2018

Synthesis and Biological Evaluation of Small Molecular Drug Candidates for the Treatment of Her2 Overexpressed Breast Cancer

Anran Zhao
Cleveland State University

SYNTHESIS AND BIOLOGICAL EVALUATION OF SMALL MOLECULAR DRUG CANDIDATES FOR THE TREATMENT OF HER2 OVEREXPRESSED BREAST CANCER

ANRAN ZHAO

Master of Science

Cleveland State University

May 2015

Bachelor of Science

South China University of Technology

May 2012

Submitted in partial fulfillment of requirements for the degree

DOCTOR OF PHILOSOPHY IN CLINICAL AND BIOANALYTICAL CHEMISTRY

at the

CLEVELAND STATE UNIVERSITY

MAY 2018

ACKNOWLEDGEMENTS

First and foremost, I want to express my sincere and utmost gratitude to my advisor Dr. Bin Su. Thank you for accepting me as your student, thank you for teaching me what research is and all the training you have giving to me. Thank you for pushing me hard and challenging me in every project. I have no words to express my appreciation for your help and guidance through all these years. Without your support and guidance, I would have not been able to complete my doctoral degree. Your rigorous attitude toward research will always be an example for me to follow.

I would like to thank my committee members, Dr. Aimin Zhou, Dr. Yana I Sandlers, Dr. Xue-Long Sun and Dr. Moo-Yeal Lee for being a part of my doctoral committee and for their insightful comments and hard question which incented me to widen my research from various perspectives. I would like to express my sincerely thanks to Dr. Aimin Zhou without your help and advice I would finish my dissertation paper so smoothly.

I would like to thank Dr. Xue-Long Sun to allow me to use his valuable instrument, and to Dr. Xiang Zhou for the training on ESI-LC-MS and HPLC-UV. I would also like to thank Joshua White for the training on Bruker NMR and Gang Xu for his valuable advice about how to better operate HPLC.

I want to thank Cleveland State University and the Department of Chemistry for providing me with the platform for my academic development and improvement. I want

to thank the professors who taught me various courses to elevate my knowledge and understand in science.

I would like to thank all my labmate who are, or were in Dr. Su's lab: Dr. Bo Zhong, Laila Alhadad, Vihanika Bobba, Nethrie Idippily, Cody M Orahoske, Yaxin Li for their support during my study, I will treasure our friendship. I would like to express my special thanks to my previous colleague Dr. Bo Zhong for teaching me many skills and techniques especially on how to become a better organic chemist. I would like to thanks Dr. Yan Xu for your help.

I also appreciate the advice and help from Qiaoyun Zheng and Dantin Liu in biological experiment.

Finally and most importantly, I want to thank my parents for their unconditional and selfless love. Thank you for your continuous support and assistance in my education. I am deeply indebted to you for all your sacrifices, advice and hard work.

SYNTHESIS AND BIOLOGICAL EVALUATION OF SMALL MOLECULAR DRUG CANDIDATES FOR THE TREATMENT OF HER2 OVEREXPRESSED BREAST CANCER

ANRAN ZHAO

ABSTRACT

In the US breast cancer is the most common cancer after skin cancer. Currently in the US the average risk of a woman to develop breast cancer in her life is roughly 12%. About 25-30% of breast cancer patients have HER2 overexpressed tumor, and the growth of tumor cell is depend on HER2 pathway. It has been well-documented that patients with over-expressed HER2 are associated with increased disease recurrence, worse prognosis and lower survival. Currently there are two type of HER2 targeting drug. The first group is HER2 monoclonal antibody drugs such as trastuzumab approved by FDA in 1998; the second type is intracellular tyrosine kinase inhibitors such as lapatinib approved by FDA in 2007. Presently trastuzumab is one of the most efficient in clinic for HER2 over-expressed breast cancer patients, however many patients didn't gain benefit due to the de novo or acquire resistance. The resistance of trastuzumab involves multiple cellular pathway, research indicates that HSP27 participate in the development of resistance. There are studies indicate that HER2 is one of the client proteins of HSP27. HER2 would be downregulated via inhibition of HSP27.

Previously, a lead compound JCC76 which generated from COX-2 inhibitor

Nimesulide was found to target HSP27. Herein, 23 analogs of JCC76 were synthesized. Cell viability assay was used for screen the analogs that selectively inhibit HER2 overexpressed cell proliferation. Western-blot and chaperone assay were used to investigate the anti-proliferate cellular mechanism. The selected compounds, 16 and 17, inhibited the protective function of small chaperone. In the HER2 downregulation experiment, the results indicate a dose-dependent downregulation of HER2 for both compounds.

In the second study we try to improve the druggable characteristics of the compounds by reducing the compound size and molecular weight. Totally 60 compounds were synthesized and screen for cell growth inhibitory ability against variance cell line, 5 compounds with potent proliferate inhibitory activity were identified. The SAR study indicates several compounds with 3-trifluoromethylbenzamide groups showed potent and selective inhibition of HER2 overexpressed breast cancer cells.

TABLE OF CONTENTS

LIST OF TABLES

Table Page

LIST OF FIGURES

LIST OF ABBREVIATIONS

IHC	immunohistochemistry
ER	estrogen receptor
PR	progesterone receptor
HER2	Human epidermal grow factor receptor 2
ErbB	Epidermal Growth Factor Receptor
RTK	Receptor tyrosine kinase\
EGF	Epidermal growth factor
TGF-α	transforming growth factor-α
AR	Amphiregulin
HB-EGF	Heparin-binding EGF-like growth factor
EPR	Epiregulin
EPG	Epigen
BTC	Betacellulin
NRG1	neuregulin-1
NRG2	neuregulin-2
NRG3	neuregulin-3
NRG4	neuregulin-4
RAF	proto-oncogene serine/threonine-protein kinase

MAPK	mitogen-activated protein kinase
Akt	Protein kinase B
PI3K	Phosphoinositide 3-kinase
STAT	signal transducer and activator of transcription
GR2	Growth factor receptor-bound protein 2
ADCC	antibody-dependent cellular cytotoxicity
DMSO	Dimethyl sulfoxide
DTT	Dithiothreitol
ESI-MS	Electrospray ionization mass spectrometry
FBS	Fetal Bovine Serum
IC50	50% inhibitory concentration
m/z	Mass to charge ratio
MTT	3-(4,5-dimethylthiazol-2-yl)-2,5-diphenyl-2H-tetrazolium bromide
SiRNA	Small interfering RNA
NmU	neuromedin U
HSP	Heat shock protein
HSP100	Heat shock protein100
HSP90	Heat shock protein90
HSP70	Heat shock protein70
HSP60	Heat shock protein60
HSP40	Heat shock protein40

ROS	Reactive oxygen species
MAPKAP-2	Mitogenactivated protein kinase-activated protein 2
DFS	disease free survival
G6DPH	Glucose-6-phosphate dehydrogenase
GR	glutathione reductase (
Apaf-1	apoptotic protease activating factor-1
dATP	Deoxyadenosine triphosphate
Bax	Bcl-2-associated X protein
JNK	c-Jun N-terminal kinase
ASK	Apoptosis signal-regulating kinase
IAPs	inhibitor of apoptosis proteins
Smac	second mitochondria-derived activator of caspases
FADD	Fas associated-death-domain
Daxx	Death-associated protein 6
Bid	BH3 interacting-domain death agonist
ASO	2’-methoxyethyl phosphorothioate antisense oligonucleotide

CHAPTER I

INTRODUCTION

1.1 Breast Cancer

Cancer is a generic term for a large group of diseases that can affect any part of the body with one defining feature of rapid generation of abnormal cells that grow beyond their usual boundaries that can then invade adjoining parts of the body and spread to other organs. [1] Most cancers will form a lump or mass called a tumor, which can proliferate and spread throughout the body in a process known as metastasis.

In the US, breast cancer is the second most common cancer in women after skin cancer, with a life time risk of about 12.4%. There are three major histopathology classifications of breast cancer: Ductal carcinoma in situ, Lobular carcinoma in situ, and Invasive breast cancer which consists of 80% of breast cancer. The American Cancer Society estimated there will be 252,710 cases of invasive breast cancer and 63,410 in situ breast carcinoma will be diagnosed among women, and 40,160 women are expected to die from breast cancer in 2017. [2]

The treatment of breast cancer depends on the stage of cancer. For early and locally advanced breast carcinoma the intention of treatment is to cure before metastasis, but for the later stage carcinoma there is no cure and the treatment is focused on increasing the overall survival rate. Various approaches employed for breast cancer management include surgery, radiation treatment, endocrine treatment and chemotherapy [3]. Lumpectomy, a surgery to remove the tumor and a small, cancer-free margin of healthy tissue around the tumor will be used for stage I and II patients followed by radiation therapy. For local advanced carcinoma and patients with former radiation therapy to the breast or chest wall will go through mastectomy, which is the surgical removal of the entire breast, instead of lumpectomy. For stage IV breast cancer, only endocrine therapy and chemotherapy is available. To achieve best therapeutic results and improve the overall survival rate, an understanding of molecular biology behind breast cancer is necessary.

Based on the expression level of classic immunohistochemistry (IHC) markers such as estrogen receptor (ER), progesterone receptor (PR) and human epidermal grow factor receptor 2 (HER-2) breast cancer can be divided into five intrinsic subtypes: Luminal A, Luminal B, HER2 over-expression, Basal and Normal-like (Table I). [4] In this study we are focusing on HER-2 over-expression subtype which tends to grow and spread more aggressively and has a poor prognosis and overall survival rate compared to the other subtypes.

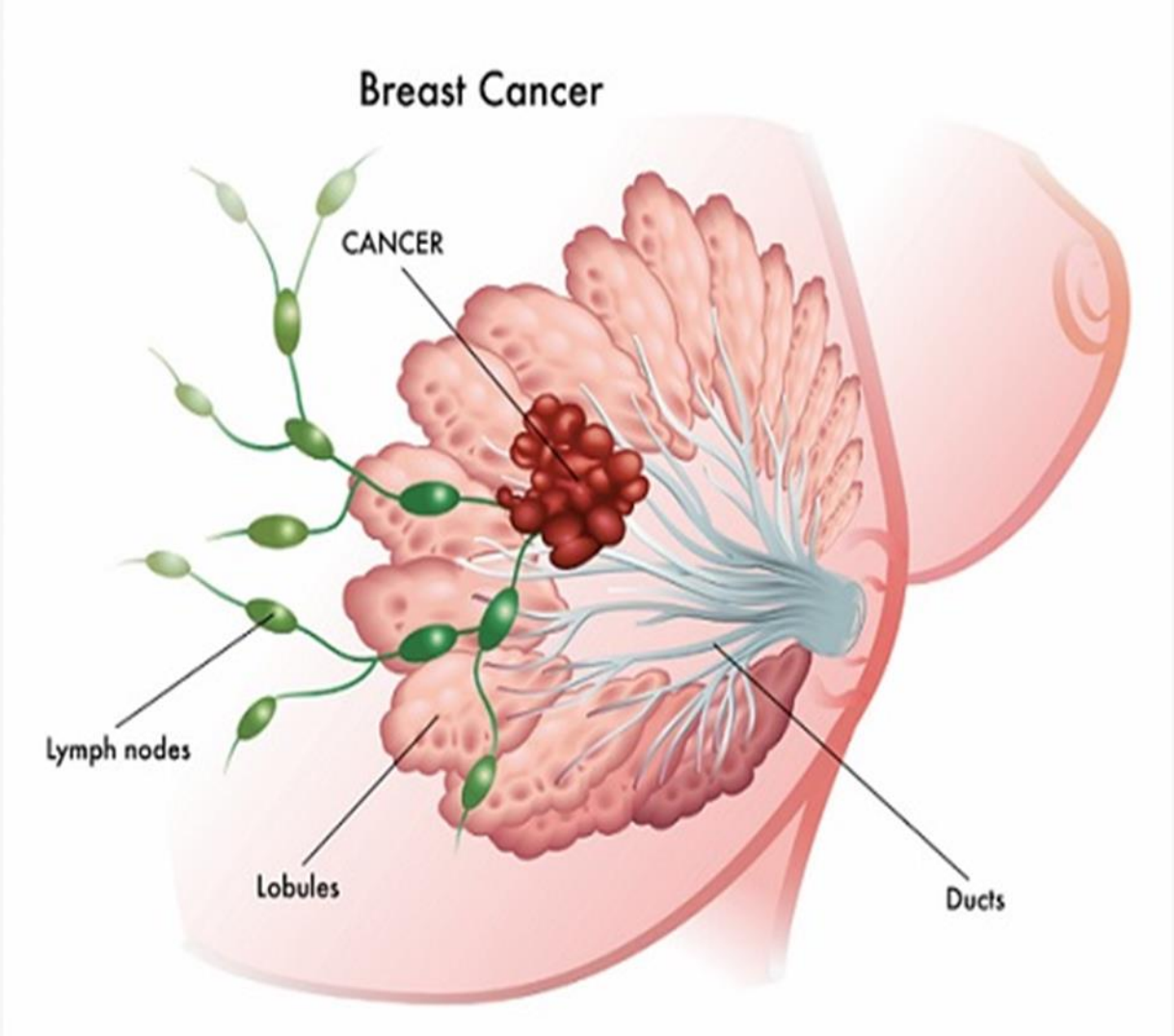

Figure 1.1 Breast Cancer
Astrid. Deodorant Alternatives for Avoiding Breast Cancer https://www.healyounaturally.com/deodorant-alternatives-for-avoiding-breast-cancer-emaxhealth/ (accessed Mar 7, 2018).

Table 1.1 Summary of the breast tumor molecular subtypes [4]

Intrinsic subtype	IHC status	Grade	Outcome
Luminal A	[ER+|PR+] HER2-KI67-	1/2	Good
Luminal B	[ER+|PR+] HER2-KI67+	2/3	Intermediate
	[ER+|PR+] HER2+KI67+		Poor
HER2 over-expression	[ER-PR-] HER2+	2/3	Poor
Basal	[ER-PR-] HER2-, basal marker+	3	Poor
Normal-like	[ER+|PR+] HER2-KI67-	1/2/3	Intermediate

1.2 Human Epidermal Growth Factor Receptor 2 (HER-2)

1.2.1 HER2 in cancer

Human Epidermal Growth Factor Receptor 2 (HER-2) is a 185 kDa glycoprotein encoded on gene 17q12 which is localized on the long arm of chromosome 17. It is normally expressed in the epithelia of various organs such as bladder, lung, breast, pancreas and prostate. HER-2 belongs to the transmembrane receptor tyrosine kinase (RTK) family, ErbB, which is a family of cell surface growth-factor receptors that play an important role in proliferation, migration, metabolism, differentiation, and survival of cells.[5]

The ErbB family of proteins consists of four members: HER1 (EGFR, ErbB1), HER2 (Neu, ErbB2), HER3 (ErbB3), and HER4 (ErbB4) which are structurally related (Figure 1.2). Members of ErbB family have three major domains: ligand binding domain, transmembrane domain and kinase domain. The ligand binding domain can recognize and bind to various ligands with different specificity. Upon ligand binding, ErbBs will be active and be ready to form a homodimer or heterodimer. The numerous ErbB ligands can be divided into four categories based on their binding affinity toward different receptors. First category includes EGF, AR and TGFα which exclusively bind to EGFR. A second family consisting of BTC, HB-EGF and EPR show dual specificity toward HER1 and HER4. NRGs comprise the third and fourth family, and NGR-1 and NRG-2 can bind HER3 and HER4, NRG-3 and NRG-4 bind HER4 but not HER3.[6] ErbB ligands have a

bivalence characteristic which shows high binding affinity toward the receptor and low affinity binding toward the dimerization partner. For instance, the ligand NRG–1's preferential dimerization partner is HER2.[7] There is no HER2 ligand that has been identified which is a characteristic related to HER2's unique extracellular domain structure. The extracellular domain of the ErbB family consists of four subdomains (I-IV): subdomain I, II and III form the ligand binding pocket and the helic fold in subdomain I and III are critical for ligand binding. During ligand binding the receptor dimerization is through interaction between a beta hairpin in subdomain II. In contrast, in the inactivated ErbB the intramolecular interactions between subdomains II and IV will prevent dimerization. HER2 has a fixed conformation that resembles a ligand-activated state, and its subdomains I and III are very close where this interaction makes ligand binding impossible. [8] This unique extracellular domain of HER-2 allows it to exhibit ligand independent activity.

Upon ligand binding and dimer formation, the intrinsic tyrosine kinase will be activated and lead to the autophosphorylation of specific C-terminal tyrosine residues, except HER3 which has an impaired autophosphorylation function.[9] Various proteins containing Src homology 2 and phosphotyrosine binding domain will bind to the C-terminal of receptor and initiate cell signaling via different pathways which include: RAS/RAF/MAPK, PI3K/AKT, Phospholipase Cγ, Src kinase pathways, and STAT pathways.[10] Apart from those tyrosine kinase pathways, there are studies that indicate that there is a novel pathway where the EGFR will be transported from the cell

membrane to the nucleus to regulate gene expression directly. [11] HER2 can only recruit Grb2 and shc on its intracellular domain to activate the RAS/RAF/MAPK pathway and the HER2 homodimer signaling is relatively weak. [6] Unlike the homodimer's weak signal, the heterodimer of HER2 has prolonged and enhanced downstream signalling through two different layers of regulation. At the ligand binding and activation layer HER2 heterodimers exhibit a relaxed ligand specificity and a decreased ligand dissociation rate which prolongs the downstream signal. At the endocytosis and recycling layer ErbB dimerizes with HER2 which will decrease the endocytosis rate. The HER2 heterodimer will readily dissociate in early endosome and will be recycled back to the membrane. [12]

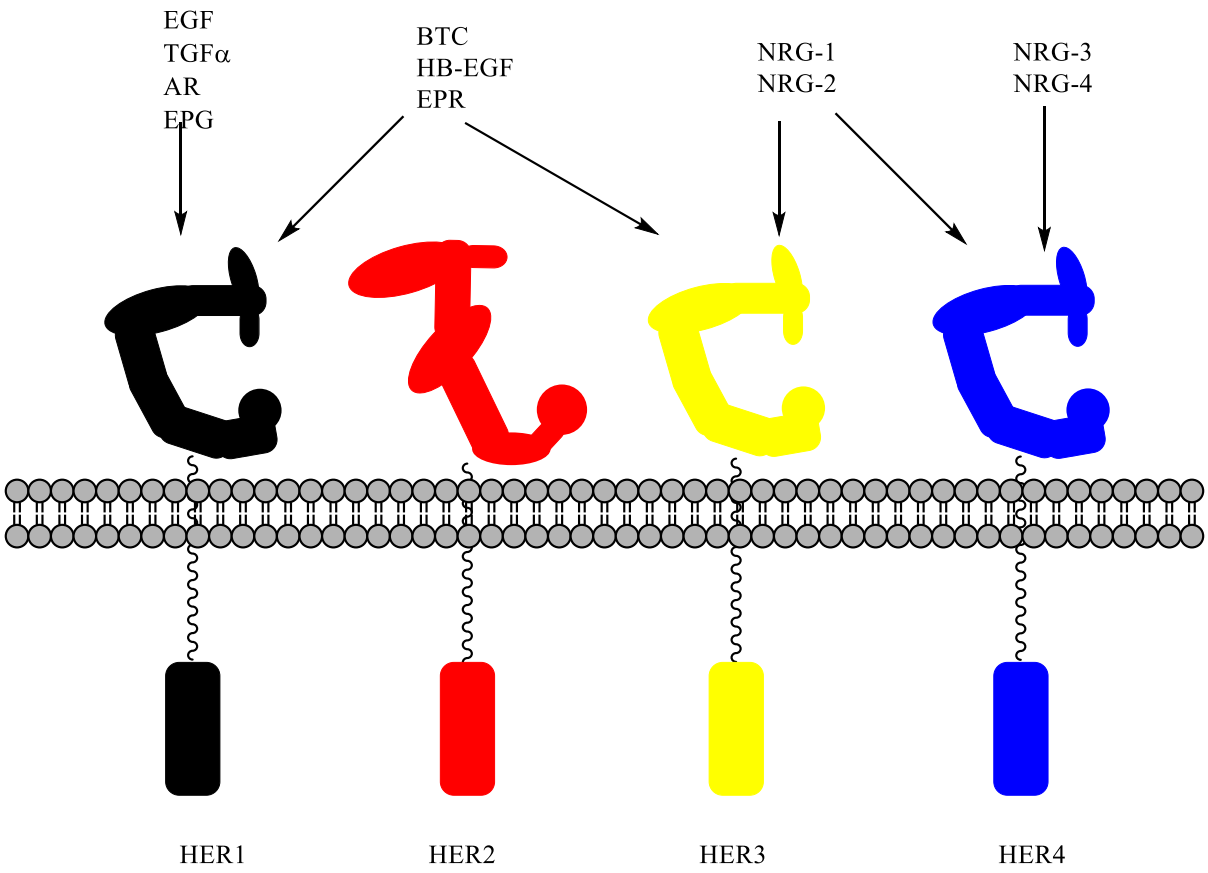

Figure 1.2 The ErbB receptors and their ligands. [6]

Binding specificities of the EGF-related peptide growth factors. There are four categories of ligands that bind ErbB family receptors. EGF, AR and TGFα bind ErbB1; BTC, HB-EGF and EPR bind ErbB1 and ErbB4; NRG-1 and NRG-2 bind ErbB3 and ErbB4; and NRG-3 and NRG-4 bind ErbB4.

Among all ErbBs heterodimers, HER2/HER3 dimer can generate the most potent downstream signal to stimulate proliferation through the PI3K/AKT pathway. Hence there is research which indicate that HER3 is an indispensable HER2 dimerization partner and is essential for HER2 overexpressed tumor cell proliferation. Therefore HER2/HER3 dimer can be regarded as an oncogenic unit of HER2 overexpressed cancer. [13]

1.2.2 HER2 targeting drug trastuzumab and its resistance

Currently, two groups of HER2 targeting drugs exist. The first group is HER2 monoclonal antibody which includes trastuzumab approved by the FDA in 1998 and pertuzumab approved in 2012. The second group is intracellular tyrosine kinase inhibitors such as lapatinib approved in 2007. [14] The exact mechanism of trastuzumab targeting HER2 overexpressed cancer remains unclear today. There are several proposed mechanisms, including blocking HER2 dimerization and extracellular domain proteolysis, recruiting immune effector cell and activating ADCC (antibody-dependent cellular cytotoxicity), receptor down regulation through endocytosis and degradation, and inhibiting DNA repair. [15],[16]

Although trastuzumab is one of the most effective treatments against HER2 overexpressed breast cancer, a great number of patients do not benefit from it due to the resistance. There are multiple reasons for the resistance and the most intensively studied

trastuzumab resistance mechanisms can be divided into four: (1) obstacles for trastuzumab binding to HER2; (2) upregulation of HER2 downstream signalling pathways; (3) enhancing signalling through alternative pathways; and (4) failure to trigger immune-mediated mechanisms to destroy tumor cells. [15]

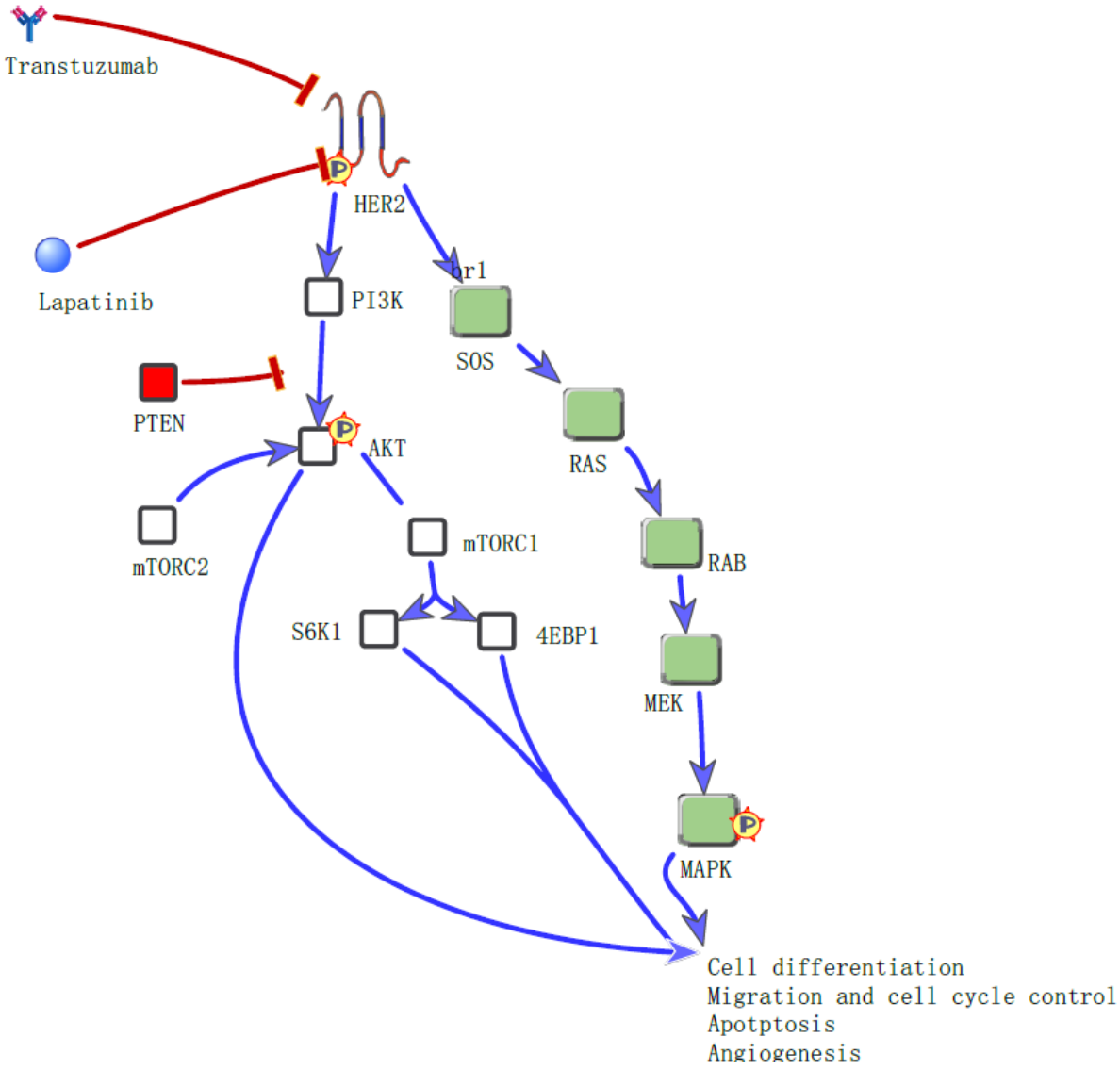

Figure 1.3 EGFR signalling pathway and targeted therapies [14]

Currently there are two type of HER2 targeting agents They are targeting extracellular domain or kinase domain of HER2, see text for more detail

Besides these well studied mechanisms HSP27 (Heat shock protein 27) was also found to be involved in trastuzumab resistance. HSP27 expression was shown to be upregulated in trastuzumab resistance cells. The sensitivity of trastuzumab resistant cells to trastuzumab increased after HSP27 suppression by specific siRNA transfection. Co-immunoprecipitation analysis indicates that HSP27 can bind to HER2 in the absence of trastuzumab. [17] Based on another study, the neuropeptide, neuromedin U (NmU), is also involved in HSP27 induced trastuzumab resistance. [18] The proposed resistance mechanism is that the overexpressed HSP27 and NmU cooperatively stabilize HER2 to downregulate its degradation which results in reduced trastuzumab susceptibility (Figure 1.4).

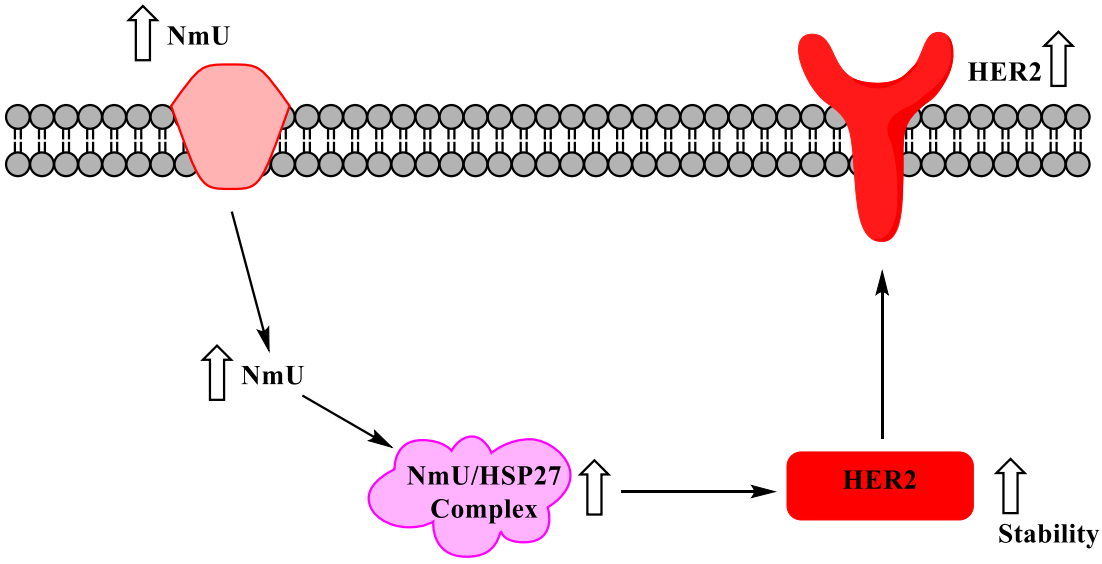

I Resistance

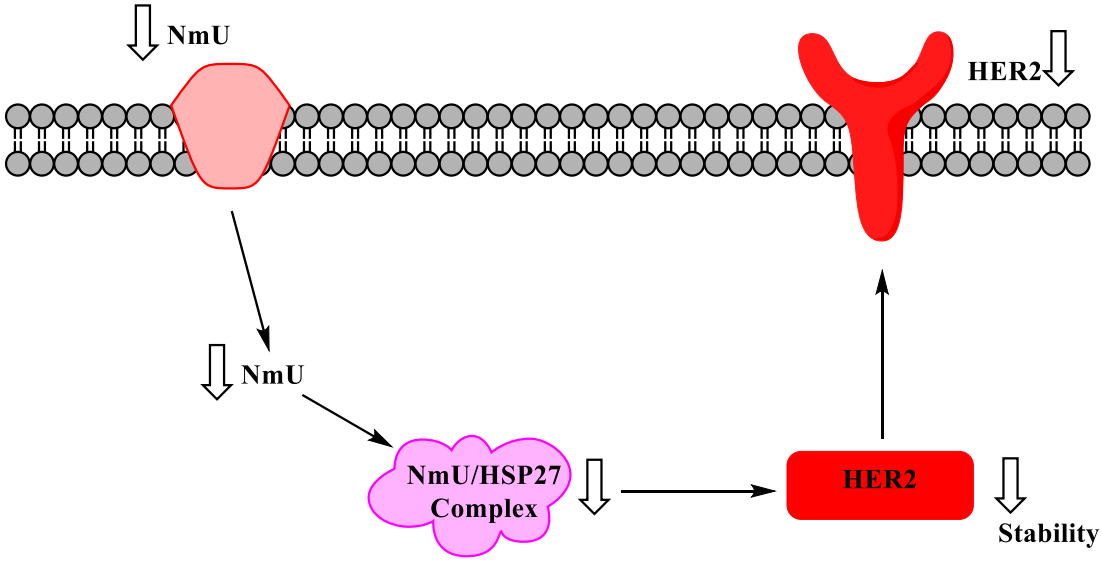

II Resensitising

Figure1.4 Proposed mechanism of HSP27 induce trastuzumab resistance [18]. HSP27 is forming complex with neuromedin U to stabilize HER2

1.3 HSP27 and its regulation on client proteins

1.3.1 HSP27 overview

Heat shock proteins (HSPs) are a family of protein produced by the cell when exposed to stress conditions. HSPs are highly conserved proteins among species which were first discovered at 1962. This family of proteins were name after heat shock because they were first described related to heat shock, but now are known to be expressed when cells are exposed to various environmental, metabolic, and pathophysiological stress conditions. [19,20] HSPs are divided into six major families based on their molecular weight: HSP100, HSP90, HSP70, HSP60, HSP40 and small HSP (30KDa-15KDa). [21] The higher molecular weight HSPs are ATP-dependent chaperones whereas small molecular HSPs are ATP-independent chaperones. Heat shock protein 27 (HSP27/HSPB1) belongs to the small heat shock protein family which contains 10 members characterized by a highly conserved central domain and less conserved N- and C-terminal domains. Small chaperone exists in monomer, dimer, and oligomers, and the dynamic oligomerization and function of the small chaperones is regulated by phosphorylation of the protein [22]

1.3.2 The ability of HSP27 regulate level of certain client proteins

Besides chaperone function and protect cell against various stress, HSP27 also play an important role in diverse cellular pathway due to its complicate and dynamic oligomer

structure and phosphorylation statue. Among these interactions there are several proteins that are stabilized by HSP27, the category of these proteins including: receptors, transcript factors and some enzymes. [23] These proteins are stabilized by HSP27 and directly interact with HSP27, they can consider as the client proteins of HSP27.

There are three transcript factors identified as the client proteins of HSP27 including: signal transducer and activator of transcription 2 (STAT2), signal transducer and activator of transcription 3 (STAT3) and zinc finger protein SNAI1 (Snail). [24] STAT2 as one of the HSP27's client proteins was report by Gibert et al. [21] In this research the downregulation of STAT2 in HSP27 depletion cell was revealed by western-blot analysis. The reduction of STAT2's activity was confirmed by monitoring the expression of luciferase in HSP27 depletion cell transfected with a STAT1/STAT2-responsive luciferase construct encoding the firefly luciferase reporter gene. In further investigation of HSP27 regulation mechanism STAT2 degradation obstructed via proteasomal pathway inhibited by MG132, in qPCR test STAT2 mRNA slightly induce when level of STAT2 decrease in HSP27 depletion cell. All these results support that HSP27 stabilizes STAT2 through preventing STAT2 degradation by proteasome. [25] In a study done by Rocchi et al, the downregulation of STAT3 via HSP27 knocked down with allele-specific oligonucleotide (ASO) has been reported. Although the exact mechanism is not clear about how HSP27 regulates STAT3, at least that HSP27 participates in STAT3 protein complex was confirmed. [26] Inhibiting HSP27 resulting in to the reduction of STAT3 was also be observed in first trimester human placenta. [27] The upregulation of Snail was found in

adenocarcinoma cell due to overexpression of transforming growth factor beta 1 (TGF-β1) or HSP27. The result of Western-blot and qPCR studies on HSP27 depleted but TGF-β1 overexpressed cell suggest that HSP27 regulate Snail at protein level instead of mRNA level. To confirm whether HSP27 stabilized Snail by decreasing proteasome degradation, HSP27 knocked down cells were treated with MG132 and the induction of Snail was restored. This result indicates that HSP27 upregulates Snail by preventing it from degradation. [28]

Two enzymes including human double minute 2 homolog (HDM2) and Histone deacetylase 6 (HDAC-6) are also identified as HSP27 client proteins. [24] In a study done by Ocallaghan-Sunol et al, HSP27 was found to stabilize HDM2 which further activates Tumor protein p53 (p53) pathway. [29] In the study done by Gibert et al, HDAC-6 was found to be downregulated in HSP27 knocked down cells and qPCR study suggests that HDAC-6 reduction was post-translationally regulated. To better understand the mechanism of HDAC-6 regulation by HSP27, HSP27 depletion HeLa cells were treated with proteasome inhibitor MG132 or ALLN. Both proteasome inhibitors were found to block the reduction of HDAC-6, suggest that HSP27 regulates HDAC-6 through degradation pathway. [25]

HER2 and androgen receptor (AR) have been identified as client proteins of HSP27 and they are important cancer therapeutic targets. [23] In a study done by Zoubeidi et al the interaction between HSP27 and AR was investigated. Androgen binding AR induces the phosphorylation of HSP27, and HSP27 could facilitate the AR complex shift to the

nucleus and induces the transcription activity of AR. HSP27 knocked down could reduce AR stability, which has been confirmed. They propose a pathway of HSP27 and AR interaction: androgen and androgen receptor binding could induce the phosphorylation of HSP27 and exchange partner from HSP90 to phosphorylated HSP27. The HSP27/AR complex will relocate into nucleus and promote transcription. inhibition of HSP27 phosphorylation or reducing HSP27 with siRNA could reduce AR translocation and increase AR degradation. [30] There is another study suggest that HSP27 also mediates AR through regulating AR mRNA level. [31]

The interaction of HSP27 and HER2 were first reported by Kang et al. They found in trastuzumab resistance breast cancer cell line that the expression of HSP27 has been upregulated. Treatment with trastuzumab could lead to HER2 degradation in both trastuzumab resistance and naïve HER2 positive cell line. However HER2 reduction in resistance cell line is much less after the treatment, suggesting that increase of HER2 stability may involve in trastuzumab resistance. The co-immunoprecipitation study shows that HSP27 can bind to HER2. After HSP27 knock down, trastuzumab resistance cell showed greater response when treated with trastuzumab and cell viability assay suggest that knock down HSP27 results in sensitizing resistance cells to trastuzumab. All this results suggest that downregulation of HER2 by trastuzumab can be blocked by the formation of HER2/HSP27 complex. [17] In another research done by the same group, the relationship between HSP27 phosphorylation and HER2 stabilization was investigated. Although HSP27 phosphorylation inhibitor suppressed cell proliferation and induced

apoptotic cell death in both HER2 positive breast cancer cell and trastuzumab resistance cells, there is no evident to support that the interaction between HER2 and HSP27 could be directly targeted by HSP27 phosphorylation inhibitor. [33] Neuromedin U (NmU) has been report to stabilize HER2 as a partner protein directly binding HSP27 [34]

1.3.3 HSP27 inhibition could induce degradation of certain client proteins

Upregulation of HSP27 results in the enhanced stability of several client proteins which are critical cancer therapeutic targets. Therefore inhibition of HSP27 serves as a promising strategy to develop new anti-cancer agents. Currently there are four class of inhibitor that can regulate the expression level and function of HSP27. [35] First class is antisense oligonucleotide (ASO) that is a chemically modified or unmodified single-stranded DNA which binding to mRNA to prevent translation. OGX-427 is an ASO HSP27 inhibitor which can sensitize no-small cell lung cancer and bladder cancer to chemotherapy. [36,37] Downregulation of HSP27 by OGX-427 leads to the increased degradation of eukaryotic translation initiation factor 4E (eIF4E) in prostate cancer cells. [38] Currently the phase II trial of OGX-427 on pancreatic cancer and no-small cell lung cancer are completed. [39] Second class of inhibitor is siRNA which is a double-stranded RNA which binding to mRNA and preventing its translation. Currently there is no siRNA drug on clinical trial but its ability to downregulate client protein of HSP27 has been reported. [25-31] The third class of inhibitor is peptide aptamers which is a selected or engineered peptide that can bind to specific target. Two sequence-specific aptamers has

been generated and prove to be able to reducing HSP27 but whether they can modify client protein or not has not been investigated. [40] The fourth class is small molecular inhibitor such as RP101, KRIBB3 and quercetin, which has been reported to inhibit HSP27 in the in vitro assays. RP101 has been prove to bind to mRNA coding therefore inhibit the translation leading to the downregulation of HSP27. [41] KRIBB3 was reported binding to HSP27 and inhibit its phosphorylation which lead to obstruct of tumor cell migration. [42] Quercetin was first reported to reduce the expression of HSP90, HSP70 and HSP27. [43] But late study indicate quercetin also capable to inhibit the phosphorylation of HSP27 [44] However there is no research investigate the interaction between these small molecular inhibitor and client proteins. Our group has identified Copalic acid and its analogs as small chaperone inhibitor. This natural product inhibits the chaperone activity of HSP27 and α-crystallin in the in vitro insulin aggregation assay. In addition, the compounds were also found to induce AR degradation. Targeting the small chaperone proteins with small molecule inhibitors has the potential to induce onco-protein degradation, and be used as novel anti-cancer agents in the future.[45]

1. 4 References

1. Cancer http://www.who.int/mediacentre/factsheets/fs297/en/ (accessed Mar 7, 2018).
2. American Cancer Society. Breast Cancer Facts & Figures 2017-2018. Atlanta: American Cancer Society, Inc. 2017
3. Anjum, F.; Razvi, N.; Masood, M. A. Breast Cancer Therapy: A Mini Review. Drug Design, Development and Therapy, 2017, 1 (2).
4. Dai, X; Li, T; Bai, Z; Yang, Y, Liu, X., Zhan, J J; & Shi, B. Breast cancer intrinsic subtype classification, clinical use and future trends. American Journal of Cancer Research, 2015;5(10):2929-2943
5. Angelica Fasolo , Luca Gianni; Hand book of HER-2-targeting agent in breast cancer , chapter 1, Switzerland: Springer International Publishing, 2016, 1-13
6. Olayioye, M. A. The ErbB signaling network: receptor heterodimerization in development and cancer. The EMBO Journal. 2000, 19 (13), 3159–3167.
7. Tzahar, E. Bivalence of EGF-like ligands drives the ErbB signaling network. The EMBO Journal. 1997, 16 (16), 4938–4950.
8. Normanno, N.; Luca, A. D.; Bianco, C.; Strizzi, L.; Mancino, M.; Maiello, M. R.; Carotenuto, A.; Feo, G. D.; Caponigro, F.; Salomon, D. S. Epidermal growth factor receptor (EGFR) signaling in cancer. Gene 2006, 366 (1), 2–16.
9. F, Shi; Telesco, S. E; Liu, Y; Radhakrishnan, R; Lemmon, M. A. ErbB3/HER3 intracellular domain is competent to bind ATP and catalyze autophosphorylation. Proceedings of the National Academy of Sciences of the United States of America.

2010, 107 (17), 7692–7697.

10. Scaltriti, M.; Baselga, J. The epidermal growth factor receptor pathway: a model for targeted therapy. Clinical Cancer Research, 2006, 12 (18), 5268–5272.
11. Lin, S.-Y.; Makino, K.; Xia, W; Matin, A.; Wen, Y.; Kwong, K. Y.; Bourguignon, L.; Hung, M.-C. Nuclear localization of EGF receptor and its potential new role as a transcription factor. Nature Cell Biology, 2001, 3 (9), 802–808.
12. Yarden, Y.; Sliwkowski, M. X. Nat. Untangling the ErbB signalling network. Nature Reviews Molecular Cell Biology, 2001, 2 (2), 127–137.
13. Holbro, T.; Beerli, R. R.; Maurer, F.; Koziczak, M.; Barbas, C. F.; Hynes, N. E. The ErbB2/ErbB3 heterodimer functions as an oncogenic unit: ErbB2 requires ErbB3 to drive breast tumor cell proliferation. Proc. Proceedings of the National Academy of Sciences of the United States of America, 2003, 100 (15), 8933–8938.
14. Loibl, S.; Gianni, L. HER2-positive breast cancer. The Lancet 2017, 389 (10087), 2415–2429.
15. Hudis, C. A. N. Engl. Trastuzumab — Mechanism of Action and Use in Clinical Practice, the New England journal of medicine 2007, 357 (1), 39–51.
16. Nahta, R.; Esteva, F. J. HER2 therapy: Molecular mechanisms of trastuzumab resistance. Breast Cancer Research, 2006, 8 (6)..
17. Kang, S. H.; Kang, K. W.; Kim, K.-H.; Kwon, B.; Kim, S.-K.; Lee, H.-Y.; Kong, S.-Y.; Lee, E. S.; Jang, S.-G.; Yoo, B. C. Upregulated HSP27 in human breast cancer cells reduces Herceptin susceptibility by increasing Her2 protein stability BMC

Cancer 2008, 8 (1).

18. Rani, S.; Corcoran, C.; Shiels, L.; Germano, S.; Breslin, S.; Madden, S.; Mcdermott, M. S.; Browne, B. C.; Odonovan, N.; Crown, J.; Gogarty, M.; Byrne, A. T.; Odriscoll, L. Neuromedin U: A Candidate Biomarker and Therapeutic Target to Predict and Overcome Resistance to HER-Tyrosine Kinase Inhibitors. Cancer Research, 2014, 74 (14), 3821–3833.
19. Ritossa, F. A new puffing pattern induced by temperature shock and DNP in drosophila. Experientia 1962, 18 (12), 571–573
20. Maio, A. D. Heat shock proteins: facts, thoughts, and dreams. Shock 1999, 11 (1), 1–12.
21. Garrido, C.; Brunet, M.; Didelot, C.; Zermati, Y.; Schmitt, E.; Kroemer, G. Heat shock proteins 27 and 70: anti-apoptotic proteins with tumorigenic properties. Cell Cycle 2006, 5 (22), 2592–2601.
22. Georg K. A. Hochberg, Justin L. P. Benesch; The big book of small heat shock protein. Chapter 3, Switzerland: Springer International Publishing, 2015. 87-100
23. Arrigo, A.-P.; Gibert, B. Protein interactomes of three stress inducible small heat shock proteins:HspB1, HspB5 and HspB8. International Journal of Hyperthermia 2013, 29 (5), 409–422.
24. Arrigo, A.-P.; Gibert, B. HspB1, HspB5 and HspB4 in Human Cancers: Potent Oncogenic Role of Some of Their Client Proteins, Cancers, 2014, 6 (1), 333–365.
25. Gibert, B.; Eckel, B.; Fasquelle, L.; Moulin, M.; Bouhallier, F.; Gonin, V.; Mellier, G.;

Simon, S.; Kretz-Remy, C.; Arrigo, A.-P.; Diaz-Latoud, C. Knock Down of Heat Shock Protein 27 (HspB1) Induces Degradation of Several Putative Client Proteins. PLOS One 2012, 7 (1).

26. Rocchi, P.; Beraldi, E.; Ettinger, S.; Fazli, L.; Vessella, R. L.; Nelson, C.; Gleave, M. Increased Hsp27 after Androgen Ablation Facilitates AndrogenIndependent Progression in Prostate Cancer via Signal Transducers and Activators of Transcription 3–Mediated Suppression of Apoptosis. Cancer Research, 2005, 65 (23), 11083–11093.
27. Shochet, G. E.; Komemi, O.; Sadeh-Mestechkin, D.; Pomeranz, M.; Fishman, A.; Drucker, L.; Lishner, M.; Matalon, S. T. Heat shock protein-27 (HSP27) regulates STAT3 and eIF4G levels in first trimester human placenta. Journal of Molecular Histology, 2016, 47 (6), 555–563.
28. Wettstein, G.; Bellaye, P.-S.; Kolb, M.; Hammann, A.; Crestani, B.; Soler, P.; Marchal-Somme, J.; Hazoume, A.; Gauldie, J.; Gunther, A.; Micheau, O.; Gleave, M.; Camus, P.; Garrido, C.; Bonniaud, P. Inhibition of HSP27 blocks fibrosis development and EMT features by promoting Snail degradation. The FASEB Journal 2013, 27 (4), 1549–1560.
29. Ocallaghan-Sunol, C.; Gabai, V. L.; Sherman, M. Y. Hsp27 modulates p53 signaling and suppresses cellular senescence. Cancer Research 2007, 67 (24), 11779–11788.
30. Zoubeidi, A.; Zardan, A.; Beraldi, E.; Fazli, L.; Sowery, R.; Rennie, P.; Nelson, C.; Gleave, M. Cooperative interactions between androgen receptor (AR) and heat-shock

protein 27 facilitate AR transcriptional activity. Cancer Research 2007, 67 (21), 10455–10465.

31. Stope, M. B.; Schubert, T.; Staar, D.; Rönnau, C.; Streitbörger, A.; Kroeger, N.; Kubisch, C.; Zimmermann, U.; Walther, R.; Burchardt, M. EVect of the heat shock protein HSP27 on androgen receptor expression and function in prostate cancer cells World Journal of Urology 2012, 30 (3), 327–331.
32. Kim, M. K.; Kim, S. C.; Kim, W. K.; Kim, K.; Kim, K.-H.; Yoo, B. C. HSP27 phosphorylation inhibitor regulates Her2 expression in human breast cancer cell line SK-BR-3 with induced Herceptin resistance; EPMA Journal 2014, 5 (S1)
33. Rani, S.; Corcoran, C.; Shiels, L.; Germano, S.; Breslin, S.; Madden, S.; Mcdermott, M. S.; Browne, B. C.; Odonovan, N.; Crown, J.; Gogarty, M.; Byrne, A. T.; Odriscoll, L. Neuromedin U: A Candidate Biomarker and Therapeutic Target to Predict and Overcome Resistance to HER-Tyrosine Kinase Inhibitors. Cancer Research 2014, 74 (14), 3821–3833
34. McAlpine, S. R.; Edkins, A. L.; Brodsky, J. L. Heat shock protein inhibitors: success stories; Springer: Switzerland, 2016.
35. Lelj-Garolla, B.; Kumano, M.; Beraldi, E.; Nappi, L.; Rocchi, P.; Ionescu, D. N.; Fazli, L.; Zoubeidi, A.; Gleave, M. E. Hsp27 Inhibition with OGX-427 Sensitizes Non–Small Cell Lung Cancer Cells to Erlotinib and Chemotherapy. Molecular Cancer Therapeutics 2015, 14 (5), 1107–1116
36. Baylot, V.; Andrieu, C.; Katsogiannou, M.; Taieb, D.; Garcia, S.; Giusiano, S.;

Acunzo, J.; Iovanna, J.; Gleave, M.; Garrido, C.; Rocchi, P. OGX-427 inhibits tumor progression and enhances gemcitabine chemotherapy in pancreatic cancer. Cell Death & Disease 2011, 2 (10).

37. Andrieu, C.; Taieb, D.; Baylot, V.; Ettinger, S.; Soubeyran, P.; De-Thonel, A.; Nelson, C.; Garrido, C.; So, A.; Fazli, L.; Bladou, F.; Gleave, M.; Iovanna, J. L.; Rocchi, P. Heat shock protein 27 confers resistance to androgen ablation and chemotherapy in prostate cancer cells through eIF4E. Oncogene, 2010, 29 (13), 1883–1896.
38. The list of currently completed OGX-427 clinical trial https://clinicaltrials.gov/ct2/results?term=ogx-427 (accessed Apr 10, 2018).
39. Gibert, B.; Hadchity, E.; Czekalla, A.; Aloy, M.-T.; Colas, P.; Rodriguez-Lafrasse, C.; Arrigo, A.-P.; Diaz-Latoud, C. Inhibition of heat shock protein 27 (HspB1) tumorigenic functions by peptide aptamers . Oncogene, 2011, 30 (34), 3672–3681.
40. Heinrich, J.-C.; Tuukkanen, A.; Schroeder, M.; Fahrig, T.; Fahrig, R. RP101 (brivudine) binds to heat shock protein Hsp27 (HSPB1) and enhances survival in animals and pancreatic cancer patients. Journal of Cancer Research and Clinical Oncology, 2011, 137 (9), 1349–1361.
41. Shin, K. D.; Lee, M.-Y.; Shin, D.-S.; Lee, S.; Son, K.-H.; Koh, S.; Paik, Y.-K.; Kwon, B.-M.; Han, D. C. Blocking Tumor Cell Migration and Invasion with Biphenyl Isoxazole Derivative KRIBB3, a Synthetic Molecule That Inhibits Hsp27 Phosphorylation. Journal of Biological Chemistry, 2005, 280 (50), 41439–41448.
42. Koishi, M.; Hosokawa, N.; Sato, M.; Nakai, A.; Hirayoshi, K.; Hiraoka, M.; Abe, M.;

Nagata, K. Quercetin, an Inhibitor of Heat Shock Protein Synthesis, Inhibits the Acquisition of Thermotolerance in a Human Colon Carcinoma Cell Line. Japanese Journal of Cancer Research, 1992, 83 (11), 1216–1222.

43. Chen, S.-F.; Nieh, S.; Jao, S.-W.; Liu, C.-L.; Wu, C.-H.; Chang, Y.-C.; Yang, C.-Y.; Lin, Y.-S. Quercetin suppresses drug-resistant spheres via the p38 MAPK–Hsp27 apoptotic pathway in oral cancer cells. PLOS One 2012, 7 (11).
44. Idippily, N. D.; Zheng, Q.; Gan, C.; Quamine, A.; Ashcraft, M. M.; Zhong, B.; Su, B. Copalic acid analogs down-regulate androgen receptor and inhibit small chaperone protein. Bioorganic & Medicinal Chemistry Letters, 2017, 27 (11), 2292–2295.

CHAPTER II

STATEMENT OF RESEARCH AND SPECIFIC AIMS

2.1 Statement of research

Cancer is the second cause of death in the US and the leading cause of death worldwide. Among various cancers, breast cancer is the most common one in females with 268,670 new cases expected in the United States in 2018. There are five intrinsic sub-types of breast cancer which are classified by the expression level of classic IHC. In this five sub-type HER2 overexpressed breast cancer accounts for about 20% of all breast cancer cases which is the most aggressive sub-type among the other four. And patients with this type of breast cancer have the lowest survival rate and the poorest prognosis. HER2 is a member of EGFR family and is overexpressed in multiple cancer types including breast cancer, ovarian cancer and lung cancer. HER2 has been a target for cancer therapy for decades; there are several drugs that have been developed. Trastuzumab, a monoclonal antibody drug, is the most successful HER2 targeting

therapeutic agent. However, half of HER2 positive breast cancer patients eventually ceased to respond to Trastuzumab due to the resistance caused by multiple different mechanisms. One of the resistance mechanisms is through the upregulation of the expression of HSP27 which stabilizes HER2. Therefore, inhibiting HSP27 could potential down-regulate HER2 protein and overcome the Trastuzumab resistance for breast cancer treatment.

HSP27 a small chaperone protein is a novel target for cancer therapy since it has anti-apoptotic effects. Currently existing HSP27 targeting agents function through reducing expression, inhibiting kinase phosphorylation of HSP27 or interrupting the interaction between HSP27 and apoptosis proteins. The present situation suggests the need for developing an HSP27 inhibitor which can specifically interrupt the HSP27-HER2 pathway.

2.2 Specific aim

(1) Synthesise a series of new compound by modify moiety B (Figure 2.1) to sulfonyl amide which should improve compounds' solubility in aqueous phase and evaluate their ability of suppress cancer cell proliferate and inhibit Hsp27 function

(2) Synthesise a series of new compound by substitute moiety A (Figure 2.1) twith smaller functional groups which should reduce the hydrophobicity and improve compounds' solubility in aqueous phase. Evaluate their anti-proliferate activity by cell viability assay.

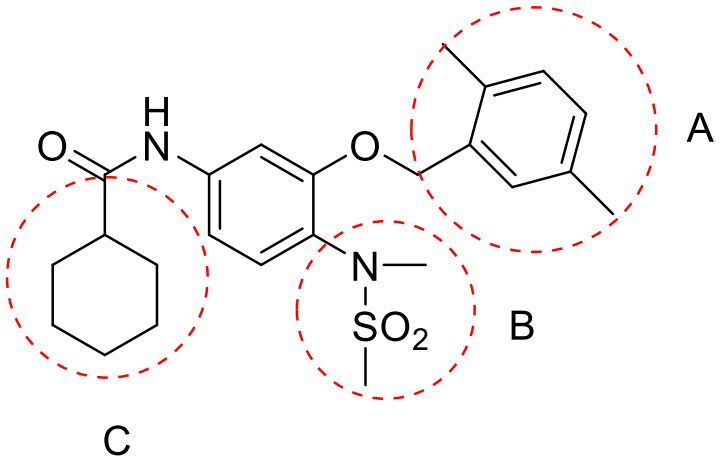

Figure 2.1 structure of HSP27 inhibitor JCC76

CHAPTER III

SYNTHESIS AND BIOLOGICAL EVALUATION OF ANTI-CANCER AGENTS THAT SELECTIVELY INHIBIT HER2 OVER–EXPRESSED BREAST CANCER CELL GROWTH VIA DOWN-REGULATION OF HER2 PROTEIN

3.1 INTRODUCTION

About 25–30% of breast cancer patients have human epidermal growth factor 2 (HER2) over-expressed tumors, and the tumor cells depend on the HER2 pathway to proliferate.[1] There are multiple factors that contribute to the high level of HER2 protein in tumors, [2,3] which results in constitutive activation of the receptor and cell growth. It has been well-documented that patients with over-expressed HER2 are associated with increased disease recurrence, worse prognosis and lower survival.[4] Targeting the extracellular domain of Her2 receptor could result in an efficient inhibition of breast

cancer cell proliferation.[1,2,5,6] In addition, inhibition of intracellular signaling pathways of HER2 downstream could lead to the suppression of cancer cell growth as well.[7] Currently,

there are two types of drugs that target HER2. The first group is HER2 monoclonal antibody drugs such as trastuzumab approved by FDA in 1998; the second type is intracellular tyrosine kinase inhibitors such as lapatinib approved by FDA in 2007. [8,9]

Even though treatment with these drugs showed great efficiency in clinic for HER2 over-expressed breast cancer patients, resistance has been reported in patients who use trastuzumab as the treatment. [9] There are multiple reasons for the resistance, and further increased HER2 expression in the cancer cells after the treatment is one of them. [10] Researchers used different strategies to reduce the HER2 level and found that the cancer cells regained the sensitivity to trastuzumab. [10] Therefore, new agents that can reduce the amount of HER2 in breast cancer cells indirectly needs to be used for the HER2 overexpressed breast cancer treatment, which may also have the potential to overcome trastuzumab resistance. [11-13]

Our goal is to identify new anti-cancer compounds that would selectively inhibit the growth of HER2 over-expressing breast cancer cells, and then investigate the mechanism of the pharmacological activity. Previously we identified a small molecule, JCC76 that showed selectivity to inhibit the growth of HER2 over-expressed breast cancer cells . In this study, structural optimization was performed to improve the biological activity and the selectivity of the lead compound. The new analogs were evaluated with a panel of breast cancer cell lines including SKBR-3, MCF-7 and MDA-MB-231. The compounds that selectively inhibited the proliferation of SKBR-3 cells that is a HER2 overexpressed breast cancer cell line were selected. They were further examined with western blot assay to analyze their effect on the HER2 protein level. The results indicate that the new compound

significantly decreased the HER2 level in breast cancer cells. In addition, the compounds inhibited the small chaperone protein in the *in vitro* assay.

3.2 RESULTS AND DISCUSSION

3.2.1 Lead optimization and summarization of the structure-activity relationship (SAR) studies

Previously, compound JCC76 was shown to selectively inhibit the growth of SKBR-3 cells with an IC_{50} of 1~3 μM. JCC76 was also found to inhibit a small chaperone protein heat shock protein 27 kDa (HSP27). It has been reported that HER2 is a client protein of HSP27, which may explain the selectivity of JCC76 to HER2 over-expressed SKBR-3 cells. To improve the potency, selectivity and ligand efficiency, we further optimized the structure of JCC76. Based on the structure activity relationship (SAR) summarized before, we either retained the 2, 5-dimethylbenzyl moiety or changed it to 2, 5-dimethoxybenzyl group (Figure 3.1). Then the sulfonamide moiety of JCC76 was changed to a flipped new sulfonamide structure and two carbons were removed to increase the ligand efficiency and solubility. Further, the amide moiety was constructed with various substituted benzamides to explore what the best function group could be for this moiety. The synthesis of the new analogs is described in schemes 1 and 2.

These new compounds were synthesized using method adapted from previous studies. Since the sulfonamide moiety was flipped in the new analogs compared to JCC76, the

construction of the sulfonamide is different to the previous synthetic method. The rest of the benzyl and amide moieties were synthesized in a similar way. A total of 23 final compounds were synthesized.

Consequently, they were examined for the potency and selectivity on the growth inhibition of three different breast cancer cells lines including SKBR-3, MCF-7, and MDA-MB-231. SKBR-3 cells are HER2 positive and estrogen receptor (ER) negative, while MCF-7 cells are HER2 negative and ER positive. MDA-MB-231 cells are HER2 and ER negative. The results are summarized in Table 3.1.

The IC_{50}s of the cell growth inhibition of the compounds range from 0.13 μM to 25.69 μM for SKBR-3 cells, 1.18 μM to 60.49 μM for MCF-7 cells, and 0.27 μM to 38.99 μM for MDA-MB-231cells. The selectivity is calculated by dividing the IC_{50}s of the compounds from different cell lines (Table 1). Most compounds exhibited more potent growth inhibition of SKBR-3 cells compared to MCF-7 and MDA-MB-231 cells, as indicated by most of the selective index that are greater than 1. For SKBR-3 cells, SAR analysis suggests that the benzamide group of these compounds is critical for the biological activity. The electron-donating substitute such as the iodo group on the benzamide moiety overall enhanced the activity, as indicated by compounds 3 and 6. The electron-withdrawing groups such as trifluromethyl harmed the activity, as indicated by compounds 7 and 15. In terms of the 2, 5-dimethoxybenzyl and 2, 5-dimethylbenzyl moiety, it seems that the methoxy group is more beneficial to the activity than the methyl group. Compounds 19-23 are relatively less potent compared to the corresponding

dimethoxy analogs, even though they have electron-donating substitutes on their benzamide moiety. Compounds 16 with a napheylamide moiety and 17 with a 4-methxyphenyl moiety showed the best potency and selectivity.

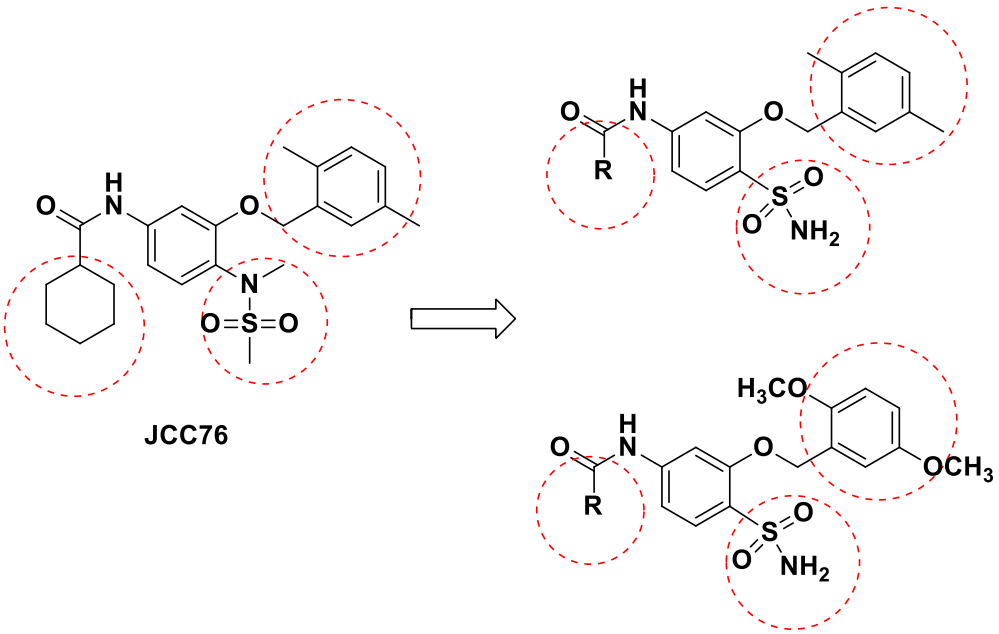

Figure 3.1. Lead optimization of JCC76 to improve the ligand efficiency and biological activity

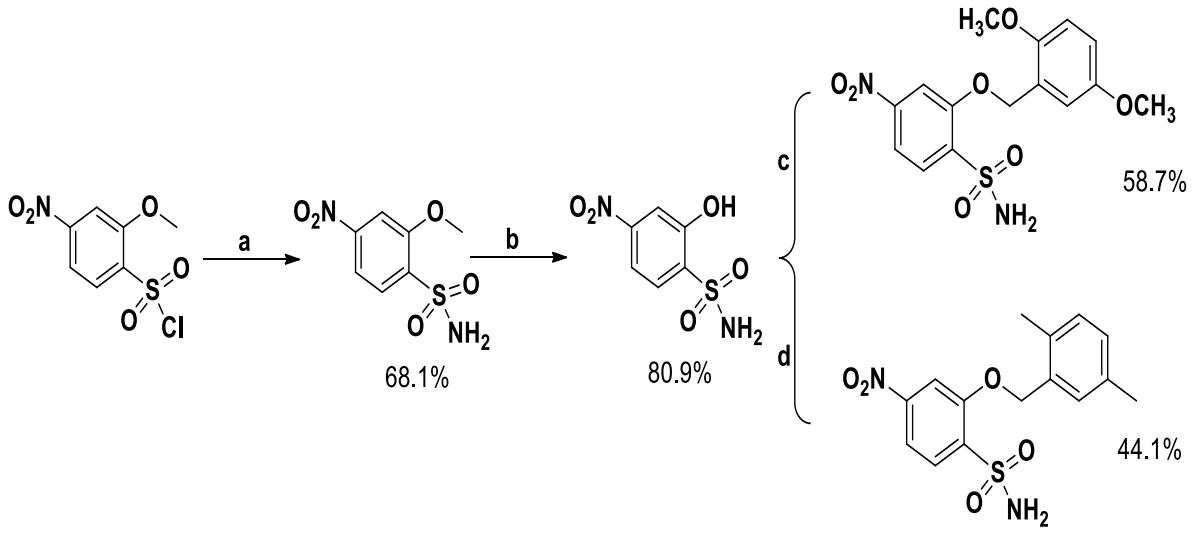

Figure 3.2 (a) NH_3,H_2O,THF; (b) CH2Cl2, BBr3; (c) 2,5-dimethoxybenzyl chloride, K_2CO_3, DMF; (d) 2,5-dimethylbenzyl chloride, K_2CO_3, DMF

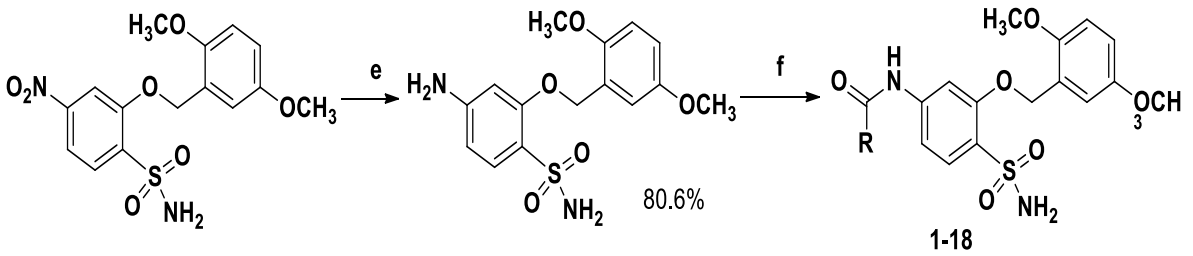

1. R=3-methoxyphenyl (71.7%)
2. R=3-methylphenyl(36.7%)
3. R=3-iodophenyl(46.3%)
4. R=3-bromophenyl(33.2%)
5. R=3-cyanophenyl(52.4%)
6. R=4-iodophenyl(%)
7. R=2,4-trifluoromethylphenyl (24.3%)
8. R=4-trifluoromethoxyphenyl(61.3%)
9. R=3-cholophenyl(52.0%)
10. R=4-ethylphenyl (56.0%)
11. R=4-cyanophenyl (31.3%)
12. R=3-nitro 4-cholophenyl(52.1%)
13. R=3-ethoxyphenyl (52.5%)
14. R=4-bromophenyl (53.3%)
15. R=3,5-trifluoromethylphenyl(30.0%)
16. R=2-napththyl(52.5%)
17. R=4-methoxyphenyl (38.6%)
18. R=cyclohexanyl(77.0%)

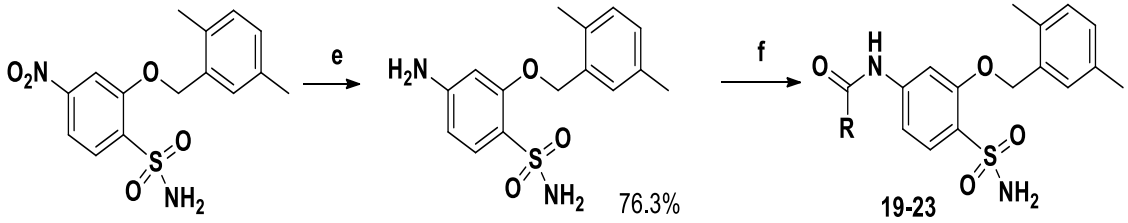

19. R=4-iodophenyl(58.3%)
20 R=3-iodophenyl(55.8%)
21. R=cyclohexanyl(53.7%)
22. R=4-methoxyphenyl(64.2%)
23 R=4-bromophenyl(58.1%)

Figure 3.3. (e) $FeCl_3$, Zn, DMF/H_2O; (f) RCOCl, K_2CO_3, 1,4-dioxane

Table 3. 1. Comparison of the growth inhibitory effects of the new analogs on different breast cancer cell lines

Entry	IC_{50}(μM) (SKBR-3)	IC_{50}(μM) (MDA-231)	IC_{50}(μM) (MCF-7)	Selectivity MDA231/SKBR-3	Selectivity MCF-7/SKBR-3
1	4.03±2.47	7.95±4.34	4.1±0.22	2.0	1.0
2	3.44±1.35	15.92±2.56	8.02±1.65	4.6	2.3
3	1.09±0.97	4.58±1.7	5.25±1.53	4.2	4.8
4	4.38±1.25	23.01±7.67	10.52±0.69	5.3	2.4
5	25.07±6.64	36.74±25.02	14.7±3.25	1.5	0.6
6	0.52±0.15	1.63±0.61	2.26±0.36	3.1	4.4
7	25.69±11.03	60.49±23.83	38.99±14.65	2.4	1.5
8	3.14±1.03	4.08±1.1	5±1.76	1.3	1.6
9	3.14±0.46	6.91±3.42	9.01±4.48	2.2	2.9
10	6.84±3.18	7.44±2.25	6.44±0.4	1.1	0.9
11	6.25±1.28	13.5±7.83	21.71±0.69	2.2	3.5
12	1.97±0.4	3.7±2.02	2.61±0.14	1.9	1.3
13	0.71±0.34	1.54±0.94	2.87±0.31	2.2	4.0
14	0.67±0.15	2.22±0.85	0.63±0.17	3.3	0.9
15	15.81±6.98	15.77±7.39	24.58±3.14	1.0	1.6

16	0.13 ±0.06	1.18 ±0.86	0.27 ±0.09	9.1	2.1
17	2.09 ±0.11	12.8 ±8.98	3.38 ±0.62	6.1	1.6
18	4.17 ±0.78	10.79 ±1.36	4.91 ±0.4	2.6	1.2
19	3.01 ±0.49	6.63 ±0.62	4.44 ±0.71	2.2	1.5
20	15.74 ±5.35	48.88 ±15.8	11.9 ±1.17	3.1	0.8
21	15.05 ±3.89	10.29 ±0.72	9.7 ±2.16	0.7	0.6
22	2.94 ±0.75	6.5 ±0.77	3.72 ±0.6	2.2	1.3
23	11.22 ±1.16	20.99 ±0.81	10.18 ±0.41	1.9	0.9

3.2.2 Compounds 16 and 17 down-regulate HER2 protein level

Based on the selectivity and potency, compounds 16 and 17 were selected for further investigation. JCC76 was demonstrated to be a small chaperone inhibitor which also selectively inhibited SKBR-3 cell growth. As a client protein of the small chaperones, we hypothesize that JCC76 may be able to increase the degradation of HER2 via the inhibition of small chaperone protein. Previously, we demonstrated that small chaperone inhibitors could induce the degradation of the client proteins of the chaperones. SKBR-3 cells were treated with JCC76 and compounds 16 and 17 for 48 h, and the Her2 level was determined by western blot assay. As exhibited in Figure 3.4,

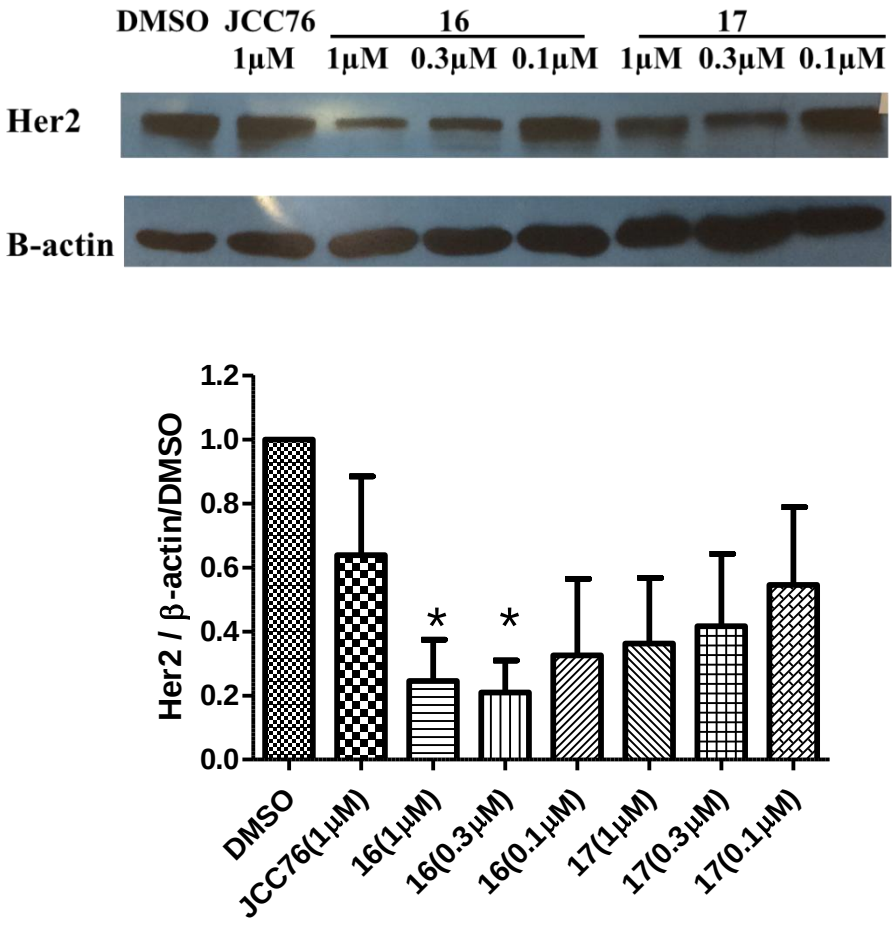

Figure 3.4 Effect of compounds 16 and 17 on Her2 protein.

SKBR-3 cells were treated with DMSO, JCC76 (1μM), compounds 16 (0.1, 0.3, 1μM) and 17 (0.1, 0.3, 1μM) for 48 h. Level of Her2 was analyzed by Western blot of cell extracts with specific antibodies. The bands of Her2 were quantified using ImageJ (NIH) and normalized to β-actin. The results are representative of three independent experiments. *$p<.05$ with unpaired t test, compound 16 vs JCC76

Her2 level was decreased by these candidates, and compounds 16 and 17 showed improved activity compared to JCC76, particularly compound 16 at 1 and 0.3 μM. The results demonstrate that the lead optimization increased the potency and selectivity of JCC76. In addition, the targeting effect of the compound is significantly increased as well.

SKBR-3 cells were treated with DMSO, JCC76 (1 μM), compound 16 (0.1, 0.3, 1 μM) and 17(0.1, 0.3, 1 μM) for 48h. The level of HER2 was analyzed by Western blot of cell extracts with specific antibody as described in experimental section. The bands of HER2 were quantified using ImageJ (NIH) and normalized to β-actin. The results are representative of three independent experiments. * $p<0.05$ with unpaired *t* test, compound 16 vs JCC76.

3.2.3 Compounds 16 and 17 slightly inhibit small chaperones

To examine if the new compounds could interfere with the chaperone function of small chaperone proteins, an *in vitro* chaperone assay was performed. As indicated in Figure 3, compounds 16 and 17 inhibited the protective function of small chaperone, α-crystalline, against DTT induced insulin denaturation and aggregation. The results demonstrate that the new analogs retained the chaperone inhibition property of the lead

compound. It has been reported that HER2 protein is a client protein of small chaperone protein HSP27, and inhibition of the small chaperone could induce HER2 degradation. Our new analogs showed inhibitory activity here. However, it is still unclear if the chaperone inhibition was the only mechanism for the decreased HER2 in SKBR-3 breast cancer cells. Further investigation is needed to look for other possible mechanisms.

The kinetics of the DTT-induced insulin aggregation was monitored in the absence of a chaperone protein, or in the presence of a chaperone protein without or with compounds. The mixture of insulin and DTT with or without other components in the assay buffer was incubated for 45min at 37 ℃ and the absorbance at 400 nm was measured. The compounds at this concentration did not interfere with DTT and insulin interaction. The results are representative of three independent experiments.

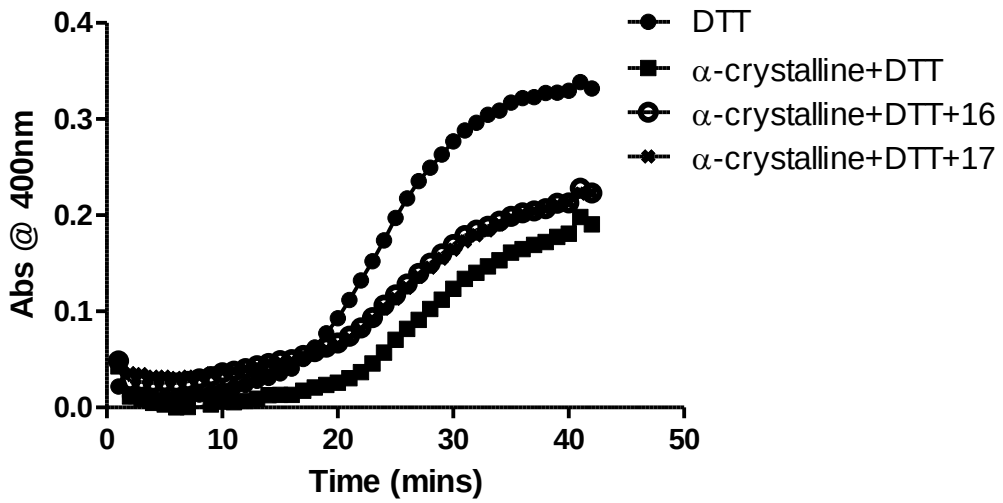

Figure 3.5 α-Crystalline lost the activity to prevent DTT induced insulin aggregation in the presence of compounds 16 (10μM) and compound 17 (10μM).

3.3 CONCLUSION

We lead optimized JCC76 to improve the selectivity and potency of the compound to inhibit HER2 over-expressed breast cancer cell growth. By flipping the sulfonamide moiety of JCC76, we generated new analogs with better ligand efficiency, potency, and selectivity against SKBR-3 cells. Two compounds, 16 and 17, decreased the HER2 protein level in SKBR-3 cells, which is speculated to be one of the main mechanisms of the selectivity and potency of the compounds. In addition, the compounds inhibited the small chaperone, α-crystalline, suggesting that they are potential small chaperone inhibitors.

3.4. EXPERIMENTAL

3.4.1. Chemistry

3.4.1.1 Synthesis of the new analogs(AZ)

Chemicals were commercially available and used as received without further purification. Moisture sensitive reactions were carried out under a dry argon atmosphere in flame-dried glassware. Thin-layer chromatography was performed on silica gel TLC plates with fluorescence indicator 254 nm (Fluka). Flash column chromatography was

performed using silica gel 60Å (BDH, 40-63 μM). Mass spectra were obtained on the ABI QStar Electrospray mass spectrometer at Cleveland State University MS facility Center. All the NMR spectra were recorded on a Bruker 400 MHz (^{13}C NMR at 100 MHz) using DMSO-d_6 as solvent. Chemical shifts (δ) for ^{1}H NMR spectra were reported in parts per million to residual solvent protons. Reversed-phase HPLC analysis of compounds was conducted on a Beckman HPLC system with an Auto Sampler. The chromatographic separation was performed on a C18 column (2.0 mm × 150 mm, 5 μm) from Phenomenex (Torrance, CA). The mobile phase of 80% acetonitrile and 20% water was employed for isocratic elution with a flow rate of 0.2 mL/min. The injection volume was 20 μL and the UV detector was set up at 260 nm.

The reaction procedure is illustrated in Schemes 1 and 2. Most of the steps follow the general methods described in our previous studies. Only the de-methylation is new and the procedure is described here.

To de-methylate the methoxy group, a solution of 2-methoxy- 4-nitrobenzene sulfonamide (2.32 g, 10.0 mmol) in CH_2Cl_2 (30 mL) was cooled to -20 ℃, and boron tri-bromide (6.01 g, 12.0 mmol) was added. The mixture was allowed to warm to room temperature over a period of 4 h and was then cooled to -20 ℃; methanol (30 mL) was added, and the solution was concentrated. The solid residue was washed with ethyl acetate to obtain 2-hydroxy-4-nitrobenzenesulfonamide.

The synthesis of the 2, 5-dimenthoxy benzyl intermediate and 2, 5-dimethyl benzyl

intermediate, the reduction of the nitro group, and the following benzamide construction are same to our previous published methods. The yield of the last step and the final compound characterization are described below.

3.4.1.2 Structural characterization of 23 compounds of the new analogs(AZ)

◆ **N-(3-((2,5-dimethoxybenzyl)oxy)-4-sulfamoylphenyl)-3-methoxybenzamide (1)**

3-methoxybenzoyl chloride was used, white solid, yield 71.7%. 1H-NMR (400MHz, DMSO-d6) δ 10.645 (1H,s), 7.810 (1H,s), 7.744 (1H,d), 7.540 (2H,t), 7.500 (1H,s), 7.464 (1H,d), 7.269 (1H,d), 7.197 (1H,d), 7.000 (1H,s), 6.929 (2H,s), 6.871 (1H,m), 5.249 (2H,s), 3.855 (3H,s), 3.817 (3H,s), 3.710 (3H,s); 13C-NMR (100MHz, DMSO-d6) δ 166.109， 159.701， 155.525， 153.728， 150.845，144.441， 136.296， 130.127， 128.744， 126.838， 125.462， 120.401， 118.101，114.720， 114.035， 113.569， 112.190， 111.596， 105.144, 65.555， 56.288， 55.866， 55.807; DUIS-MS calculated for $C_{23}H_{24}N_2O_7S$, [M-H]-: 471.14, found 471.0; Purity: 99.8%.

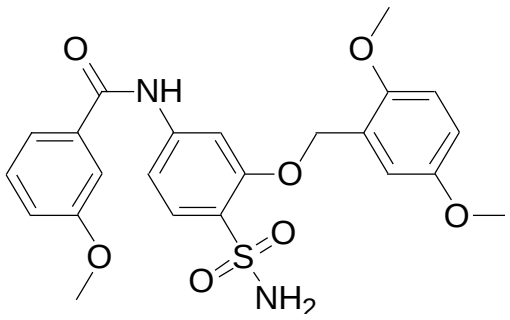

Figure 3.6 The Chemical construction of N-(3-((2,5-dimethoxybenzyl) oxy)-4-sulfamoylphenyl)-3-methoxybenzamide

◆ **N-(3-((2,5-dimethoxybenzyl)oxy)-4-sulfamoylphenyl)-3-methylbenzamide(2)**

3-methylbenzoyl chloride was used, white solid, yield 36.7%. 1H-NMR (400MHz, DMSO-d6) δ 10.462 (1H,s), 7.798 (2H,d), 7.744 (2H,d), 7.552 (1H,s), 7.439 (2H,d) 7.272 (1H,d), 7.000 (1H,d), 6.928 (2H,s), 6.871 (1H,m), 5.251 (2H,s), 3.818 (3H,s), 3.711 (3H,s), 2.418 (3H,s); 13C-NMR (100MHz, DMSO-d6) δ 166.502, 155.530, 153.729, 150.842, 144.556, 138.282, 134.925, 132.998, 128.849, 128.752, 128.639, 126.743, 125.478, 125.402, 114.716, 114.019, 112.194, 111.489, 105.047, 65.557, 56.294, 55.811, 21.424; DUIS-MS calculated for $C_{23}H_{24}N_2O_6S$, [M-H]-: 455.15, found 455.0; Purity: 99.7%

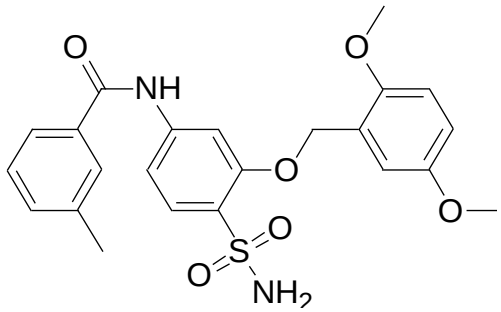

Figure 3.7 The Chemical construction of N-(3-((2,5-dimethoxy benzyl)oxy)-4-sulfamoylphenyl)-3-methylbenzamide

◆ **N-(3-((2,5-dimethoxybenzyl)oxy)-4-sulfamoylphenyl)-3-iodobenzamide (3)**

3-iodobenzoyl chloride was used, white solid, yield 46.3%. 1H-NMR (400MHz, DMSO-d6) δ 10.555 (1H,s), 8.309 (1H,s) 7.976 (2H,t), 7.751 (2H,d), 7.530 (1H,d), 7.366 (1H,t), 7.263 (1H,d), 7.000 (1H,d), 6.944 (2H,s), 6.870 (1H,m), 5.251 (2H,s), 3.817 (3H,s), 3.781 (3H,s); 13C-NMR (100MHz, DMSO-d6) δ 164.838, 155.521, 153.729, 150.826, 144.222, 140.932, 136.909, 136.451, 131.113, 128.792, 127.769, 127.026, 125.446, 114.679, 114.022, 112.188, 111.639, 105.181, 95.192, 65.564, 56.293, 55.811; DUIS-MS calculated for $C_{22}H_{21}IN_2O_6S$, [M-H]-: 567.03, found 566.9; Purity: 93.7%

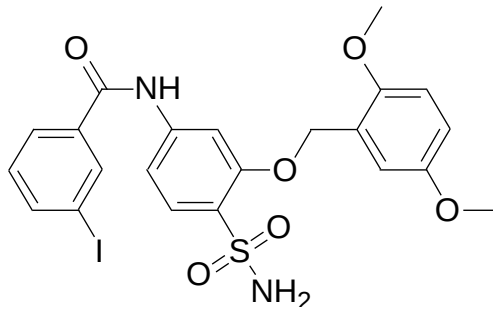

Figure 3.8 The Chemical construction of N-(3-((2,5-dimethoxy benzyl)oxy)-4-sulfamoylphenyl)-3-iodobenzamide

◆ **3-bromo-N-(3-((2,5-dimethoxybenzyl)oxy)-4-sulfamoylphenyl)benzamide(4)**

3-bromobenzoyl chloride was used, white solid, yield 33.2%. 1H-NMR (400MHz, DMSO-d6) δ 10.581 (1H,s), 8.159 (1H,s), 7.969 (1H,d), 7.833 (1H,d), 7.758 (2H,d), 7.540 (2H,d), 7.264 (1H,s), 7.002 (1H,d), 6.949 (2H,s), 6.871 (1H,m), 5.255 (2H,s), 3.819 (3H,s), 3.710 (3H,s); 13C-NMR (100MHz, DMSO-d6) δ 164.828, 155.520, 153.723, 150.813, 144.187, 137.056, 135.136, 131.213, 130.771, 128.809, 127.466, 127.062, 125.437, 122.185, 114.657, 113.999, 112.171, 111.642, 105.177, 65.549, 56.283, 55.801;DUIS-MS calculated for $C_{22}H_{21}BrN_2O_6S$, [M-H]-: 519.04, found 520.9; Purity: 99.5%

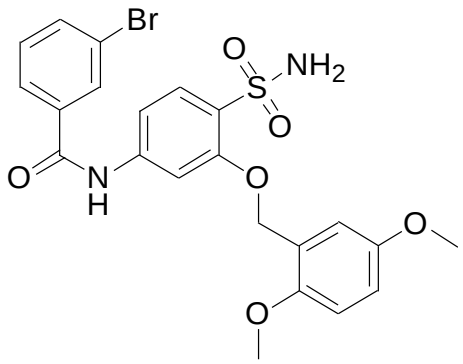

Figure 3.9 The Chemical construction of 3-bromo-N-(3-((2,5-dimethoxybenzyl)oxy)-4-sulfamoylphenyl)benzamide

◆ **3-cyano-N-(3-((2,5-dimethoxybenzyl)oxy)-4-sulfamoylphenyl)benzamide (5)**

3-cyanobenzoyl chloride was used, white solid, yield 52.4 %. 1H-NMR (400MHz, DMSO-d6) 10.663 (1H,s), 8.417 (1H,s), 8.259 (1H,d), 8.104 (1H,s), 7.779 (1H,s), 7.758 (2H,s), 7.528 (1H,s), 7.253 (1H,s), 7.001 (1H,d), 6.980 (2H,s), 6.870 (1H,d), 5.259 (2H,s), 3.816 (3H,s), 3.703 (3H,s); 13C-NMR (100MHz, DMSO-d6) δ 164.542, 155.533, 153.709, 150.790, 144.044, 135.930, 135.797, 133.095, 131.862, 130.393, 128.877, 127.184, 125.405, 118.728, 114.601, 113.959, 112.156, 112.047, 111.632, 105.127, 65.525, 56.280, 55.790; DUIS-MS calculated for $C_{23}H_{21}N_3O_6S$, [M-H]-: 466.13, found 466.0; Purity: 99.9%

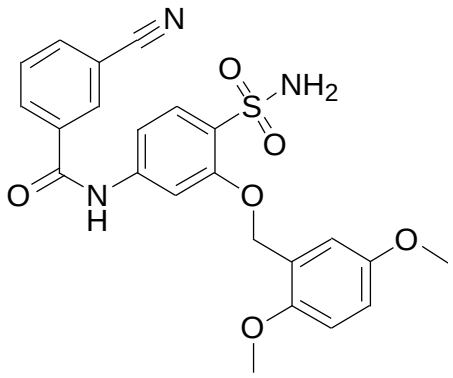

Figure 3.10 The Chemical construction of 3-cyano-N-(3-((2,5-dimethoxybenzyl)oxy)-4-sulfamoylphenyl)benzamide

◆ **N-(3-((2,5-dimethoxybenzyl)oxy)-4-sulfamoylphenyl)-4-iodobenzamide (6)**

4-iodobenzoyl chloride was used, white solid, yield %. 1H-NMR (400MHz, DMSO-d6) 10.539 (1H,s), 7.950 (1H,d), 7.747 (2H,s), 7.727 (1H,s), 7.701 (1H,d), 7.523 (1H,d), 7.250 (1H,s), 6.997 (1H,d), 6.952 (2H,s), 6.876 (1H,d), 5.243 (2H,s), 3.811(3H,s), 3.700 (3H,s); 13C-NMR (100MHz, DMSO-d6) δ 165.715, 155.517, 153.718, 150.848, 144.280, 137.835, 137.476 , 134.251, 131.923, 130.135, 128.774, 126.937, 125.433, 114.705, 114.026, 112.210, 111.612, 105.158, 100.257, 65.556, 56.296, 55.807; DUIS-MS calculated for $C_{22}H_{21}IN_2O_6S$, [M-H]-: 567.03, found 567.0; Purity: 94.2%

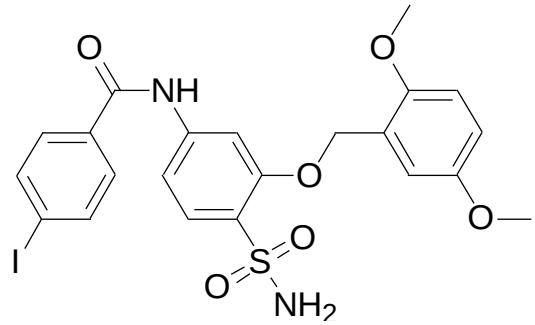

Figure 3.11 The Chemical construction of N-(3-((2,5-dimethoxy benzyl)oxy)-4-sulfamoylphenyl)-4-iodobenzamide

◆ **N-(3-((2,5-dimethoxybenzyl)oxy)-4-sulfamoylphenyl)-2,4-bis(trifluoromethyl)benzamide(7)**

2,4-bis(trifluoromethyl)benzoyl chloride was used, white solid, yield 24.3%. 1H-NMR (400MHz, DMSO-d6) 10.992 (1H,s), 8.246 (2H,d), 8.018 (1H,d), 7.763 (1H,d), 7.630(1H,s), 7.356 (1H,s), 7.235 (1H,s), 6.986 (3H,s) 6.872(1H,d), 5.248 (2H,s), 3.793 (3H,s), 3.698 (3H,s); 13C-NMR (100MHz, DMSO-d6) δ 165.128, 155.658, 153.679, 150.928, 143.607, 139.659, 131.295, 130.973, 130.508, 129.058, 127.449, 125.250, 124.900, 124.686, 124.005, 122.187, 121.960, 114.806, 114.153, 112.230, 111.115, 104.628, 65.535, 56.266, 55.785; DUIS-MS calculated for $C_{24}H_{20}F_6N_2O_6S$, [M-H]-: 577.10, found 576.9; Purity: 99.5%

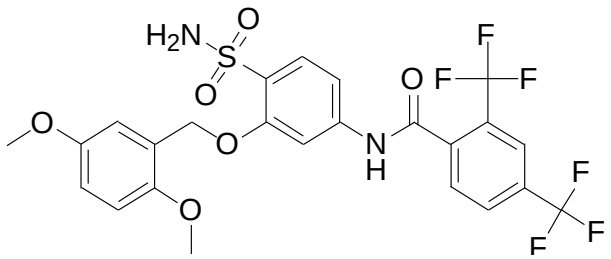

Figure 3.12 The Chemical construction of N-(3-((2,5-dimethoxy benzyl)oxy)-4-sulfamoylphenyl)-2,4-bis(trifluoromethyl)benzamide

◆ **N-(3-((2,5-dimethoxybenzyl)oxy)-4-sulfamoylphenyl)-4-(trifluoromethoxy)benzamide (8)**

4-trifluoromethoxybenzoyl chloride was used, white solid, yield 61.3%. 1H-NMR (400MHz, DMSO-d6) 10.593 (1H,s), 8.092 (2H,d), 7.772 (1H,s), 7.751 (1H,d), 7.555 (2H,d), 7.518 (1H,d), 7.251 (1H,s), 7.000 (1H,d), 6.944 (2H,s), 6.874 (1H,m), 5.253 (2H,s), 3.815 (3H,s), 3.704 (3H,s); 13C-NMR (100MHz, DMSO-d6) δ 165.213, 155.514, 153.701, 151.161, 150.813, 144.258, 134.033, 130.673, 128.813, 126.981, 125.415, 121.226, 114.647, 113.971, 112.161, 111.570, 105.0855, 65.510, 56.274, 55.786; DUIS-MS calculated for $C_{23}H_{21}F_3N_2O_7S$, [M-H]-: 525.11, found 525.0; Purity: 99.9%

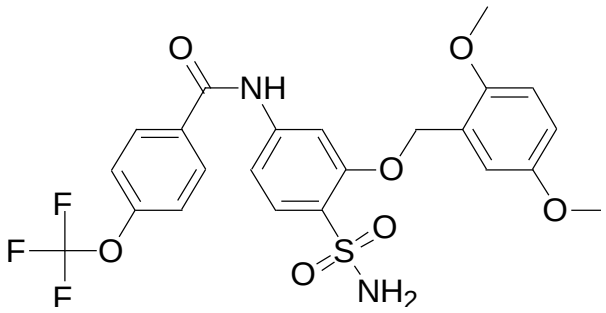

Figure 3.13 The Chemical construction of N-(3-((2,5-dimethoxy benzyl)oxy)-4-sulfamoylphenyl)-4-(trifluoromethoxy)benzamide

◆ **3-chloro-N-(3-((2,5-dimethoxybenzyl)oxy)-4-sulfamoylphenyl)benzamide (9)**

3-chlorobenzoyl chloride was used, white solid, yield 52.0 %. 1H-NMR (400MHz, DMSO-d6) 8.031 (1H,s), 7.936 (1H,d), 7.768 (2H,d), 7.734 (1H,d), 7.605 (1H,d), 7.549 (1H,d), 7.271 (1H,s), 7.000 (1H,d), 6.877 (2H,m), 5.262 (2H,s), 3.821 (3H,s), 3.713 (3H,s); 13C-NMR (100MHz, DMSO-d6) δ 164.924, 155.521, 153.716, 150.812, 144.202, 136.863, 133.741, 132.236, 130.963, 128.815, 127.953, 127.086, 127.050, , 125.429, 114.660, 113.979, 112.151, 111.639, 105.168, 65.549, 56.268, 55.791; DUIS-MS calculated for $C_{22}H_{21}ClN_2O_6S$, [M-H]-: 475.09, found 475.0; Purity: 99.6%

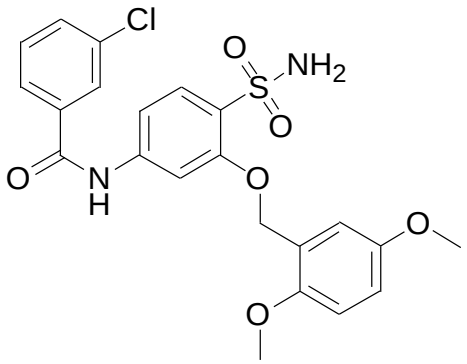

Figure 3.14 The Chemical construction of 3-chloro-N-(3-((2,5-dimethoxybenzyl)oxy)-4-sulfamoylphenyl)benzamide

◆ **N-(3-((2,5-dimethoxybenzyl)oxy)-4-sulfamoylphenyl)-4-ethylbenzamide(10)**

4-ethylbenzoyl chloride was used, white solid, yield 56.0 %. 1H-NMR (400MHz, DMSO-d6) 10.417 (1H,s), 7.98 (2H,d), 7.810 (1H,s), 7.734 (1H,d), 7.543 (1H,d), 7.394 (2H,d), 7.267 (1H,s), 7.000 (1H,d), 6.922 (2H,s), 6.870 (1H,d), 5.247 (2H,s), 3.817 (3H,s), 3.709 (3H,s), 2.705(2H,m), 1.228 (3H,t); 13C-NMR (100MHz, DMSO-d6) δ 166.255, 155.523, 153.725, 150.841, 148.675, 144.618, 132.335, 128.736, 128.355, 128.303, 126.665, 125.479, 114.711, 114.020, 112.183, 111.458, 105.006, 65.538, 56.286, 55.806, 28.555, 15.799; DUIS-MS calculated for $C_{24}H_{26}N_2O_6S$, [M-H]-: 469.16, found 468.9;Purity: 99.9%.

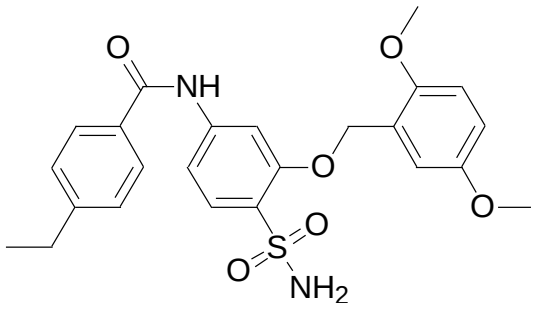

Figure 3.15 The Chemical construction of N-(3-((2,5-dimethoxybenzyl)oxy)-4-sulfamoylphenyl)-4-ethylbenzamide

◆ **4-cyano-N-(3-((2,5-dimethoxybenzyl)oxy)-4-sulfamoylphenyl)benzamide (11)**

4-cyanobenzoyl chloride was used, white solid, yield 31.3 %. 1H-NMR (400MHz, DMSO-d6) δ 10.720 (1H,s), 8.114 (2H,d), 8.044 (2H,d), 7.772 (1H,s), 7.760(1H,d), 7.246 (1H,d), 6.995 (1H,d), 6.967(2H,s), 6.866 (1H,m), 5.255 (2H,s), 3.812 (3H,s), 3.701 (3H,s); 13C-NMR (100MHz, DMSO-d6) δ 165.041, 155.544, 153.739, 150.843, 144.019, 138.922, 132.991, 129.092, 128.842, 127.273, 125.426, 118.705, 114.661, 114.034, 112.215, 111.715, 105.254, 65.564, 56.306, 55.809; DUIS-MS calculated for $C_{23}H_{21}N_3O_6S$, [M-H]-: 466.13, found 466.0; Purity: 91.3%.

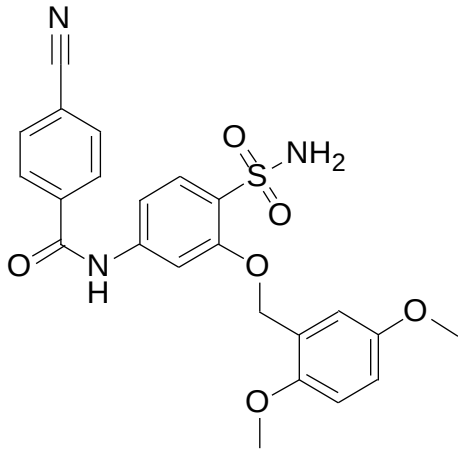

Figure 3.16 The Chemical construction of 4-cyano-N-(3-((2,5-dimethoxybenzyl)oxy)-4-sulfamoylphenyl)benzamide

- **4-chloro-N-(3-((2,5-dimethoxybenzyl)oxy)-4-sulfamoylphenyl)-3-nitrobenzamide (12)**

4-chloro-3-nitrobenzoyl chloride was used, white solid, yield 52.1 %. 1H-NMR (400MHz, DMSO-d6) δ 10.761 (1H,s), 8.642 (1H,s), 8.266 (1H,d), 7.995 (1H,s), 7.778 (1H,s), 7.737 (1H,s), 7.516 (1H,d), 7.250 (1H,s), 7.000 (1H,d), 6.973 (2H,s), 6.871 (1H,d), 5.262 (2H,s), 3.817 (3H,s), 3.704 (3H,s); 13C-NMR (100MHz, DMSO-d6) δ 163.368, 155.543, 153.728, 150.805, 147.838, 143.819, 134.904, 133.415, 132.510, 128.895, 127.392, 125.409, 114.615, 113.997, 112.191, 111.798, 105.299, 65.561, 60.226, 56.298, 55.800; DUIS-MS calculated for $C_{22}H_{20}ClN_3O_8S$, [M-H]-: 520.08, found 520.0; Purity: 97.6%

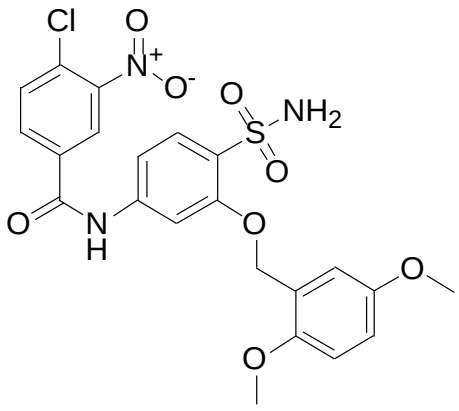

Figure 3.17 The Chemical construction of 4-chloro-N-(3-((2,5-dimethoxybenzyl)oxy)-4-sulfamoylphenyl)-3-nitrobenzamide

◆ **N-(3-((2,5-dimethoxybenzyl)oxy)-4-sulfamoylphenyl)-3-ethoxybenzamide(13)**

3-ethoxybenzoyl chloride was used, white solid, yield 52.5 %. 1H-NMR (400MHz, DMSO-d6) δ 10.445 (1H,s), 7.816 (1H,s), 7.749 (1H,d), 7.545 (2H,d), 7.500 (1H,s), 7.460 (1H,t), 7.276 (1H,s), 7.181 (1H,d), 7.000 (1H,d), 6.929 (2H,s), 6.875 (1H,d), 5.254 (2H,s), 4.123 (2H,m), 3.819 (3H,s), 3.714 (3H,s), 1.375 (3H,t);13C-NMR (100MHz, DMSO-d6) δ 166.128, 158.944, 155.507, 153.705, 150.869, 144.432, 136.199, 130.163, 128.718, 126.789, 125.424, 120.318, 118.437, 114.766, 114.070, 114.048, 112.209, 111.604, 105.155, 65.563, 63.8435, 56.282, 55.799, 15.049; DUIS-MS calculated for $C_{24}H_{26}N_2O_7S$, [M-H]-: 485.16, found 485.1; Purity: 98.6%

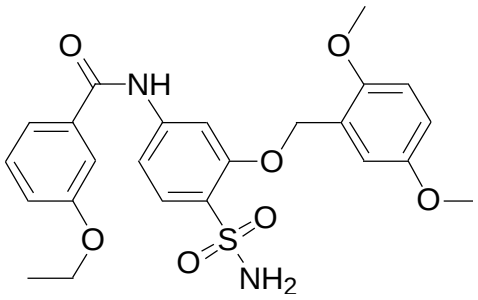

Figure 3.18 The Chemical construction of N-(3-((2,5-dimethoxybenzyl)oxy)-4-sulfamoylphenyl)-3-ethoxybenzamide

◆ **4-bromo-N-(3-((2,5-dimethoxybenzyl)oxy)-4-sulfamoylphenyl)benzamide(14)**

4-bromobenzoyl chloride was used, white solid, yield 53.3 %. 1H-NMR (400MHz, DMSO-d6) δ 10.563 (1H,s), 7.922 (2H,d), 7.788 (1H,s), 7.770 (2H,s), 7.743 (1H,d), 7.525 (1H,d), 7.251 (1H,s), 7. 000(1H,d), 6.957 (2H,s), 6.867 (1H,d), 5.246 (2H,s), 3.8115 (3H,s), 3.700 (3H,s); 13C-NMR (100MHz, DMSO-d6) δ 165.412, 155.505, 153.704, 150.803, 144.274, 133.948, 131.978, 130.360, 128.798, 126.945, 126.263, 125.425, 114.640, 113.968, 112.156, 111.584, 105.110, 65.516, 56.273, 55.790; DUIS-MS calculated for $C_{22}H_{21}BrN_2O_6S$, [M+H]+: 521.04, found 520.9; Purity: 98.7%

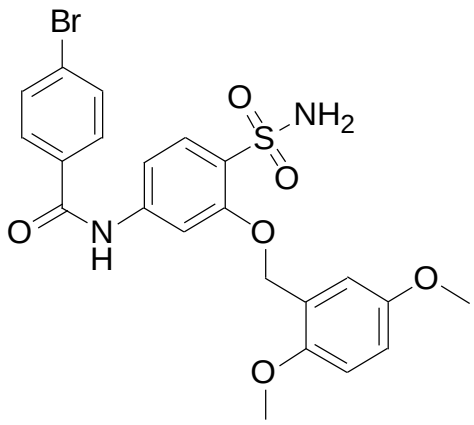

Figure 3.19 The Chemical construction of 4-bromo-N-(3-((2,5-dimethoxybenzyl)oxy)-4-sulfamoylphenyl)benzamide

- **N-(3-((2,5-dimethoxybenzyl)oxy)-4-sulfamoylphenyl)-3,5-bis(trifluoromethyl) benzamide(15)**

3,5-bistrifluoromethylbenzoyl chloride was used, white solid, yield 30.0 %. 1H-NMR (400MHz, DMSO-d6) δ 10.875 (1H,s), 8.612 (2H,s), 8.394 (1H,s), 7.802 (1H,d), 7.7571 (1H,s), 7.264 (1H,s), 7.000 (1H,d), 6.986 (2H,s), 6.871 (1H,m), 5.275 (2H,s), 3.818 (3H,s), 3.709 (3H,s); 13C-NMR (100MHz, DMSO-d6) δ 163.489, 155.557, 153.723, 150.791, 143.758, 137.180, 131.158, 130.827, 129.130, 128.902, 127.482, 125.376, 124.909, 122.195, 114.608, 113.990, 112.168, 111.971, 105.422, 65.587, 56.259, 55.776; DUIS-MS calculated for $C_{24}H_{20}F_6N_2O_6S$, [M-H]-: 577.10, found 577.0; Purity: 97.6%.

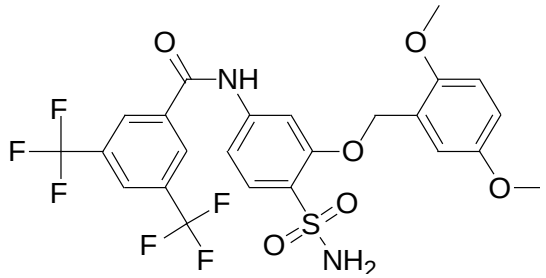

Figure 3.20 The Chemical construction of N-(3-((2,5-dimethoxybenzyl)oxy)-4-sulfamoylphenyl)-3,5-bis(trifluoromethyl)benzamide

◆ **N-(3-((2,5-dimethoxybenzyl)oxy)-4-sulfamoylphenyl)-1-naphthamide(16)**

1-naphthoyl chloride was used, white solid, yield 52.8 %. 1H-NMR (400MHz, DMSO-d6) δ 8.606 (1H,s), 8.110 (1H,d), 8.073 (1H,s), 8.040 (2H,s), 7.845 (1H,s), 7.768 (1H,s), 7.663 (2H,m), 7.280 (1H,s), 7.007 (1H,d), 6.877 (1H,d), 5.2720 (2H,s), 3.825 (3H,s), 3.714 (3H,s); 13C-NMR (100MHz, DMSO-d6) δ 166.466, 155.557, 153.721, 150.835 144.635, 134.893, 132.490, 132.208, 129.499, 128.802, 128.734, 128.596, 128.520, 128.180, 127.428, 126.778, 125.479, 124.869, 114.713, 113.988, 112.169, 111.562, 105.108, 65.578, 56.282, 55.806; DUIS-MS calculated for $C_{26}H_{24}N_2O_6S$, [M-H]-: 491.15, found 491.1;Purity: 98.7%

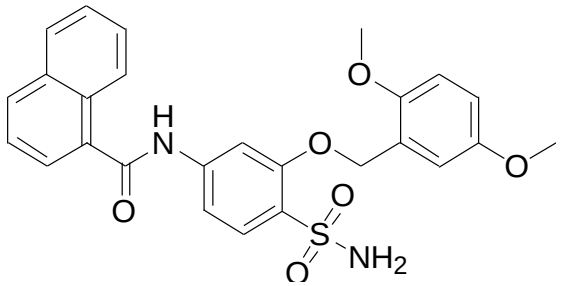

Figure 3.21 The Chemical construction of N-(3-((2,5-dimethoxy benzyl)oxy)-4-sulfamoylphenyl)-1-naphthamide

◆ **N-(3-((2,5-dimethoxybenzyl)oxy)-4-sulfamoylphenyl)-4-methoxybenzamide(17)**

4-methoxybenzoyl chloride was used, white solid, yield 38.6 %. 1H-NMR (400MHz, DMSO-d6) 10.468 (1H,s), 7.807 (1H,s), 7.742 (1H,d), 7.520 (4H,m), 7.264(1H,s), 7.200(1H,d), 7.003 (1H,d), 6.932 (2H,s), 6.870 (1H,m), 5.248 (2H,s), 3.856 (3H,s), 3.817 (3H,s), 3.711 (3H,s); 13C-NMR (100MHz, DMSO-d6) δ 166.116, 159.700, 155.520, 153.721, 150.849, 144.431, 136.287, 130.136, 128.739, 126.831, 125.453, 120.401, 118.111, 114.726, 114.041, 113.555, 112.199, 111.603, 105.145, 65.553, 56.290, 55.867, 55.807; DUIS-MS calculated for $C_{23}H_{24}N_2O_7S$, [M-H]-: 471.14, found 471.0; Purity: 98.1%

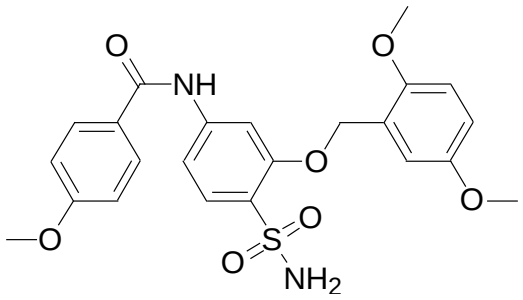

Figure 3.22 The Chemical construction of N-(3-((2,5-dimethoxy benzyl)oxy)-4-sulfamoylphenyl)-4-methoxybenzamide

◆ **N-(3-((2,5-dimethoxybenzyl)oxy)-4-sulfamoylphenyl)cyclohexanecarboxamide(18)**

Cyclohexanecarbonyl chloride was used, white solid, yield 77.0 %. 1H-NMR (400MHz, DMSO-d6) δ 10.149 (1H,s), 7.660 (2H,d), 7.246 (2H,m), 6.992 (2H,d), 6.864 (2H,m), 5.200 (2H,s), 3.807 (3H,s), 3.701 (3H,s), 2.341 (1H,t), 1.785 (4H,t), 1.658 (1H,d), 1.3939 (32H,m), 1.228 (3H,m); 13C-NMR (100MHz, DMSO-d6) δ 175.370, 155.614, 153.704, 150.867, 144.766, 128.774, 126.128, 125.463, 114.732, 114.069, 112.199, 110.359, 103.865, 65.482, 56.298, 55.802, 45.4049, 29.484, 25.629;DUIS-MS calculated for $C_{22}H_{28}N_2O_6S$, [M-H]-: 447.18, found 447.0; Purity: 99.0%

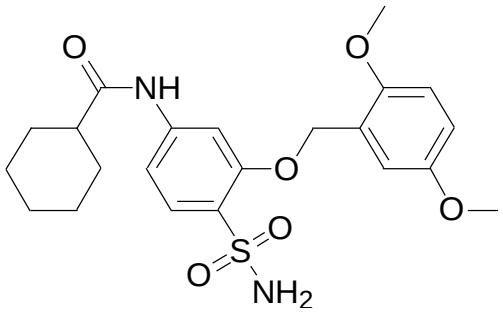

Figure 3.23 The Chemical construction of N-(3-((2,5-dimethoxy benzyl)oxy)-4-sulfamoylphenyl)cyclohexanecarboxamide

◆ **N-(3-((2,5-dimethylbenzyl)oxy)-4-sulfamoylphenyl)-4-iodobenzamide (19)**

4-iodobenzoyl chloride was used, white solid, yield 58.3%. 1H-NMR (400MHz, DMSO-d6) 10.547 (1H,s), 7.939 (2H,d), 7.776 (1H,s), 7.731 (3H,d), 7.461 (1H,d), 7.362 (1H,s), 7.076 (2H,m), 6.963 (2H,s), 5.241 (2H,s), 2.333 (3H,s), 2.251 (3H,s); 13C-NMR (100MHz, DMSO-d6) δ 165.846, 155.849, 144.190, 137.844, 135.154, 134.473, 134.289, 133.421, 131.549, 130.515, 130.143, 129.074, 128.937, 126.930, 111.492, 105.264, 100.226, 68.702, 21.151, 18.504; DUIS-MS calculated for $C_{22}H_{21}IN_2O_4S$, [M-H]-: 535.04, found 534.9; Purity: 96.7%

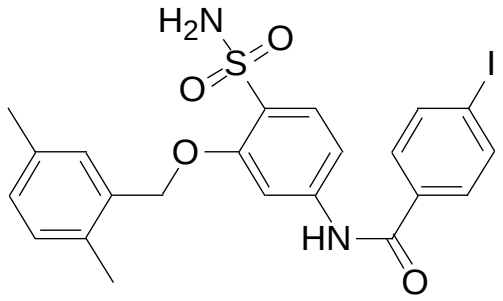

Figure 3.24 The Chemical construction of N-(3-((2,5-dimethylbenzyl)oxy)-4-sulfamoylphenyl)-4-iodobenzamide

◆ **N-(3-((2,5-dimethylbenzyl)oxy)-4-sulfamoylphenyl)-3-iodobenzamide(20)**

3-iodobenzoyl chloride was used, white solid, yield 55.8%.1H-NMR (400MHz, DMSO-d6) 10.566 (1H,s), 8.288 (1H,s), 7.975 (2H,t), 7.779 (1H,s), 7.745 (1H,d), 7.477 (1H,d), 7.380 (1H,s), 7.084 (2H,m), 6.942 (2H,s), 5.248 (2H,s), 2.343 (3H,s), 2.264 (3H,s); 13C-NMR (100MHz, DMSO-d6) δ 164.960, 155.859, 144.124, 136.953, 136.440, 134.484, 131.148, 130.515, 129.117, 128.944, 127.757, 127.045, 111.550, 105.342, 95.157, 68.749, 21.151, 18.510; DUIS-MS calculated for $C_{22}H_{21}IN_2O_4S$, [M-H]-: 535.04, found 534.9; Purity: 99.8%

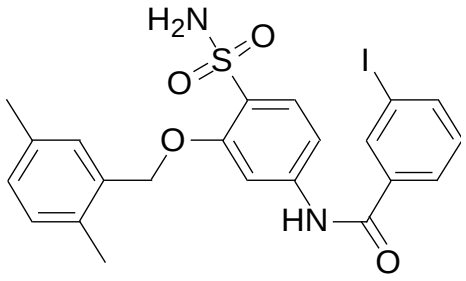

Figure 3.25 The Chemicalstruction of N-(3-((2,5-dimethylbenzyl)oxy)-4-sulfamoylphenyl)-3-iodobenzamide

◆ **N-(3-((2,5-dimethylbenzyl)oxy)-4-sulfamoylphenyl)cyclohexanecarboxamide (21)**

Cyclohexanecarbonyl chloride was used, white solid, yield 53.7%. 1H-NMR (400MHz, DMSO-d6) 10.097 (1H,s), 7.659 (2H,d), 7.352 (1H,s), 7.227 (1H,d), 7.110 (1H,d), 7.075 (2H,m), 6.872 (2H,s), 5.205 (2H,s), 2.327 (3H,s), 2.252 (3H,s), 1.778 (4H,t), 1.654 (1H,d), 1.399 (2H,m), 1.239 (3H,m); 13C-NMR (100MHz, DMSO-d6) δ 175.386, 155.934, 144.688, 135.088, 134.522, 133.429, 130.477, 129.149, 128.952, 128.881, 126.086, 110.156, 103.935, 68.587, 45.421, 29.485, 25.815, 25.622, 21.143, 18.512. UIS-MS calculated for $C_{22}H_{28}N_2O_4S$, [M-H]-: 415.19, found 415.6; Purity: 95.3%

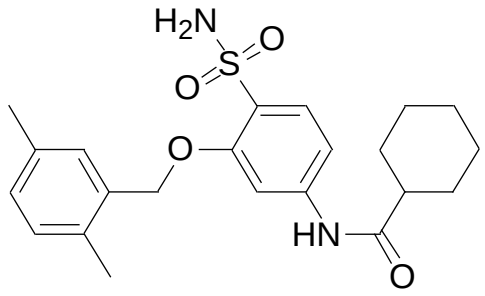

Figure 3.26 The Chemical construction of N-(3-((2,5-dimethylbenzyl)oxy)-4-sulfamoylphenyl)cyclohexanecarboxamide

◆ **N-(3-((2,5-dimethylbenzyl)oxy)-4-sulfamoylphenyl)-4-methoxybenzamide(22)**

4-methoxybenzoyl chloride was used, white solid, yield 64.2%.1H-NMR (400MHz, DMSO-d6) 10.347 (1H,s), 7.964 (2H,d), 7.818 (1H,s), 7.718 (1H,d), 7.382 (1H,s), 7.082 (4H,m), 6.9072(2H,s), 5.241(2H,s), 3.390(3H,s), 2.343 (3H,s), 2.261 (3H,s); 13C-NMR (100MHz, DMSO-d6) δ 162.679, 155.872, 144.659, 135.153, 134.543, 133.437, 130.509, 130.248, 129.149, 128.940, 128.822, 126.919, 126.546, 114.194, 111.3683, 105.1611, 68.731, 55.962, 21.151, 18.512 ; DUIS-MS calculated for $C_{23}H_{24}N_2O_5S$, [M-H]-: 439.15, found 439.0; Purity: 98.9%

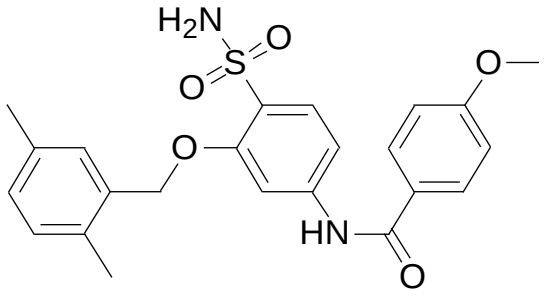

Figure 3.27 The Chemical construction of N-(3-((2,5-dimethylbenzyl)oxy)-4-sulfamoylphenyl)-4-methoxybenzamide

◆ **4-bromo-N-(3-((2,5-dimethylbenzyl)oxy)-4-sulfamoylphenyl)benzamide(23)**

4-bromobenzoyl chloride was used, white solid, yield 58.1%.1H-NMR (400MHz, DMSO-d6) δ 10.561 (1H,s), 7.921 (1H,s), 7.901 (1H,s), 7.788 (2H,s), 7.767(1H,s), 7.743 (1H,d), 7.479 (1H,d), 7.378 (1H,s), 7.118 (1H,d), 7.047 (1H,d), 6.940 (2H,s), 5.248 (2H,s), 2.343(3H,s), 2.261 (3H,s); 13C-NMR (100MHz, DMSO-d6) δ 165.491, 155.862, 144.211, 135.134, 134.525, 134.021, 133.388, 131.979, 130.496, 130.373, 129.061, 128.915, 127.004, 111.485, 105.266, 68.698, 21.176, 18.527; DUIS-MS calculated for $C_{22}H_{21}BrN_2O_4S$, [M+H]+: 489.05, found 488.9; Purity: 99.4%

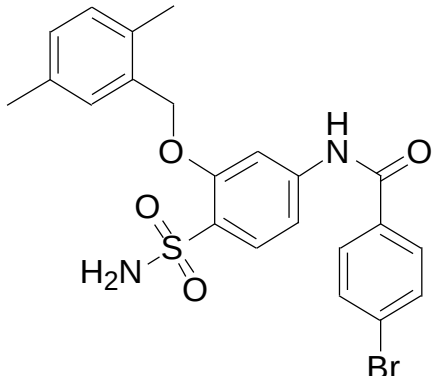

Figure 3.28 The Chemical construction of 4-bromo-N-(3-((2,5-dimethylbenzyl)oxy)-4-sulfamoylphenyl)benzamide

3.4.2. Biological studies

3.4.2.1. Cell culture.

Three breast cancer cell lines including SKBR-3, MCF-7, and MDA-MB-231 were obtained from ATCC (Rockville, MD). The cells were maintained in RPMI1640 medium supplemented with 10% fetal bovine serum (FBS), 2 mmol/L L-Glutamine, 1 mmol/L sodium pyruvate, 100 U/mL penicillin-streptomycin. FBS was heat inactivated for 30 min in a 56 ℃ water bath before use. Cell cultures were grown at 37 ℃, in a humidified atmosphere of 5% CO_2 in a VWR CO_2 incubator (Bridgeport NJ).

3.4.2.2. Cell viability analysis

The effects of the new derivatives on the viability of three breast cancer cell lines were assessed using the 3-(4,5-dimethylthiazol-2-yl)-2,5-diphenyl-2H- tetrazolium bromide assay in four replicates. Cells were grown in RPMI1640 medium in 96-well, flat-bottomed plates for 24 h, and were exposed to various concentrations of the compounds dissolved in DMSO (DMSO final concentration ≤0.1%) in media for 48 h. Controls received DMSO vehicle at a concentration equal to that in drug-treated cells. The medium was removed, replaced by 200 μL of 0.5 mg/ml of 3-(4,5-dimethylthiazol-2-yl) -2,5-diphenyl-2H- tetrazolium bromide in fresh media, and cells were incubated in the CO_2 incubator at 37 ℃ for 2 h. Supernatants were removed from the wells, and the reduced

3-(4,5-dimethylthiazol-2-yl) -2,5-diphenyl- 2H-tetrazolium bromide dye was solubilized in 200 µL/well DMSO. Absorbance at 570 nm was determined on a plate reader. Statistical and graphical information was determined using GraphPad Prism software (GraphPad Software Incorporated) and Microsoft Excel (Microsoft Corporation). IC_{50} values were determined using nonlinear regression analysis.

3.4.2.3. Western blot

SKBR-3 cells were treated with JCC76 (1 µM), compound 16 (0.1, 0.3, 1 µM) and compound 17 (0.1, 0.3, 1 µM) for 48 h. The cells were lysed, briefly sonicated, and centrifuged at 12000*g* for 10 min. 30 g of protein for each sample was boiled with 4x loading buffer for 5 minutes, electrophoresed on a 10% SDS-polyacrylamide gel, and transferred onto polyvinylidene difluoride (PVDF) membrane. The membrane was blocked for 1 hour with 5% nonfat milk in PBST and then incubated with specific primary antibody (Cell Signaling). After washing, the membrane was incubated with horseradish-conjugated secondary antibody (Cell Signaling). The bands were visualized by chemiluminescence with ECL reagent (Thermo Scientific).

3.4.2.4. Small chaperone activity assay.

Alpha-crystalline chaperone activity assay: 24 µlmg/ml insulin stock solution was added to the single well of 384 well plate, 3 µl 5mg/ml alpha-crystalline, 71 µl PBS buffer with appropriate concentration of compound dissolved inside were added as well. The mixture was thoroughly mixed and incubated at 37 ℃ for 5 min, whereupon 2 µL of 1M DTT in water was added to initiate the insulin aggregation. The absorbance (A) at 400 nm was monitored over 45min using a plate reader. A mixture of insulin in the absence or presence of alpha-crystalline with 0.1% DMSO was used as control.

3.5. ACKNOWLEDGEMENTS

This research was supported by Center for Gene Regulation in Health and Disease (GRHD) of Cleveland State University and the Summer Undergraduate Research program. Aicha Quamine was supported by a McNair scholarship. The instruments used in the study were supported by National Science Foundation Major Research Instrumentation Grants (CHE-0923398 and CHE-1126384).

3.6 REFERENCES

1. Figueroa-Magalhães, M. C.; Jelovac, D.; Connolly, R. M.; Wolff, A. C. Treatment of HER2-positive breast cancer The Breast 2014, *23*(2), 128–136.
2. Ahmed, S.; Sami, A.; Xiang, J. HER2-directed therapy: current treatment options for HER2-positive breast cancer. Breast Cancer 2015, 22 (2), 101–116.
3. Verma, S.; Miles, D.; Gianni, L.; Krop, I. E.; Welslau, M.; Baselga, J.; Pegram, M.; Oh, D.-Y.; Diéras, V.; Guardino, E.; Fang, L.; Lu, M. W.; Olsen, S.; Blackwell, K. Trastuzumab Emtansine for HER2-Positive Advanced Breast Cancer. New England Journal of Medicine 2012, 367 (19), 1783–1791.4. A.A. Onitilo, J.M. Engel, R.T. Greenlee, B.N. Mukesh, Clinical Medicine & Research 7 (2009).
4. Onitilo, A. A.; Engel, J. M.; Greenlee, R. T.; Mukesh, B. N. Breast cancer subtypes based on ER/PR and Her2 expression: comparison of clinical pathologic features and survival. Clinical Medicine & Research 2009, 7 (1-2), 4–13.
5. Loibl, S.; Gianni, L. HER2-positive breast cancer. The Lancet 2016, 389 (10087), 2415–2429.
6. Swain, S. M.; Baselga, J.; Kim, S.-B.; Ro, J.; Semiglazov, V.; Campone, M.; Ciruelos, E.; Ferrero, J.-M.; Schneeweiss, A.; Heeson, S.; Clark, E.; Ross, G.; Benyunes, M. C.; Cortés, J. Pertuzumab, Trastuzumab, and Docetaxel in HER2-Positive Metastatic Breast Cancer. New England Journal of Medicine 2015, 372 (8), 724–734.

7. Rexer, B. N.; Arteaga, C. L. Optimal targeting of HER2-PI3K signaling in breast cancer: Mechanistic insights and clinical implications. Cancer Research 2013, 73 (13), 3817–3820.
8. Ryan, Q.; Ibrahim, A.; Cohen, M. H.; Johnson, J.; Ko, C.-W.; Sridhara, R.; Justice, R.; Pazdur, R. FDA drug approval summary: lapatinib in combination with capecitabine for previously treated metastatic breast cancer that overexpresses HER-2.. The Oncologist 2008, 13 (10), 1114–1119.
9. Valabrega, G.; Montemurro, F.; Aglietta, M. Trastuzumab: mechanism of action, resistance and future perspectives in HER2-overexpressing breast cancer. Annals of Oncology 2007, 18 (6), 977–984.
10. Kang, S. H.; Kang, K. W.; Kim, K.-H.; Kwon, B.; Kim, S.-K.; Lee, H.-Y.; Kong, S.-Y.; Lee, E. S.; Jang, S.-G.; Yoo, B. C. Upregulated HSP27 in human breast cancer cells reduces Herceptin susceptibility by increasing Her2 protein stability. BMC Cancer 2008, 8 (1).
11. Wong, A. L. A.; Lee, S.-C. Mechanisms of Resistance to Trastuzumab and Novel Therapeutic Strategies in HER2-Positive Breast Cancer. International Journal of Breast Cancer 2012, 2012, 1–13.
12. Vu, T.; Sliwkowski, M. X.; Claret, F. X. Biochimica et Biophysica Acta (BBA) - Personalized drug combinations to overcome trastuzumab resistance in HER2-positive breast cancer. Reviews on Cancer 2014, 1846 (2), 353–365.

13. Arteaga, C. L.; Sliwkowski, M. X.; Osborne, C. K.; Perez, E. A.; Puglisi, F.; Gianni, L Treatment of HER2-positive breast cancer: current status and future perspectives. Nature Reviews Clinical Oncology 9 (2011) 16.

CHAPTER IV

SYNTHESIS AND BIOLOGICAL EVALUATION OF SMALL MOLECULES WITH IMPROVED DRUG CHARACTERISTICS TO INHIBIT THE GROWTH OF HER2 OVER-EXPRESSED BREAST CANCER CELL

4.1 INTRODUCTION

About 25-30% of breast cancer patient have human epidermal growth factor receptor 2 (HER2) overexpressed tumors, and the tumor cell rely on HER2 pathway to survive and proliferate. [1] HER2 is a ligand independent RTK, overexpress HER2 result in constitutive activation of the receptor which stimulate cell growth and metastasis. [2] It has been well documented that overexpressed HER2 in breast cancer relate to poor prognosis and lower survival rate. [3] Targeting HER2 has become a promising strategy to develop breast cancer therapeutic agent. Currently there are three type of drug that targeting HER2. The first group is HER2 monoclonal antibody drugs such as trastuzumab approved by FDA in 1998;

the second group is antibody-drug conjugate base on first group drug such as trastuzumab emtansine approved by FDA in 2013; the third group is intracellular tyrosine kinase inhibitors such as lapatinib approved by FDA in 2007.[4-6]

Even though trastuzumab has become a successful drug for treating HER2 overexpressed breast cancer, still there are a great number of patient didn't gain benefit from this therapy due to de novo or acquire resistance. [5] There is several pathways involve in trastuzumab resistance development. [7] Up-regulated HER2 is one of the resistance mechanisms. It has been reported that long term treatment of breast cancer cells with trastuzumab leads to HER2 expression increase. The further increased HER2 compensate the targeting effect of trastuzumab, which is the main reason of the resistance. Based on the resistance mechanism, targeting HER2 to decrease its expression and increase its degradation could solve the resistance.

Previously, we found that small chaperone inhibitors have the potential to increase HER2 degradation. In this study our goal is to develop drug candidates with better druggable characteristics to selectively target HER2 overexpressed breast cancer, and further examine if the identified compounds induce HER2 degradation via small chaperone inhibition. Ligand efficiency is an important factor that may affect the efficacy of the compound. Drug candidates with better ligand efficacy have better permeability in the in vivo system. Therefore, the in vivo activity of these compounds should be better than compounds with lower ligand efficacy. In this study we tried to reduce the size and hydrophobicity of lead compound JCC76 from our previous study to maintain selectivity and improve solubility and cell uptake.

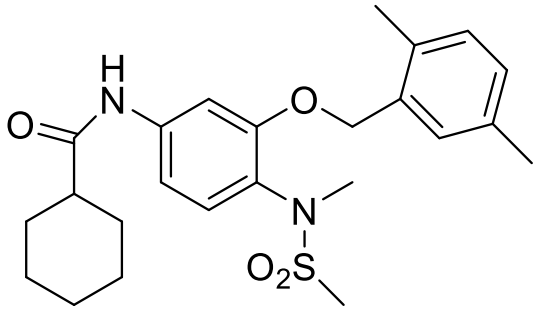

JCC76

Figure 4.1 structure of lead compound JCC76

4.2 RESULTS AND DISCUSSION

4.2.1 Lead optimization and summarization of structure-activity relationship (SAR) studies

In last chapter, we tried to improve compound's solubility by flipping the sulfonamide moiety of JCC76. Via flipping the sulfonamide we expose two hydrogen bond proton donors which should improve compound's aqueous phase solubility. Through biology study we have confirmed those compound preserve ability to inhibit small chaperone, and induce HER2 degradation. Following the same principle, we hypothesize that further increase the ligand efficacy may even lead to better drug candidates.

In this study we attempt to improve compound's solubility and cell uptake by reduce molecule size and increase polarity. In previously study we have confirmed that by replace the 2,5-dimethylbenzyl in B moiety with 2,5-dimethoxylbenzyl the potency of inhibitor induce. We wonder if remove this highly hydrophobic group on the compound will it preserve the ability to inhibit HSP27 and selectively constrain the growth of HER2 overexpressed breast cancer cell. To reduce molecule weight the 2,5-dimethylbenzyl group in B moiety was substitute with smaller function groups including methyl, methoxy, fluoro and chloro.

In previously study the general order of potency of sulfonamides for inhibition of SKBR-3 cell growth has been identity which is methanesulfonamides >

ethanesulfonamides ≥ propylsulfonamides > benzylsulfoylamides > phenylsulfonamides. The larger of the sulphonamide the less cell growth inhibition which suit our compound design. In A moiety three sulfonamide substitutions: methanesulfonamide, ethanesulfonamide and trifluoromethanesulfonamide were choose to synthesized the new derivatives, methanesulfonamide and ethanesulfonamide were choose because of their potency and low molecular weight. We select trifluoromethanesulfonamide not just because of its small molecule size but we also interesting in whether this highly polar substitution could be tolerated or not.

In previously study we discover that at C moiety bulky electron donating group is favour over electron withdraw group. However bulky electron donating group will induce the hydrophobicity of the compound and limit the solubility and cell uptake. From the result of cell viability assay of previously study 5 highly polar substitution groups exhibit potent SKBR-3 cell proliferate inhibition were choose. The substation group at C moiety are: 4-chloro benzylamide, 4-cyano benzylamide, 3-trifluroumethyl benzylamide, 3-nitro, 4-chloro benzylamide and 3,5-bis trifluroumethyl benzylamide. The potency of synthesized compounds inhibition against HER2 overexpressed breast cancer cell growth inhibition were test by cell viability assay.

For SKBR-3 cell only two types of analogs exhibited potent anti-proliferate activity. First type is compound with 3-nitro, 4-chloro benzoyl amide substitution group. However, this category of analogs lack selectivity which may be related to the general cytotoxicity of the nitro group. The second type of analogs contain 3-trifluoromethybenzoyl amide

substitution group. The SAR analysis indicates that the strong electronegative group on B moiety favor SKBR-3 proliferation inhibition whereas the electron withdrawing group trifluoromethyl on sulfonamide negatively affects the compounds' activity.

In C38 cells, several compounds with 3,5-bistrifluoromethybenzoyl amide substitution group showed some potent anti-proliferate activity, especially compound 5 with IC_{50} value at 0.9μM. This result suggests that the new analogs may interfere with unknown cell growth pathway other than the HER2-HSP27 pathway.

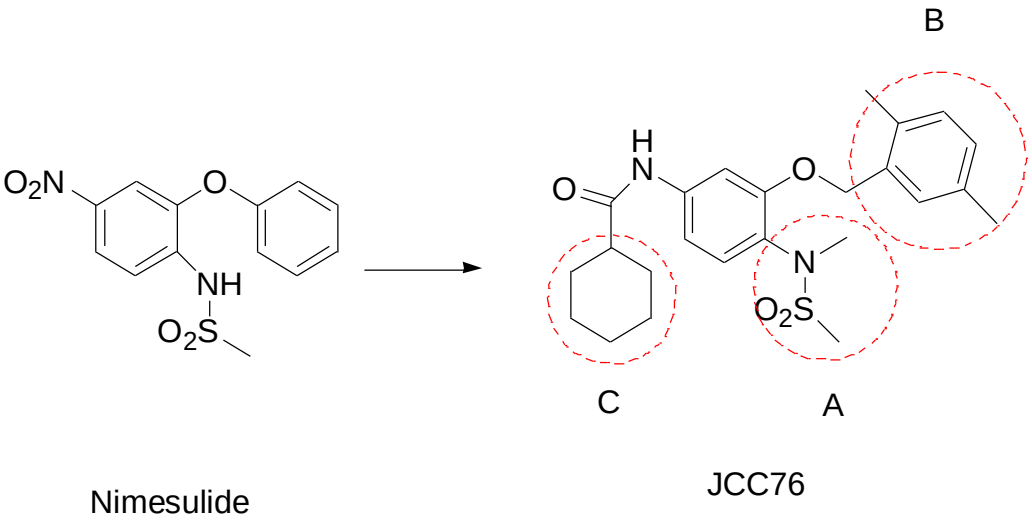

Nimesulide

JCC76

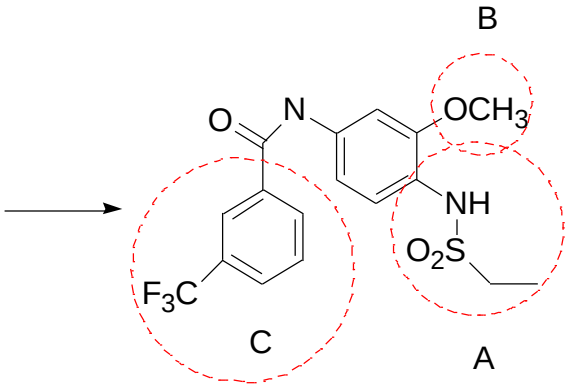

Compound 23

Figure 4.2 Development of HSP27 inhibitor

Table 4.1 Comparison of the growth inhibitory effects of the new analogs on different cell lines(the specific structures of the compounds are included in the experimental section)

Entry	IC_{50}(μM) (SKBR-3)	IC_{50}(μM) (MDA-231)	IC_{50}(μM) (MCF-7)	IC_{50}(μM) (HEK293)	IC_{50}(μM) (C38)
1	240.13±83.26	>250	>250	50.26±13.57	69.05±20.12
2	>250	>250	142.85±45.63	43.53±8.54	171.12±68.07
3	126.28±23.43	79.76±5.69	84.41±41.5	17.49±14.24	13.87±6.70
4	18.32±7.43	15.28±4.47	15.78±4.46	39.86±7.11	20.41±5.73
5	>250	84.41±7.80	122.28±21.25	>250	0.98±0.74
6	159.95±14.86	91.73±36.28	>250	125.43±27.20	68.71±11.88
7	>250	145.45±21.86	>250	>250	108.76±16.77
8	105.71±21.65	54.95±13.86	90.83±22.86	209.63±56.26	113.91±28.44
9	19.33±20.10	28.34±8.83	28.1±14.28	35.47±8.99	71.23±29.97
10	126.12±35.72	112.9±31.99	125.15±22.49	>250	30.60±11.92
11	39.21±11.34	57.25±10.66	52.84±30.60	200.5±62.06	35.36±14.04
12	233.65±49.92	>250	>250	>250	135.4±24.58
13	65.36±9.84	153.58±32.67	247.45±120.26	130.60±32.20	8.72±6.18
14	>250	211.6±66.65	130.99±34.85	>250	89.78±24.65
15	37.73±6.27	0.63±0.73	74.93±25.09	38.73±14.75	19.66±7.35

16	>250	215.48±49.05	210.93±94.35	>250	70±16.32
17	>250	142.98±26.55	191.2±51.02	>250	>250
18	29.89±25.57	96.48±7.53	>250	>250	84.77±27.70
19	19.98±14.37	>250	17.25±3.79	164.4±37.51	>250
20	218.73±61.27	90.61±21.10	118.2±52.1	41.97±17.57	>250
21	240.79±162.24	91.43±47.52	172.28±37.97	>250	60.09±31.85
22	>250	149.47±42.46	>250	>250	66.44±29.82
23	7.05±4.77	194.58±90.04	183.5±32.90	>250	84.83±41.66
24	17.04±2.39	20.05±3.15	17.25±3.79	63.65±18.13	5.66±2.95
25	>250	>250	>250	>250	32.71±18.78
26	61.57±20.75	116.63±80.60	174.5±37.98	>250	108.48±46.66
27	55.43±20.54	109.60±75.54	>250	>250	201.47±80.81
28	107.47±40.26	100.14±36.64	>250	>250	75.23±14.75
29	41.80±17.44	37.57±23.79	102.41±15.53	180.65±45.41	54.08±20.70
30	>250	67.72±47.29	98.51±53.21	>250	>250
31	147.7±47.33	217.68±15.38	>250	167.45±30.03	79.94±49.27
	>250	156.99±41.6	>250	>250	>250
32					
33	178.59±104.35	>250	>250	>250	>250
34	60.98±9.15	181.225±48.86	127.23±13.38	203.57±29.44	43.60±22.23

35	101.37±15.48	90.32±13.23	156.25±26.92	132.33±49.16	62.40±37.52
36	51.89±7.99	25.24±14.54	99.07±13.13	45.64±11.6	22.18±6.19
37	>250	126.5±16.76	>250	>250	226.08±114.47
38	10.56±5.59	36.84±7.34	148.01±44.73	106.79±33.36	49.09±14.51
39	14.78±3.45	8.48±3.87	10.39±5.75	35.33±6.45	8.65±4.21
40	12.23±4.58	75.25±34.49	73.08±35.02	43.33±18.33	11.84±9.00
41	77.14±11.92	75.70±33.31	83.74±41.06	190.9±63.12	47.15±6.39
42	107.72±16.70	125.06±43.83	>250	>250	97.77±40.81
43	49.98±7.08	129.3±17.82	137.2±21.13	209.85±39.02	55.82±7.79
44	97.65±15.87	106.74±28.5	116.32±33.98	228.48±44.82	31.68±7.26
45	79.07±15.83	113.97±38.49	79.35±57.63	>250	136.06±51.81
46	121.66±38.63	110.63±16.50	74.25±30.12	216.2±9.88	22.25±6.64
47	>250	97.47±9.76	>250	>250	>250
48	21.88±12.09	88.52±51.93	>250	>250	32.29±15.69
49	57.78±24.03	105.06±5.12	191.69±95.93	23.08±3.13	101.79±45.41
50	67.61±22.46	141.69±89.26	>250	>250	124.94±70.28
51	108.25±57.74	65.13±10.71	>250	53.37±4.83	151.92±73.77
52	58.37±4.4	50.02±16.01	>250	26.36±6.79	107.38±49.13
53	12.35±1.53	44.58±8.96	165.34±90.71	94.84±29.38	119.17±43.96
54	9.42±3.5	25.84±8.64	24.59±14.81	6.69±0.83	34.66±14.98

55	92.43±9.22	163.28±42.03	104.21±18.2	>250	58.26±31.56
56	85.86±18.92	147.97±103.29	198.82±90.25	78.98±41.12	3.27±1.78
57	233.55±163.8	>250	0.11±0.07	171.6±40.12	>250
58	24.79±2.46	196.165±186.2 6	>250	151.7±31.83	34.44±20.47
59	28.47±6.21	9.97±4.48	8.60±5.32	22.66±9.82	26.99±15.74
60	66.41±13.63	>250	3.59±1.24	81.61±27.32	71.54±10.98

4.2.2 Study on the structural characterization of fluorinated compounds.

The NMR spectra of fluorinated compounds are very complex. The reason is that the atomic number(I) of fluorine atoms is also 1/2. In ^{1}HNMR, it can couple and splite of the H atoms separated by 1-4 bonds. The corresponding coupling constants are $^{2}J_{HF}$=40-60Hz，$^{3}J_{HF}$=2-15Hz and $^{4}J_{HF}$=0-5Hz[11,12,13]. When there is a fluorine atom on the benzene ring, there are coupling and splitting between the fluorine atom and the ortho-position H atoms. and even the meta-position H atoms. In ^{13}C NMR there are coupling and splitting between the fluorine atom and the C atoms separated by 1-4 bonds. The corresponding coupling constants are $^{1}J_{CF}$=150-350, $^{2}J_{CF}$=20-60Hz，$^{3}J_{CF}$=4-20Hz，$^{4}J_{CF}$=0-5Hz[11,12,13]. If there is a fluorine atom on the benzene ring, it's going to couple and split the five carbon atoms but para-position carbon atoms. The three fluorine atoms in CF_3 can divide the carbon atoms that are directly connected to the fluorine atoms or two or three bonds apart with the fluorine atoms into four peaks. . In this experiment the coupling and splitting of H-C-C-F($^{2}J_{HF}$)，***C*-*F***($^{1}J_{CF}$)，***C***-C-***F***($^{2}J_{CF}$)，***C***-C-C-***F***($^{3}J_{CF}$) were detected. According to the chemical shift and the coupling and splitting, compound (50) is used for the identification of ^{1}HNMR and ^{13}C NMR,as shown in figure 4X and figure 4X

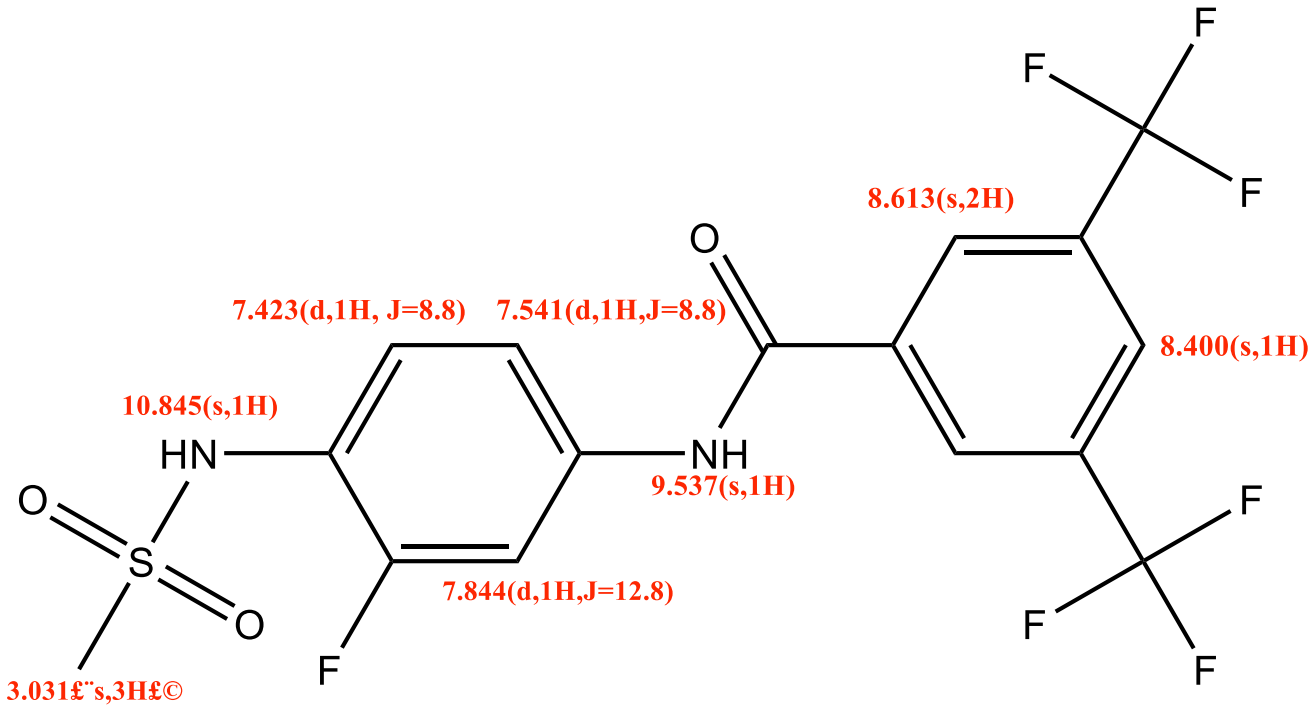

Figure 4.3 The hydrogen spectrum signal belongs of the compound(50)

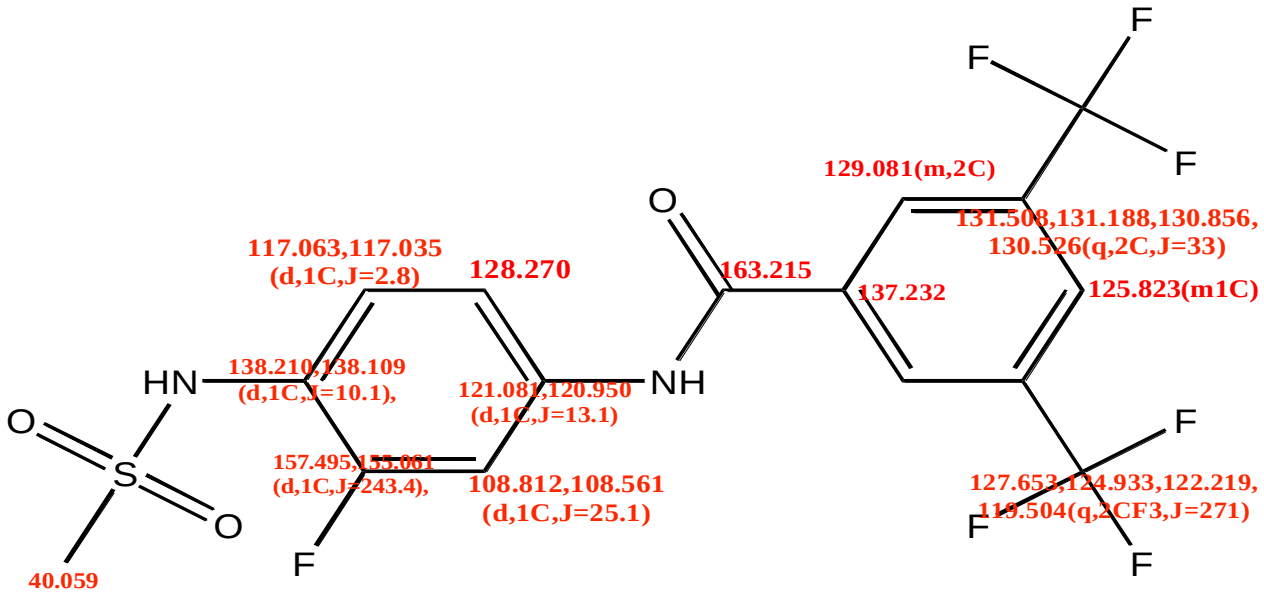

Figure 4.4 The carbon spectrum signal belongs of the compound(50)

4.3 CONCLUSION

Some compounds from the new analogs selectively inhibited SKBR-3 cell proliferation with IC50 values at 10μM. However some compounds show unexpected potent inhibition against C38 cell proliferation, the most potent compound with IC50 value at 0.8μM, which suggest that these compounds may have toxicity to the immune system, since C38 is a macrophage cell line and used here as a model of the immune system.

4.4 EXPERIMENTAL

4.4.1 Chemistry

Chemicals were commercially available and used as received without further purification. Moisture sensitive reactions were carried out under a dry argon atmosphere in flame-dried glassware. Thin-layer chromatography was performed on silica gel TLC plates with fluorescence indicator 254 nm (Fluka). Flash column chromatography was performed using silica gel 60Å (BDH, 40-63 M). Mass spectra were obtained on the ABI QStar Electrospray mass spectrometer at Cleveland State University MS facility Center. All the NMR spectra were recorded on a Bruker 400 MHz (13C NMR at 100 MHz) using DMSO-d6 as solvent. Chemical shifts (δ) for 1H NMR spectra were reported in parts per million to residual solvent protons. Reversed-phase HPLC analysis of

compounds was conducted on a Beckman HPLC system with an Auto Sampler. The chromatographic separation was performed on a C18 column (2.0 mm × 150 mm, 5 μm) from Phenomenex (Torrance, CA). The mobile phase of 80% acetonitrile and 20% water was employed for isocratic elution with a flow rate of 0.2 mL/min. The injection volume was 20 μL and the UV detector was set up at 260 nm.

4.4.1.1 Synthesis of the new analogs(HB)

The reaction procedure is illustrated in the scheme 1 and 2. The general synthesis method describe below, as Figure 4.5 and Figure 4.6.

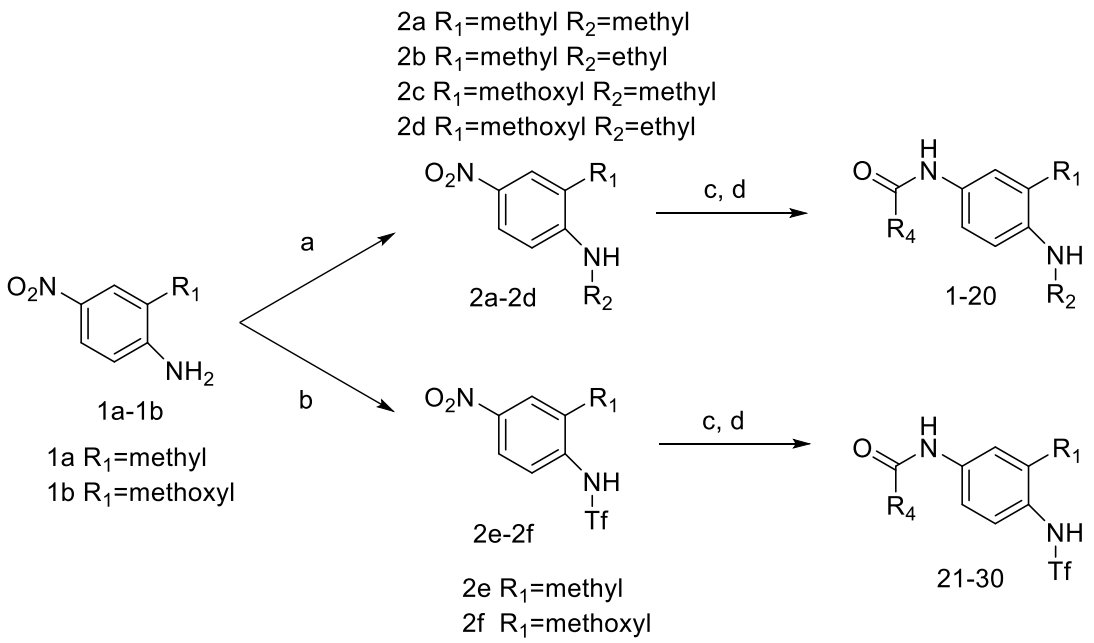

Figure 4.5 (a) NaH, DMF, Ethanesulfonyl chloride/ Methanesulfonyl chloride ; NaOH, Methanol, H2O; (b) DCM, K_2CO_3, Trifluoromethanesulfonic anhydride; (c) Acetone, Zn, $FeCl_3$; (d) Acetone, Brine, saturated Na_2CO_3 solution, corresponding Benzoyl chloride

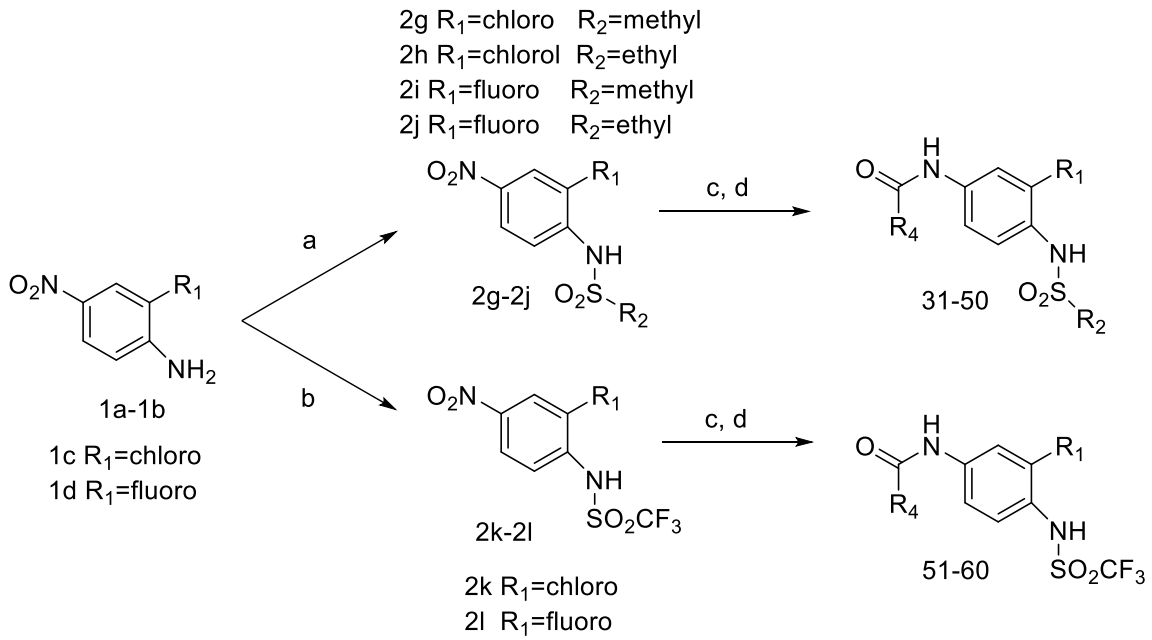

Figure 4.6 (a) TEA, DCM, Ethanesulfonyl chloride/ Methanesulfonyl chloride ; NaOH, Methanol, H_2O; (b) DCM, K_2CO_3, Trifluoromethanesulfonic anhydride; (c) Acetone, Zn, $FeCl_3$; (d) Acetone, Brine, saturated Na_2CO_3 solution, corresponding Benzoyl chloride.

◆ **General method for the preparation of 2a-2d**

Sulfonamides 2a-2d were prepared from arylsubstituted 2-amino-5-nitrophenols 1a-1b. Dissolve arylsubstituted 2-amino-5-nitrophenol (15.0mmol) in 40ml anhydride DMF add NaH (95% powder, 1.325 g, 52.5 mmol, 3.5equiv) into the solution stir at room temperature for 30min. After stir at room temperature for 30min corresponding sulfonyl chloride (45mmol, 3equiv) was added to the mixture the reaction continued overnight at room temperature. Quench the reaction with water and the mixture was neutralized with 6N HCl until pH=1-2, yellow intermediate precipitated. Intermediate was collect by filtration and wash with water, which was used to the next reaction without further purification

The intermediate was dissolve in 100ml methanol and 50ml 4N NaOH aq solution was added into the solution, stir at room temperature for 2h. After reaction completed neutralized the solution with 6N HCl until pH=1-2. The precipitate was collect by filtration and was with water and cold ether to provide desire product.

◆ **General method for the preparation of 2g-2j**

Sulfonamides 2g-2j were prepared from arylsubstituted 2-amino-5-nitrophenols 1c-1d. Dissolve arylsubstituted 2-amino-5-nitrophenol (15.0mmol) in 150ml anhydride DCM, TEA was added into solution (105.0mmol, 7equiv). After TEA added corresponding sulfonyl chloride (45mmol, 3equiv) added into solution, reacted at room temperature overnight. After reaction completed DCM evaporated under vacuum added

200ml water added into the flask neutralized with 6N HCl until pH=1-2. Collect the solid intermediate by filtration. Wash the intermediate with water, which was used to the next reaction without further purification.

The intermediate was dissolve in 100ml methanol and 50ml 4N NaOH aq solution was added into the solution, stir at room temperature for 2h. After reaction completed neutralized the solution with 6N HCl until pH=1-2. The precipitate was collect by filtration and was with water and cold ether to provide desire product

◆ **General method for the preparation of 2e-2f and 2k-2l**

Trifluoroumethylsulfonamides 2e-2f and 2k-2l were prepared from arylsubstituted 2-amino-5-nitrophenols 1a-1d. Dissolve arylsubstituted 2-amino-5-nitrophenol (15.0mmol) in 150ml anhydride DCM and K_2CO_3 (75mmol) was added to solution, then cool to 0℃. Trifluoromethanesulfonic anhydride (45mmol) was added into the solution dropwise. The resulting mixture was continuously stirred for 3 h at 0-5 ℃. Water (30 mL) was added to quench the reaction. DCM was evaporated under vacuum, and then 6N HCl (10mL) was added to acidify the residue. The product was collected by filtration and washed with water and cool ether, then used for the next reaction without further purification.

◆ **General method for the preparation of product 1-60**

Dissolve intermediates 2a-2l 1mmol in acetone 10ml and water 1ml. After intermediates dissolve into solvent Zn (10mmol, 10equiv) and $FeCl_3$ (4mmol, 4equiv) were added into solution, the result mixture was stirred at room temperature for 1h. After the reaction completed the mixture was filtrate through celite to remove inorganic precipitate. The eluent was evaporated under vacuum.

Redissolve the intermediate into 10ml acetone, the corresponding benzoyl chloride (1.1mmol, 1.1equiv) was added then 10ml brine and 10ml saturated K_2CO_3 solution. The result mixture was stirred at room temperature for 1h. After the reaction completed neutralized with 6N HCl until PH=1-2, acetone was evaporated under vacuum. The product was collect by filtration and purify by recrystallization in ethanol/ water (3:1).

4.4.1.2 Structural characterization of 60 compounds of the new analogs (HB)

◆ **4-chloro-N-(4-(methylsulfonamido)-3-methylphenyl)benzamide（1）**

Yield 56.7%. ^{1}H-NMR (400MHz, DMSO-d_6) δ: 10.427(s,1H), 8.362(s,1H), 8.013 (d,2H,J=8.0), 7.753(s,1H), 7.738(d,1H,J=8.0), 7.634(d,2H,J=8.0), 7.325 (d,1H,J=8.0), 3.248(s,3H), 2.344(s,3H). ^{13}C-NMR (100MHz, DMSO-d_6) δ: 164.950, 138.947, 137.065, 133.812, 133.458, 130.119(2C), 128.992(2C), 128.945, 125.696, 123.006, 119.310, 43.628, 18.173. DUIS-MS calculated for $C_{15}H_{15}ClN_2O_3S$, [M-H]-: 337.04 , found336.9;

Purity: 95.3%.

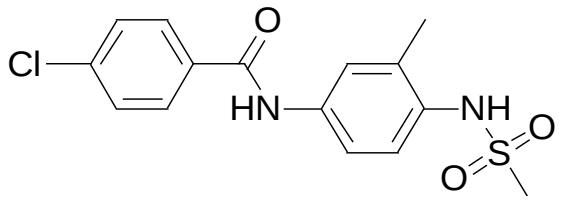

Figure 4.7 The Chemical construction of 4-chloro-N-(4-(methyl sulfonamido)-3-methylphenyl)benzamide

◆ **4-cyano-N-(4-(methylsulfonamido)-3-methylphenyl)benzamide (2)**

Yield 60.5%.^{1}H-NMR (400MHz, DMSO-d_6) δ: 10.607 (s,1H), 8.362 (s,1H), 8.136 (d,2H,J=8.4), 8.049(d,2H,J=8.4), 7.758(s,1H), 7.744 (d,1H, J=8.0),7.339 (d,1H, J=8.0), 3.250(s,3H), 2.349(s,3H). ^{13}C-NMR (100MHz, DMSO-d_6) δ: 164.659， 139.127，133.491，132.981(2C), 132.952, 129.029,(2C), 128.964, 125.616, 123.066, 119.386, 118.748, 114.483,43.585,18.188. DUIS-MS calculated for $C_{16}H_{15}N_3O_3S$, [M-H]-: 328.08, found 328.0, Purity: 97.3%.

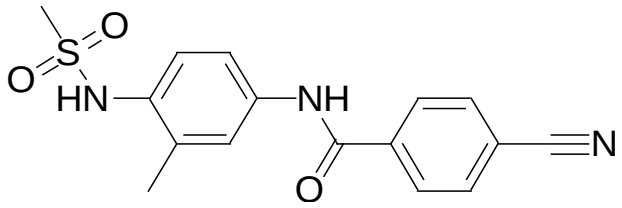

Figure 4.8 The Chemical construction of 4-cyano-N-(4-(methylsulfonamido)-3-methylphenyl)benzamide

◆ **N-(4-(methylsulfonamido)-3-methylphenyl)-3-(trifluoromethyl)benzamide (3)**

Yield 62.7%. ^{1}H-NMR (400MHz, DMSO-d_6) δ: 10.447(s,1H), 9.008(s,1H), 8.301(s,1H), 8.270(d,1H,J=8.0), 7.980, (d,1H,J=8.0) 7.799(t,1H,J=8.0), 7.679(s,1H), 7.628(d,1H,J=8.8), 7.279(d,1H,J=8.8), 2.981(s,3H), 2.333(s,3H). ^{13}C-NMR (100MHz, DMSO-d_6) δ: 164.387, 137.523, 136.180, 135.468, 132.293, 131.706, 130.218, 130.160,129.838,129.518,129.212(q,1C), 128.644(m,1C), 127.520, 124.732,124.694,124.655,124.620(q,1C), 123.137, 119.159, 31.144, 18.840. DUIS-MS calculated for $C_{16}H_{15}F_3N_2O_3S$, [M-H]-: 371.07, found 370.9, Purity: 97.8%.

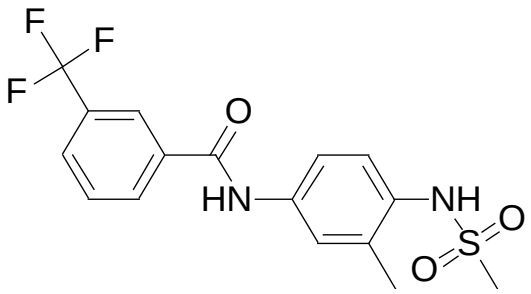

Figure 4.9 The Chemical construction of N-(4-(methyl sulfonamido)-3-methylphenyl)-3-(trifluoromethyl)benzamide

◆ **4-chloro-N-(4-(methylsulfonamido)-3-methylphenyl)-3-nitrobenzamide (4)**

Yield 61.7%. ^{1}H-NMR (400MHz, DMSO-d_6) δ: 10.733 (s,1H), 8.694(s,1H), 8.375(s,1H), 8.316(d,1H, J=8.4), 7.790(d,1H,J=8.4), 7.757(s,1H), 7.750 (d,1H,J=8.8), 7.353(d,1H,J=8.8), 3.270(s, 3H), 2.363(s,3H). ^{13}C-NMR (100MHz, DMSO-d_6) δ: 162.997, 147.960, 139.503, 135.091, 133.599, 133.379, 132.566, 132.477, 128.694,

125.771, 125.377, 123.150, 119.449, 43.609. 18.230. DUIS-MS calculated for $C_{15}H_{14}ClN_3O_2S$, [M-H]-: 382.03, found381.9; Purity: 98.2%.

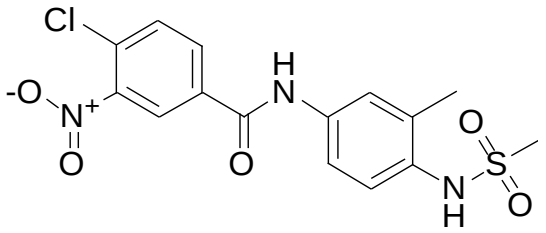

Figure 4.10 The Chemical construction of 4-chloro-N-(4-(methylsulfonamido)-3-methylphenyl)-3-nitrobenzamide

◆ **N-(4-(methylsulfonamido)-3-methylphenyl)-3,5-bis(trifluoromethyl)benzamide (5)**

Yield 55.4%. ^{1}H-NMR (400MHz, DMSO-d_6) δ: 10.593(s,1H), 9.573(s,1H), 8.619(s,2H), 8.379 (s,1H), 7.640(s,1H) ， 7.741(d,1H,J=8.6),7.582 (d,1H,J=8.6), 3.326(s,3H) ,2.256(s,3H), ^{13}C-NMR (100MHz, DMSO-d_6) δ: 160.290, 137.568, 135.467, 132.523, 131.474,131.147,130.812,130.430(q,1C), 128.964(m,2C), 125.511(m,1C), 124.975, 123.780, 123.086, 122.264, 119.028, 40.074，18.514 . DUIS-MS calculated for $C_{17}H_{14}F_6N_2O_3S$, [M-H]-: 439.06, found 439.0, Purity: 98.8%.

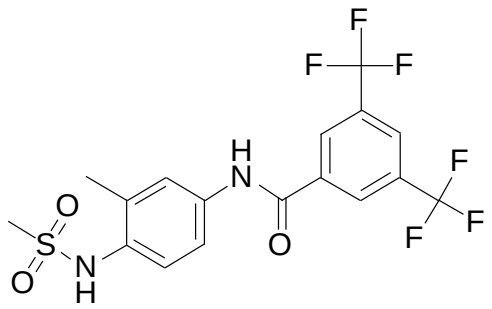

Figure 4.11 The Chemical construction of N-(4-(methyl sulfonamido)-3-methylphenyl)-3,5-bis(trifluoromethyl)benzamide

◆ **4-chloro-N-(4-(ethylsulfonamido)-3-methylphenyl)-benzamide (6)**

Yield 68.9%. ^{1}H-NMR (400MHz, DMSO-d_6) δ: 10.295(s,1H), 8.985(s,1H), 7.985 (d,2H,J=8.8), 7.662(d,1H,J=2.4), 7.618(d,2H,J=8.8), 7.583(dd,1H, J_1=2.4, J_2=8.8), 7.233(d,1H,J=8.8), 3.075(q, 2H,J=8.0), 2.324(S,3H), 1.275(t,3H, J=8.0). ^{13}C-NMR (100MHz, DMSO-d_6) δ: 164.779, 137.547, 136.895, 135.290, 134.012, 131.542，130.064(2C), 128.940(2C), 127.299, 122.992, 119.043, 46.672, 18.917, 8.560 . DUIS-MS calculated for $C_{16}H_{17}ClN_2O_3S$, [M-H]-: 351.06 , found 351.0; Purity: 96.7%.

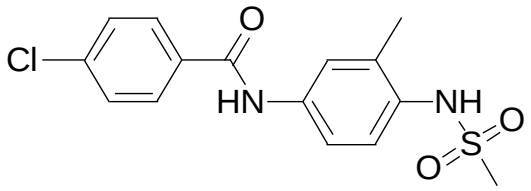

Figure 4.12 The Chemical construction of 4-chloro-N-(4-(ethylsulfonamido)-3-methylphenyl)-benzamide

◆ **4-cyano-N-(4-(ethylsulfonamido)-3-methylphenyl)benzamide (7)**

Yield 60.7%. ^{1}H-NMR (400MHz, DMSO-d_6) δ: 10.449 (s, 1H), 8.999 (s,1H), 8.106 (d,2H, J=8.4), 8.035 (d,2H, J=8.4), 7.668 (d,1H, J=2.4), 7.588 (dd,1H, J_1= 2.4, J_2= 8.4,), 7.250 (d,1H, J=8.4), 3.079 (q,2H, J=7.6), 2.328 (s,3H), 1.274 (t,3H, J=7.6). ^{13}C-NMR (100MHz, DMSO-d_6) δ: 164.493, 139.338, 137.279, 135.285, 132.949, 131.817, 128.872, 127.274, 123.027, 119.091, 118.779, 114.342, 46.702, 18.914, 8.561. DUIS-MS calculated for $C_{17}H_{17}N_3O_3S$, [M-H]-: 342.09, found 341.8, Purity: 96.8%.

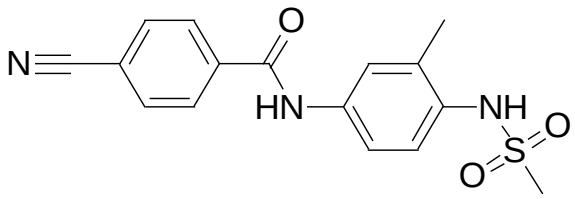

Figure 4.13 The Chemical construction of 4-cyano-N-(4-(ethyl sulfonamido)-3-methylphenyl)benzamide

◆ **N-(4-(ethylsulfonamido)-3-methylphenyl)-3-(trifluoromethyl)benzamide (8)**

Yield 61.7%. ^{1}H-NMR (400MHz, DMSO-d_6) δ: 10.433(s,1H), 8.990(s,1H), 8.300(s,1H), 8.269(d,1H,J=7.6), 7.980 (d,1H,J=7.6), 7.799(t,1H,J=7.6), 7.667(s,1H), 7.610 (d,1H,J=8.4), 7.259(d,1H,J=8.4), 3.087(q,2H,J=7.2), 2.339(s,3H), 1.282 (t,3H,J=7.2). ^{13}C-NMR (100MHz, DMSO-d_6) δ: 164.373, 137.352, 136.191, 135.288, 132.287, 131.763, 130.214, 130.162,129.842,129.524,129.183(q,1C), 128.628(m,1C),

127.273, 124.690(m,1C), 123.139, 119.171, 46.733, 18.995, 8.555. DUIS-MS calculated for $C_{17}H_{17}F_3N_2O_3S$, [M-H]-: 385.08, found 384.8, Purity: 97.5%.

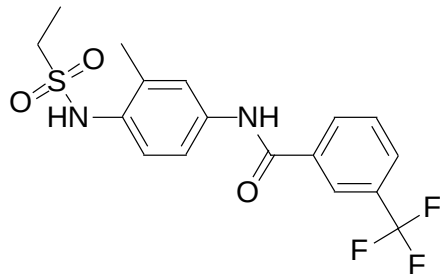

Figure 4.14 The Chemical construction of N-(4-(ethylsulfonamido)-3-methylphenyl)-3-(trifluoromethyl)benzamide

◆ **4-chloro-N-(4-(ethylsulfonamido)-3-methylphenyl)-3-nitrobenzamide (9)**

Yield 64.3%. ^{1}H-NMR (400MHz, DMSO-d_6) δ: 10.516 (s,1H), 9.015 (s,1H), 8.632 (d,1H, J=2.0), 8.258 (dd,1H, J=8.4, 2.0), 7.981(d,1H, J=8.4), 7.645 (d,1H, J=2.0), 7.586(dd,1H, J_1=2.0, J_2=8.6), 7.260 (d,1H, J=8.6), 3.083 (q,2H, J=7.3),2.331(s,3H), 1.274 (t,3H, J=7.3). ^{13}C-NMR (100MHz, DMSO-d_6) δ: 162.913, 137.060, 135.315, 135.279, 133.299, 132.452, 131.961, 128.564, 127.292, 125.274, 123.091, 119.147, 117.059, 46.743, 18.998, 8.554. DUIS-MS calculated for $C_{16}H_{16}ClN_3O_5S$, [M-H]-: 396.04, found 396.0 Purity: 98.8%.

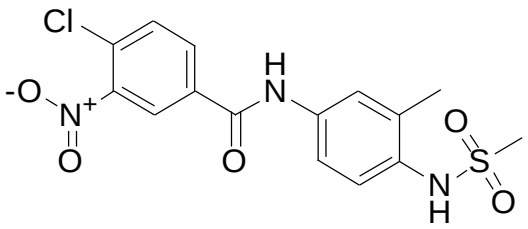

Figure 4.15 The Chemical construction of 4-chloro-N-(4-(ethyl sulfonamido)-3-methylphenyl)-3-nitrobenzamide

◆ **N-(4-(ethylsulfonamido)-3-methylphenyl)-3,5-bis(trifluoromethyl)benzamide (10)**

Yield 54.6%. ^{1}H-NMR (400MHz, DMSO-d_6) δ: 10.633(s,1H), 9.015(s,1H), 8.621(s,2H), 8.377(s,1H), 7.658 (s,1H), 7.625(d,1H,J=8.4), 7.285(d,1H,J=8.4), 3.081 (q,2H,J=7.2), 2.347(s,3H), 1.285, (t,3H,J=7.2). ^{13}C-NMR (100MHz, DMSO-d_6) δ: 162.948, 137.509, 136.979, 135.287, 132.094, 131.490,131.156,130.824,130.490(q,1C), 129.018(m,2C), 127.242, 125.564(m,1C), 123.261, 119.290, 46.786, 18.881, 8.556. DUIS-MS calculated for $C_{18}H_{16}F_6N_2O_3S$, [M-H]-: 453.07, found 453.0, Purity: 98.8%.

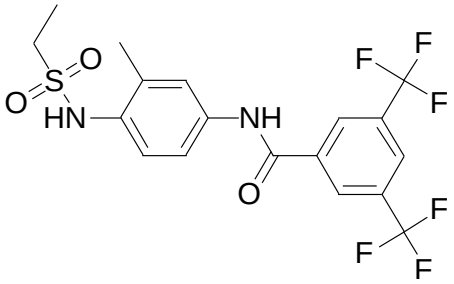

Figure 4.16 The Chemical construction of N-(4-(ethylsulfonamido)-3-methylphenyl)-3,5-bis(trifluoromethyl)benzamide

◆ **4-Chloro-N-(3-methyl-4-trifluoromethanesulfonylamino-phenyl)-benzamide (11)**

Yield 59.7%. ^{1}H-NMR (400MHz, DMSO-d_6) δ: 11.341(s,1H), 10.367(s,1H), 7.987 (d,2H,J=8.4), 7.740(s,1H), 7.636(m,3H), 7.299(d,1H,J=8.8), 2.320(s,3H). ^{13}C-NMR (100MHz, DMSO-d_6) δ: 164.98, 139.21, 137.02, 136.34, 133.89, 130.10,(2C) , 128.96(2C), 128.91, 128.38, 122.90, 121.80, 119.19. DUIS-MS calculated for $C_{15}H_{12}ClF_3N_2O_3S$, [M-H]-: 391.01, found 390.9, Purity: 95.7%.

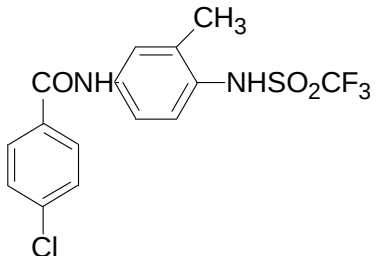

Figure 4.17 The Chemical construction of 4-Chloro-N-(3-methyl-4-trifluoromethanesulfonylamino-phenyl)-benzamide

◆ **4-Cyano-N-(3-methyl-4-trifluoromethanesulfonylamino-phenyl)-benzamide (12)**

Yield 52.7%. ^{1}H-NMR (400MHz, DMSO-d_6) δ: 11.398(s, 1H), 10.543 (s, 1H), 8.106 (d, 2H, J=8.0), 8.041(d, 2H, J=8.0), 7.752(s, 1H)， 7.654(d, 2H, J=8.8), 7.248 (d, 1H, J=8.8), 2.326 (s, 3H). ^{13}C-NMR (100MHz, DMSO-d_6) δ: 164.720, 139.211, 138.969, 136.400, 132.867(2C), 129.013(2C), 128.965, 128.636, 122.942, 119.426, 118.750,

114.454, 18.342. DUIS-MS calculated for $C_{16}H_{12}F_3N_3O_3S$, [M-H]-: 382.05, found 381.9, Purity: 97.9%.

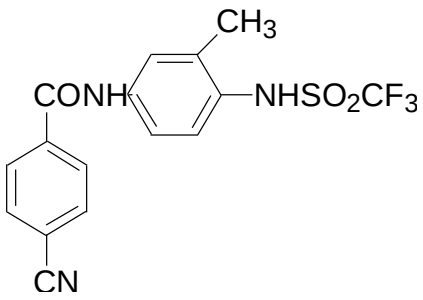

Figure 4.18 The Chemical construction of 4-Cyano-N-(3-methyl-4-trifluoromethanesulfonylamino-phenyl)-benzamide

◆ **N-(3-Methyl-4-trifluoromethanesulfonylamino-phenyl)-3-trifluoromethyl-benzamide (13)**

Yield 55.4%. ^{1}H-NMR (400MHz, DMSO-d_6) δ: 10.550 (s,1H), 8.274 (s,1H), 8.246 (d, 1H, J= 8.0), 7.973 (d, 1H, J=8.0), 7.791 (t, 1H, J=8.0), 7.721 (s, 1H), 7.656 (d,1H, J=8.4), 7.241 (d, 1H, J=8.4), 2.321 (s,3H) . ^{13}C-NMR (100MHz, DMSO-d_6) δ: 164.716, 138.999, 136.502, 135.978, 132.282, 130.288, 130.197,129.877,129.557,129.241(q,1C), 129.001, 128.771(m,1C), 128.512, 124.703(m,1C), 123.111, 119.372, 18.290. DUIS-MS calculated for $C_{16}H_{12}F_6N_2O_3S$, [M-H]-: 425.04, found 424.8, Purity: 98.7%.

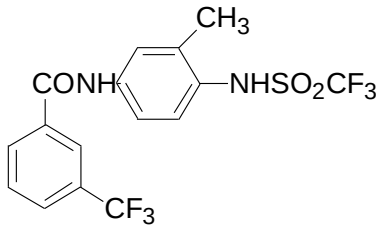

Figure 4.19 The Chemical construction of N-(3-Methyl-4-trifluoromethane sulfonylamino-phenyl)-3-trifluoromethyl-benzamide

◆ **4-Chloro-N-(3-methyl-4-trifluoromethanesulfonylamino-phenyl)-3-nitro-benzamide (14)**

Yield 52.9%. ^{1}H-NMR (400MHz, DMSO-d_6) δ: 11.382(s,1H), 10.633 (s,1H), 8.645 (s,1H), 8.272 (d,1H, J=8.4), 7.985 (d,1H, J=8.4), 7.738 (s, 1H), 7.664 (d, 1H, J=8.6), 7.259 (d, 1H, J=8.6), 2. 332 (s,3H) . ^{13}C-NMR (100MHz, DMSO-d_6) δ: 163.025, 147.858, 138.814, 136.456, 135.153, 133.340, 132.465, 129.014, 128.716, 128.671, 125.341, 123.008, 119.301, 18.339. DUIS-MS calculated for $C_{15}H_{11}ClF_3N_3O_5S$, [M-H]-: 436.00, found 435.9, Purity: 96.8%.

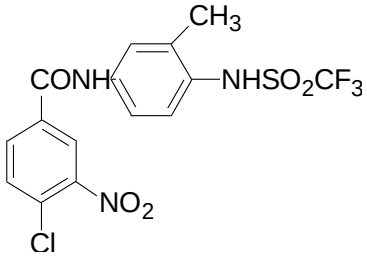

Figure 4.20 The Chemical construction of 4-Chloro-N-(3-methyl-4-trifluoromethanesulfonylamino-phenyl)-3-nitro-benzamide

◆ **N-(3-Methyl-4-trifluoromethanesulfonylamino-phenyl)-3,5-bis-trifluoromethyl-benzamide (15)**

Yield 53.6%. ^{1}H-NMR (400MHz, DMSO-d_6) δ: 10.693 (s, 1H), 8.611 (s,2H), 8.462(s,1H), 8.391 (s,1H), 7.724 (s, 1H), 7.673 (d,1H,J=8.8), 7.275 (d,1H, J=8.8), 2.338 (s, 3H). NMR (100MHz, DMSO-d_6) δ: 163.073, 138.647, 137.409, 136.417, 131.498,131.167,130.837,130.505(q,2C), 129.017(m,2C), 128.965, 125.719(m,1C), 127.660,124.946,122.232,119.517(q,2CF_3), 123.163, 121.898, 119.406, 18.319. DUIS-MS calculated for $C_{17}H_{11}F_9N_2O_3S$, [M-H]-: 493.03, found 492.8, Purity: 98.1%.

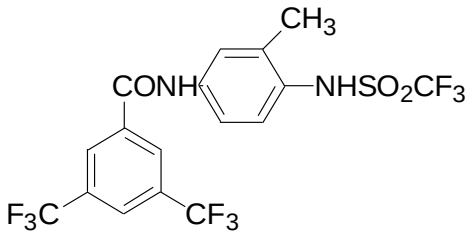

Figure 4.21 The Chemical construction of N-(3-Methyl-4-trifluoro methanesulfonylamino-phenyl)-3,5-bis-trifluoromethyl-benzamide

◆ **4-chloro-N-(4-(methylsulfonamido)-3-methoxylphenyl)benzamide (16)**

Yield 69.8%. ^{1}H-NMR (400MHz, DMSO-d6) δ: 10.339 (s,1H), 8.837 (s,1H), 7.997 （ d,2H,J=8.4 ）,7.627 （ d,2H,J=8.4 ）, 7.622(s,1H), 7.353 (d,1H,J=8.8), 7.217(d,1H,J=8.8), 3.836(s,3H), 2.929(s,3H). ^{13}C-NMR (100MHz, DMSO-d_6) δ: 164.83，153.563， 139.435， 136.595， 134.001，130.056（2C） 129.922（2C）， 127.373，121.532， 112.756， 104.901， 56.151 ， 40.062. DUIS-MS calculated for

$C_{15}H_{15}ClIN_2O_4S$, [M-H]-: 353.04 , found 352.9; Purity: 96.7%.

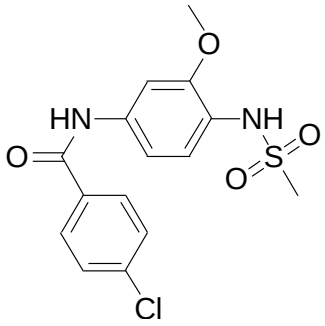

Figure 4.22 The Chemical construction of 4-chloro-N-(4-(methylsulfonamido)-3-methoxylphenyl)benzamide

◆ **4-cyano-N-(4-(methylsulfonamido)-3-methoxylphenyl)benzamide (17)**

Yield 65.3%. ^{1}H-NMR (400MHz, DMSO-d_6) δ: 10.511 (s, 1H), 8.865 (s,1H), 8.116 (d,2H,J=8.4), 8.045 (d,2H, J=8.4), 7.623 (d, 1H,J=2.0), 7.336 (dd,1H, J_1= 2.0, J_2= 8.8), 7.233 (d,1H, J=8.8), 3.838 (s,3H), 2.933 (s,3H). ^{13}C-NMR (100MHz, DMSO-d_6) δ:164.56, 153.53, 139.31, 138.29, 132.96, 128.96, 127.33, 121.99, 118.77, 114.40, 112.81, 104.91, 56.16, 40.07. DUIS-MS calculated for $C_{16}H_{15}N_3O_4S$, [M-H]-: 344.07, found 344.0, Purity: 98.0%.

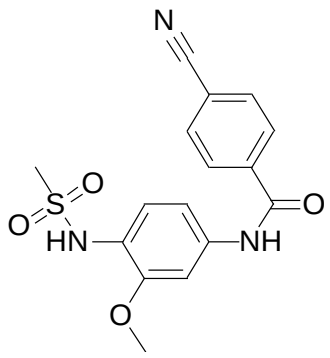

Figure 4.23 The Chemical construction of 4-cyano-N-(4-(methylsulfonamido)-3-methoxylphenyl)benzamide

◆ **N-(4-(methylsulfonamido)-3-methoxylphenyl)-3-(trifluoromethyl) benzamide (18)**

yield 65.3%. ^{1}H-NMR (400MHz, DMSO-d_6) δ: 10.499 (s, 1H), 8.856 (s,1H), 8.303 (s,1H), 8.279 (d, 1H, J=7.6), 7.989 (d, 1H, J= 7.6), 7.808 (t,1H, J=7.6), 7.618 (s, 1H), 7.374 (d, 1H, J=8.8), 7.241 (d, 1H, J=8.8), 3.848 (s, 3H), 2.939 (s, 3H). ^{13}C-NMR (100MHz, DMSO-d_6) δ: 164.463, 153.535, 138.351, 136.179，132.281，130.233，130.180,129.859,129.539,129.219(q,1C), 128.655(m,1C), 127.288, 124.692(m,1C), 121.962, 112.922, 105.051, 56.187, 40.070. DUIS-MS calculated for $C_{16}H_{15}F_3N_2O_4S$, [M-H]-: 387.06, found 386.9, Purity: 97.0%.

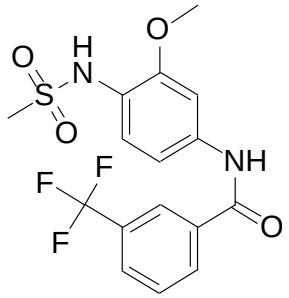

Figure 4.24 The Chemical construction of N-(4-(methyl sulfonamido)-3-methoxylphenyl)-3-(trifluoromethyl) benzamide

◆ **4-chloro-N-(4-(methylsulfonamido)-3-methoxylphenyl)-3-nitrobenzamide (19)**

Yield 70.1%. ^{1}H-NMR (400MHz, DMSO-d_6) δ: 10.572 (s, 1H), 8.876 (s, 1H), 8.645 (s,1H), 8.275 (d, 1H, J=8.4), 7.994 (d, 1H, J=8.4), 7.589 (s, 1H), 7.358 (d,1H,J=8.4), 7.247 (d, 1H,J=8.4), 3.844 (s,3H), 2.940 (s,3H). ^{13}C-NMR (100MHz, DMSO-d_6) δ: 162.972, 153.502, 147.974, 138.041, 135.272, 133.279, 132.466, 128.602, 127.255, 125.262, 122.195, 112.916, 106.007, 56.196, 40.064. DUIS-MS calculated for $C_{15}H_{14}ClN_3O_6S$, [M-H]-:398.02, found 397.9; Purity: 98.3 %.

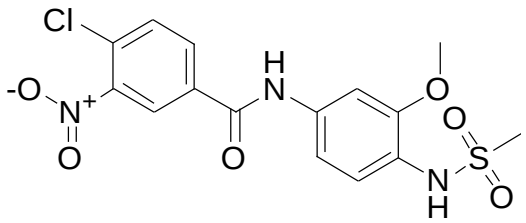

Figure 4.25 The Chemical construction of 4-chloro-N-(4-(methylsulfonamido)-3-methoxylphenyl)-3-nitrobenzamide

◆ **N-(4-(methylsulfonamido)-3-methoxylphenyl)-3,5-bis(trifluoromethyl) benzamide (20)**

Yield 63.4%. ^{1}H-NMR (400MHz, DMSO-d_6) δ: 10.694 (s,1H), 8.901 (s,1H), 8.621 (s,2H), 8.394 (s,1H), 7.589 (d, 1H, J=2.0), 7.373 (dd,1H, J_1= 2.0, J_2= 8.8), 7.266 (d, 1H,J=8.8), 3.854 (s, 3H), 2.948 (s,3H). ^{13}C-NMR (100MHz, DMSO-d_6) δ: 162.952, 153.483, 137.924, 137.486, 131.488,131.159,130.829,130.495(q,2C)，129.017(m,2C), 127.209, 125.631(m,1C), 127.675,124.959,122.245,199.531(q,2CF3), 122.311, 113.082, 105.149, 56.214, 40.039. DUIS-MS calculated for $C_{17}H_{14}F_6N_2O_4S$, [M-H]-: 455.05, found 454.9, Purity: 96.1%.

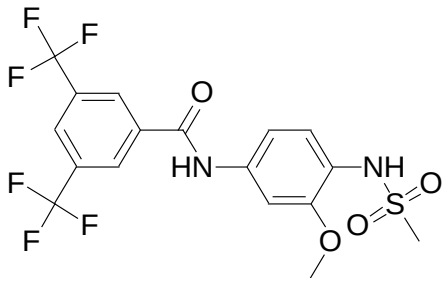

Figure 4.26 The Chemical construction of N-(4-(methylsulfonamido) -3-methoxylphenyl)-3,5-bis(trifluoromethyl) benzamide

◆ **4-chloro-N-(4-(ethylsulfonamido)-3-methoxylphenyl)benzamide (21)**

Yield 69.9%. ^{1}H-NMR (400MHz, DMSO-d_6) δ: 10.345(s,1H), 8.843(s,1H), 7.994 (d,2H,J=8.4), 7.628(d, 2H,J=8.4), 7.608(d, 1H,J=2.0), 7.337 (dd,1H, J_1= 2.0, J_2= 8.4) ,7.225(d,1H,J=8.4), 3.824(s,3H), 2.992(q,2H, J=7.2), 1.257 (t,3H,J=7.2). ^{13}C-NMR

(100MHz, DMSO-d_6) δ: 164.932，153.380，138.439，136.950，133.996，130.059，128.962， 127.245， 121.733， 112.736， 104.803， 56.108， 46.606， 8.482. DUIS-MS calculated for $C_{16}H_{17}ClN_2O_4S$, [M-H]-: 367.05, found366.9, Purity: 97.5%.

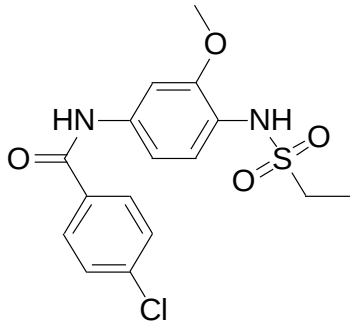

Figure 4.27 The Chemical construction of 4-chloro-N-(4-(ethylsulfonamido)-3-methoxylphenyl)benzamide

◆ **4-Cyano-N-(4-ethanesulfonylamino-3-methoxy-phenyl)-benzamide (22)**

Yield 65.8%. ^{1}H-NMR (400MHz, DMSO-d_6) δ: 10.503 (s,1H), 8.856 (s,1H), 8.114 (d,2H, J=8.4), 8.045 (d,2H,J=8.4), 7.607(d.1H, J=2.0), 7.339(dd,1H, J_1= 2.0, J_2= 8.4), 7.243 (d,1H, J=8.4), 3.828 (s,3H), 2.999 (q,2H,J=7.2), 1.258 (t,3H,J=7.2) . ^{13}C-NMR (100MHz, DMSO-d_6) δ: 164.54, 153.32, 139.32, 138.13, 132.95, 128.96, 127.11, 122.07, 118.76, 114.40, 112.83, 104.87, 56.14, 46.65, 8.47. DUIS-MS calculated for $C_{17}H_{17}N_3O_4S$, [M-H]-: 358.09, found 357.9, Purity: 96.9%.

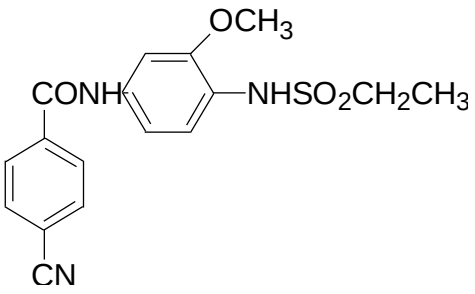

Figure 4.28 The Chemical construction of 4-Cyano-N-(4-ethane sulfonylamino-3-methoxy-phenyl)-benzamide

◆ **N-(4-(ethylsulfonamido)-3-methoxylphenyl)-3-(trifluoromethyl)benzamide(23)**

Yield 62.3%. ^{1}H-NMR (400MHz, DMSO-d_6) δ: 10.495(s,1H), 8.853(s,1H), 8.301(s,1H), 7.276(d,1H,J=7.6), 7.988(d,1H,J=7.6), 7.806(t,1H,J=7.6), 7.603(s,1H), 7.358(d,1H,J=8.8), 7.252 (d,1H,J=8.8), 3.838(s,3H), 3.006(q,2H,J=7.2), 1.264(t,3H,J=7.2). ^{13}C-NMR (100MHz, DMSO-d_6) δ: 164.442, 153.344, 138.199, 136.181, 132.276, 130.228, 130.183,129.855,129.534,129.218(q,1C), 128.677(m,1C), 127.135, 128.524,125.813,123.102,120.379(q,CF_3), 124.649(m,1C)， 121.997， 112.910， 104.968， 56.151， 46.654， 8.481. DUIS-MS calculated for $C_{17}H_{17}F_3N_2O_4S$, [M-H]-: 401.08, found 400.9, Purity: 97.8%.

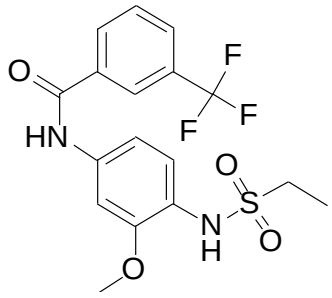

Figure 4.29 The Chemical construction of N-(4-(ethylsulfonamido) -3-methoxylphenyl)-3-(trifluoromethyl)benzamide

◆ **4-chloro-N-(4-(ethylsulfonamido)-3-methoxylphenyl)-3-nitrobenzamide (24)**

Yield 69.7.4%. ^{1}H-NMR (400MHz, DMSO-d_6) δ: 10.561(s,1H), 8.858(s,1H), 8.639 (d,1H, J=2.0), 8.268 (dd,1H,J=8.4,2.0), 7.992(d,1H,J=8.4), 7.570(d,1H,J=1.6), 7.339(dd,1H, J_1=1.6 J_2=8.8,), 7.256 (s,1H,J=8.8), 3.834(s,3H), 3.006(q,2H,J=7.2), 1.260(t,3H,J=7.2). ^{13}C-NMR (100MHz, DMSO-d_6) δ: 162.856, 152.327 , 147.865, 137.902, 135.267, 133.276, 132.466, 128.600, 127.149, 125.265, 122.203, 112.899,104.897, 56.153, 45.667, 8.484. DUIS-MS calculated for $C_{16}H_{16}ClN_3O_6S$, [M-H]-: 412.04, found 411.9, Purity: 96.7%.

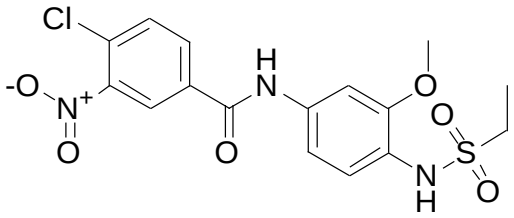

Figure 4.30 The Chemical construction of 4-chloro-N-(4-(ethyl sulfonamido)-3-methoxylphenyl)-3-nitrobenzamide

◆ **N-(4-(ethylsulfonamido)-3-methoxylphenyl)-3,5-bis(trifluoromethyl)benzamide (25)**

Yield 62.4%. ^{1}H-NMR (400MHz, DMSO-d_6) δ: 10.684 (s,1H), 8.883 (s,1H), 8.618 (s,2H), 8.397 (s,1H), 7.573 (d ,1H, J=2.0), 7.354 (q, 1H, J_1=2.0, J_2= 8.6), 7.275 (d, 1H, J=8.6), 3.844 (s,3H), 3.013 (q,2H, J=7.3), 1.263 (t,3H, J=7.3). ^{13}C-NMR (100MHz, DMSO-d_6) δ: 162.932, 153.296, 137.773, 137.512, 131.497,131.168,130.836,130.506(q,2C), 129.006(m,2C), 127.675,124.962,122.250,119.532(q,2CF3), 127.030, 125.669(m,1C), 122.382, 113.094, 105.107, 56.196, 46.715, 8.481. DUIS-MS calculated for $C_{18}H_{16}F_6N_2O_4S$, [M-H]-: 469.07, found 468.9, Purity: 98.2%.

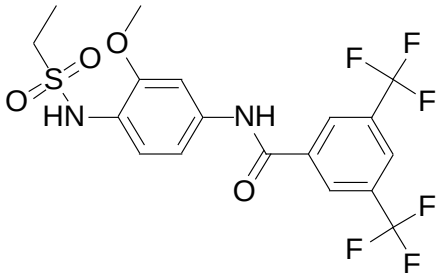

Figure 4.31 The Chemical construction of N-(4-(ethylsulfonamido)-3-methoxylphenyl)-3,5-bis(trifluoromethyl)benzamide

◆ **4-Chloro-N-(3-methoxy-4-trifluoromethanesulfonylamino-phenyl)-benzamide (26)**

Yield 45.5%. ^{1}H-NMR (400MHz, DMSO-d_6) δ: 11.141(s,1H),10.439 (s, 1H), 7.999 (d, 2H, J=8.4), 7.662 (s, 1H), 7.635 (d, 2H, J=8.4), 7.402 (d,1H, J=8.4), 7.223 (d,1H, J=8.4), 3.836 (s,3H). ^{13}C-NMR (100MHz, DMSO-d_6) δ: 165.061, 155.451, 140.658, 137.086, 133.862, 130.110,(2C), 129.724, 128.992(2C), 118.028, 112.583,104.755, 56.230. DUIS-MS calculated for $C_{15}H_{12}ClF_3N_2O_4S$, [M-H]-: 407.01, found 406.9, Purity: 97.4%.

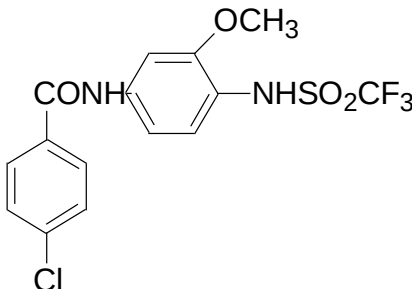

Figure 4.32 The Chemical construction of 4-Chloro-N-(3-methoxy-4-trifluoromethanesulfonylamino-phenyl)-benzamide

◆ **4-Cyano-N-(3-methoxy-4-trifluoromethanesulfonylamino-phenyl)-benzamide (27)**

Yield 45.0 %. ^{1}H-NMR (400MHz, DMSO-d_6) δ: 11.219(s,1H), 10.595(s,1H)，8.115(d,2H, J=8.4), 8.052(d,2H,J=8.4), 7.659(d,1H, J=1.6)， 7.400(dd,1H, J_1= 1.6, J_2= 8.4), 7.241(d,1H, J=8.4), 3.840(s, 3H). ^{13}C-NMR (100MHz, DMSO-d_6) δ: 164.797,

155.459, 140.410, 139.185, 132.987(2C), 129.775, 129.009(2C), 118.747, 114.507, 112.656, 107.673, 104.788, 56.254. DUIS-MS calculated for $C_{16}H_{12}F_3N_3O_4S$, [M-H]-: 398.04, found 397.9, Purity: 96.2%.

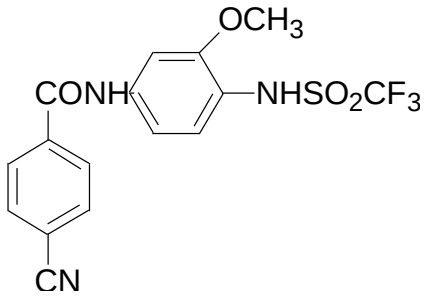

Figure 4.33 The Chemical construction of 4-Cyano-N-(3-methoxy-4-trifluoromethanesulfonylamino-phenyl)-benzamide

◆ **N-(3-Methoxy-4-trifluoromethanesulfonylamino-phenyl)-3-trifluoromethyl-benzamide (28)**

Yield 45.8%. ^{1}H-NMR (400MHz, DMSO-d_6) δ: 11.208(s,1H), 10.578(s,1H), 8.300(s,1H), 8.277(d,1H, J=7.6), 7.998(d,1H, J=7.6), 7.815(t,1H, J=7.6), 7.652(s,1H), 7.419(d,1H, J=8.4), 7.247(d,1H, J=8.4), 3.337(s, 1H). ^{13}C-NMR (100MHz, DMSO-d_6) δ: 164.691, 155.474, 140.490, 138.515, 136.072, 132.033, 131.067, 130.780,130.269,129.744,129.240(q,1C), 128.852, 128.472(m,1C), 124.739(m,1C), 112.747, 104.912, 56.273. DUIS-MS calculated for $C_{16}H_{12}F_6N_2O_4S$, [M-H]-: 441.03, found 440.9, Purity: 98.7%.

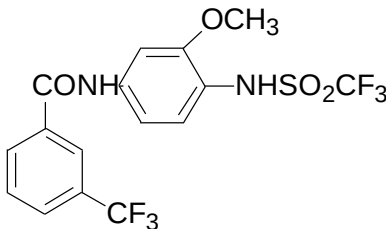

Figure 4.34 The Chemical construction of N-(3-Methoxy-4-trifluoro methanesulfonylamino-phenyl)-3-trifluoromethyl-benzamide

◆ 4-Chloro-N-(3-methoxy-4-trifluoromethanesulfonylamino-phenyl)-3-nitro-benzamid e (29)

Yield 50.7%. ^{1}H-NMR (400MHz, DMSO-d_6) δ: 11.219(s,1H), 10.657(s,1H), 8.647(s,1H), 8.276(d,1H, J=8.0), 7.999(d,1H, J=8.0), 7.628(s,1H), 7.407(d,1H, J=8.4), 7.257(d,1H, J=8.4), 56.291(s,3H). ^{13}C-NMR (100MHz, DMSO-d_6) δ:163.107, 155.466, 147.879, 140.188, 135.157, 133.322, 132.491, 129.761, 128.721, 125.318, 118.479, 112.755, 104.900, 56.291. C15H11ClF3N3O6S, [M-H]-: 452.01, found 451.9, Purity: 97.8%

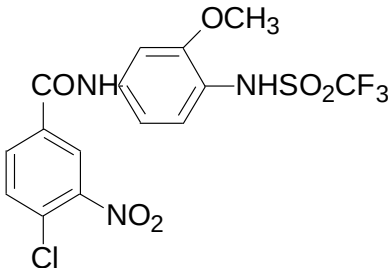

Figure 4.35 The Chemical construction of 4-Chloro-N-(3-methoxy-4-trifluoromethanesulfonylamino-phenyl)-3-nitro-benzamide

◆ **N-(3-Methoxy-4-trifluoromethanesulfonylamino-phenyl)-3,5-bis-trifluoromethyl -benzamide (30)**

Yield 52.7%. ^{1}H-NMR (400MHz, DMSO-d_6) δ: 11.249(s,1H), 10.769(s,1H), 8.618(s,2H), 8.395(s,1H), 7.630(s,1H), 7.422(d,1H, J=8.6), 7.276(d,1H, J=8.6), 3.860(s,3H). ^{13}C-NMR (100MHz, DMSO-d_6) δ: 163.194, 155.471, 140.141, 137.404, 131.508,131.179,130.947,130.516(q,2C), 129.789, 129.066(m,2C), 125.700(m,1C)，127.656,124.939,122.226,119.515(q,2CF_3), 118.529，112.900，105.016，56.302. DUIS-MS calculated for $C_{17}H_{11}F_9N_2O_4S$, [M-H]-: 509.03, found 508.9, Purity: 97.7%.

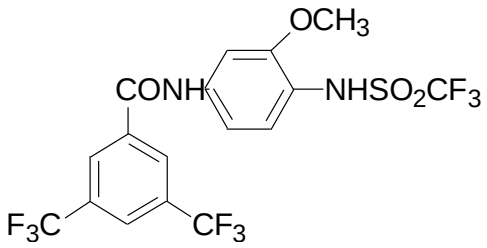

Figure 4.36 The Chemical construction of N-(3-Methoxy-4-trifluoro methanesulfonylamino-phenyl)-3,5-bis-trifluoromethyl-benzamide

◆ **4-chloro-N-(3-chloro-4-(methylsulfonamido)phenyl)benzamide (31)**

Yield 56.7%. ^{1}H-NMR (400MHz, DMSO-d_6) δ: 10.492(s,1H), 9.409(s,1H), 8.062(s,1H), 7.994 (d,2H, J=8.4), 7.710(d,1H,J=8.4), 7.639(d,2H,J=8.4), 7.444(d,1HJ=8.4), 3.032(S,3H). ^{13}C-NMR (100MHz, DMSO-d_6) δ: 165.095, 138.749, 137.200, 133.623, 130.143(2C), 130.093, 129.765, 129.221, 129.033(2C), 212.422,

119.971, 41.305. DUIS-MS calculated for $C_{14}H_{12}Cl_2N_2O_3S$, [M-H]-:356.99, found 356.8; Purity: 98.9%.

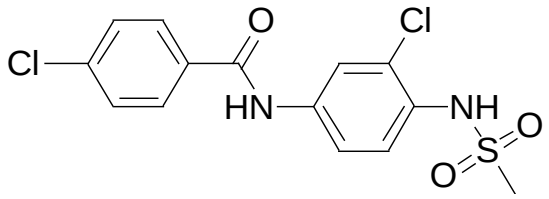

Figure 4.37 The Chemical construction of 4-chloro-N-(3-chloro-4-(methylsulfonamido)phenyl)benzamide

◆ **4-cyano-N-(3-chloro-4-(methylsulfonamido)phenyl)benzamide (32)**

Yield 66.8%. ^{1}H-NMR (400MHz, DMSO-d_6) δ: 10.662 (s, 1H), 9.434 (s,1H), 8.116 (d, 2H, J=8.4), 8.066(s,1H), 8.056 (d,2H,J=8.4), 7.712 (d,1H,J=8.4), 7.461 (d,1H, J=8.4), 3.037 (s, 3H) . ^{13}C-NMR (100MHz, DMSO-d_6) δ: 164.824, 138.938, 138.462, 133.011(2C), 130.051, 129.187, 129.044(2C), 121.509, 120.054, 118.721, 114.594, 99.985, 41.323. DUIS-MS calculated for $C_{15}H_{12}ClN_3O_3S$, [M-H]-: 348.02, found 347.9, Purity: 98.7%.

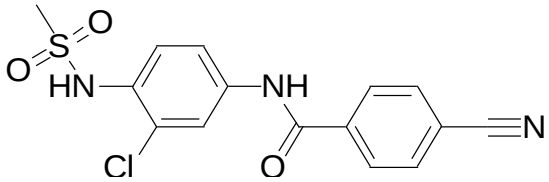

Figure 4.38 The Chemical construction of 4-cyano-N-(3-chloro-4-(methylsulfonamido)phenyl)benzamide

◆ **N-(3-chloro-4-(methylsulfonamido)phenyl)-3-(trifluoromethyl)benzamide (33)**

Yield 69,8%. ^{1}H-NMR (400MHz, DMSO-d_6) δ: 10.842(s,1H), 9.451(s,1H), 8.343(s,1H), 8.113(s,1H), 7.994 (d,1H,J=6.8), 7.803(m,3H), 7.459(d,1H,J=8.4), 3.039(s,3H). ^{13}C-NMR (100MHz, DMSO-d_6) δ: 164.708, 138.724, 135.710, 132.546, 130.193, 130.161,129.842,129.523,129.210(q,1C), 130.130,129.928, 129.106, 128.846(m,1C), 125.004(m,1H), 121.759, 120.242, 41.287. DUIS-MS calculated for $C_{15}H_{12}ClF_3N_2O_3S$, [M-H]-: 391.01, found 390.9, Purity: 98.7%.

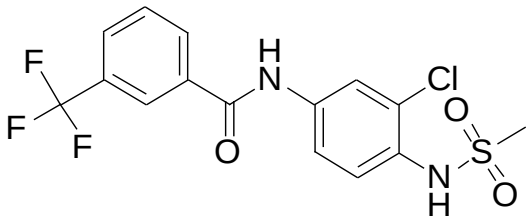

Figure 4.39 The Chemical construction of N-(3-chloro-4-(methyl sulfonamido)phenyl)-3-(trifluoromethyl)benzamide

◆ **4-chloro-N-(3-chloro-4-(methylsulfonamido)phenyl)-3-nitrobenzamide (34)**

Yield 68.8%. ^{1}H-NMR (400MHz, DMSO-d_6) δ: 10.716(s,1H), 9.450(s,1H), 8.645(s,1H), 8.268 (d,1H, J=8.4), 8.045(s,1H), 8.001(d,1H,J=8.4), 7.704(d,1H,J=8.8), 7.473(d,1H,J=8.8), 3.041(s,3H). ^{13}C-NMR (100MHz, DMSO-d_6) δ: 163.134, 147.875, 138.237, 134.910, 133.350, 132.534, 130.207, 130.029, 129.161, 128.934, 125.354, 121.599, 120.116, 41.344. DUIS-MS calculated for $C_{14}H_{11}Cl_2N_3O_5S$, [M-H]-:401.97, found 401.8; Purity: 98.6%.

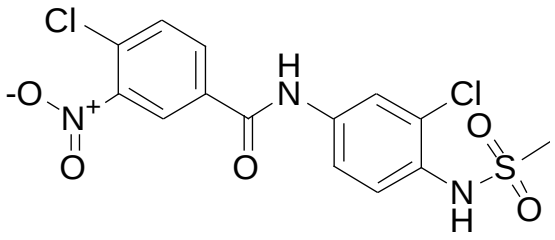

Figure 4.40 The Chemical construction of 4-chloro-N-(3-chloro-4-(methylsulfonamido)phenyl)-3-nitrobenzamide

◆ **N-(3-chloro-4-(methylsulfonamido)phenyl)-3,5-bis(trifluoromethyl)benzamide (35)**

Yield 51.2%. ^{1}H-NMR (400MHz, DMSO-d_6) δ: 10.803(s,1H), 9.445(s,1H), 8.618(s,2H), 8.402(s,1H), 8.051(s,1H), 7.727(d,1H,J=8.8), 7.495(d,1H,J=8.8), 3.052(s,3H). ^{13}C-NMR (100MHz, DMSO-d_6) δ: 163.210, 138.142, 137.200, 131.539,131.214,130.879,130.551,(q,2C) 130.334, 130.004, 129.105, 129.067(m,2C), 127.643,124.934,122.225,119.509(q,2CF_3), 125.830(m,1C), 121.803, 120.260, 40.077. DUIS-MS calculated for $C_{16}H_{11}ClF_6N_2O_3S$, [M-H]-: 459.00, found 458.8, Purity: 99.2%.

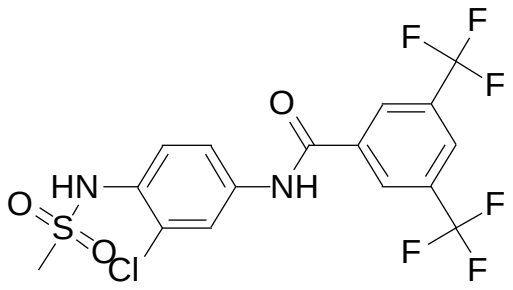

Figure 4.41 The Chemical construction of N-(3-chloro-4-(methyl sulfonamido)phenyl)-3,5-bis(trifluoromethyl)benzamide

◆ **4-chloro-N-(3-chloro-4-(ethylsulfonamido)phenyl)benzamide (36)**

Yield 66.3%. ^{1}H-NMR (400MHz, DMSO-d_6) δ: 10.477(s,1H), 9.382(s,1H), 8.050(s,1H), 7.992 (d,2H, J=8.0), 7.693(d,1H,J=8.6), 7.634(d,2H,J=8.0), 7.447(d,1H,J=8.6), 3.121(q,2H,J=7.2), 1.295 (t,3H,J=7.2). ^{13}C-NMR (100MHz, DMSO-d_6) δ: 165.074, 138.571, 137.191, 133.632, 130.136, 129.874, 129.827, 129.020, 121.399, 119.964, 99.992, 47.608, 8.564. DUIS-MS calculated for $C_{15}H_{14}Cl_2N_2O_3S$, [M-H]-: 371.00, found 370.9, Purity: 98.1%.

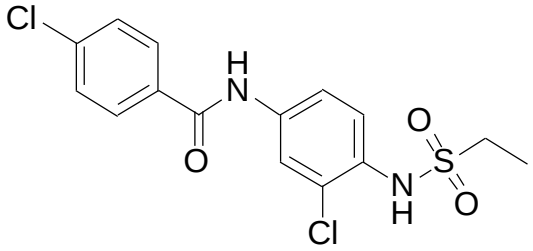

Figure 4.42 The Chemical construction of 4-chloro-N-(3-chloro-4-(ethylsulfonamido)phenyl)benzamide

◆ **4-cyano-N-(3-chloro-4-(ethylsulfonamido)phenyl)benzamide (37)**

Yield 62.7%. ^{1}H-NMR (400MHz, DMSO-d_6) δ: 10.649(s,1H), 9.412(s,1H), 8.058(s,1H), 8.113(d,2H, J=8.0), 8.048(d,2H,J=8.0), 7.694 (d,1H, J=8.6), 7.463 (d,1H, J=8.6), 3.125(q,2H,J=7.2), 1.294 (t,3H,J=7.2). ^{13}C-NMR (100MHz, DMSO-d_6) δ: 164.801, 138.943, 138.283, 133.000(2C), 130.162, 129.787, 129.039(2C), 128.976, 121.475, 120.047, 118.720, 114.599, 47.631, 8.562. DUIS-MS calculated for $C_{16}H_{14}ClN_3O_3S$, [M-H]-: 362.04, found 361.9, Purity: 97.8%.

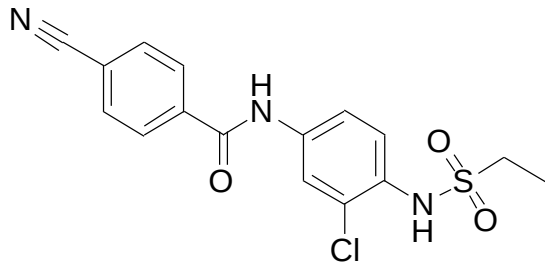

Figure 4.43 The Chemical construction of 4-cyano-N-(3-chloro-4-(ethylsulfonamido)phenyl)benzamide

◆ **N-(3-chloro-4-(ethylsulfonamido)phenyl)-3-(trifluoromethyl)benzamide (38)**

Yield 62.5%. ^{1}H-NMR (400MHz, DMSO-d_6) δ: 10.661 (s,1H), 9.410 (s,1H), 8.309 (s, 1H), 8.283 (d,1H, J=7.4), 8.061 (s, 1H), 7.997 (d,1H, J=7.4), 7.811 (t,1H, J=7.4), 7.719 (d,1H, J=8.6), 7.467 (d, 1H, J=8.6), 3.130 (q, 2H, J=7.2), 1.299 (t, 3H ,J=7.2) . ^{13}C-NMR (100MHz, DMSO-d_6) δ: 164.678, 138.382, 135.818, 132.381, 130.285, 130.082, 130.211,129.892,129.571,129.251(q,1C), 129.800, 128.970, 128.879(m,1C),

128.487,125.781,123.073,120.360(q,CF_3), 124.787(m), 121.579, 120.112，47.629，8.563. DUIS-MS calculated for $C_{16}H_{14}ClF_3N_2O_3S$, [M-H]-: 405.03, found 404.9, Purity: 99.1%.

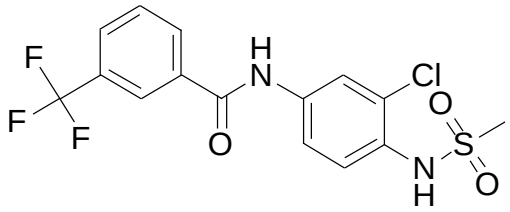

Figure 4.44 The Chemical construction of N-(3-chloro-4-(ethyl sulfonamido)phenyl)-3-(trifluoromethyl)benzamide

◆ 4-chloro-N-(3-chloro-4-(ethylsulfonamido)phenyl)-3-nitrobenzamide (39)

Yield 67.7%. ^{1}H-NMR (400MHz, DMSO-d_6) δ: 10.699(s,1H), 9.424(s,1H), 8.642(s,1H), 8.266 (d,1H, J=8.4), 8.033(s,1H), 7.999 (d,1H,J=8.4), 7.686(d,1H,J=8.8), 7.475(d,1H,J=8.8), 3.130(q,2H,J=7.2), 1.295 (t,3H,J=7.2). ^{13}C-NMR (100MHz, DMSO-d_6) δ: 163.11, 147.88, 138.06, 134.92, 133.34, 132.53, 130.31, 129.77, 128.97, 128.82, 125.35, 121.55, 120.10, 47.65, 8.56. DUIS-MS calculated for $C_{15}H_{13}Cl_2N_3O_5S$, [M-H]-: 415.99, found 415.8, Purity: 98.8%.

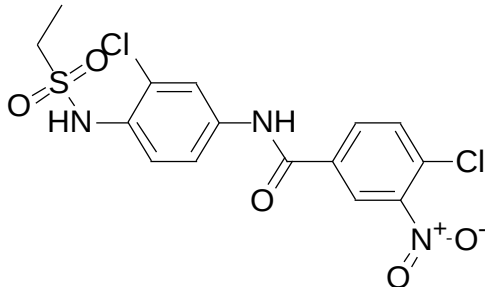

Figure 4.45 The Chemical construction of 4-chloro-N-(3-chloro-4-(ethylsulfonamido)phenyl)-3-nitrobenzamide

◆ **N-(3-chloro-4-(ethylsulfonamido)phenyl)-3,5-bis(trifluoromethyl)benzamide (40)**

Yield 54.1%. ^{1}H-NMR (400MHz, DMSO-d_6) δ: 10.808(s,1H), 9.434 (s,1H), 8.607 (s, 2H), 8.380 (s, 1H), 8.034 (s, 1H), 7.703 (d,1H, J=8.6), 7.488 (d, 1H, J=8.6), 3.135 (q,2H, J=7.2), 1.299(t, 3H,J=7.2). ^{13}C-NMR (100MHz, DMSO-d_6) δ: 163.182, 137.951, 137.164, 131.537,131.204,130.873,130.539(q,2C), 130.452, 129.730, 129.062(m,2C), 128.886, 125.777(m,1C), 127.624, 124.911,122.198,119.483(q,2CF_3), 121.754, 120.242, 47.668, 8.532. DUIS-MS calculated for $C_{17}H_{13}ClF_6N_2O_3S$, [M-H]-: 473.02, found 472.9, Purity: 97.2%.

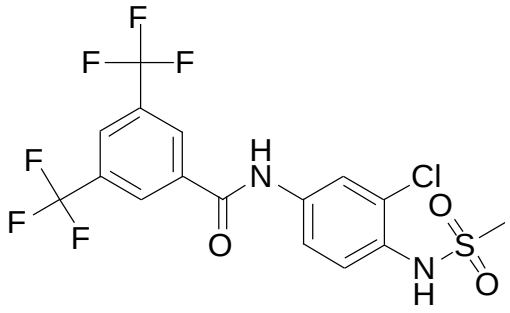

Figure 4.46 The Chemical construction of N-(3-chloro-4-(ethyl sulfonamido)phenyl)-3,5-bis(trifluoromethyl)benzamide

◆ **4-chloro-N-(3-chloro-4-(trifluoromethylsulfonamido)phenyl)benzamide (41)**

Yield 48.2%. ^{1}H-NMR (400MHz, DMSO-d_6) δ: 10.719(s,1H), 8.113 (d,2H, J=8.4), 8.102(s,1H), 8.056 (d,2H, J=8.4),7.745 (d,1H, J=8.8),7.457 (d,1H, J=8.8). ^{13}C-NMR (100MHz, DMSO-d_6) δ:164.960, 139.664, 138.866, 133.017(2C),131.734, 130.443, 129.076(2C), 121.499, 120.081, 118.705, 114.657. DUIS-MS calculated for $C_{14}H_9Cl_2F_3N_2O_3S$, [M-H]-: 410.96, found 410.8, Purity: 98.2%.

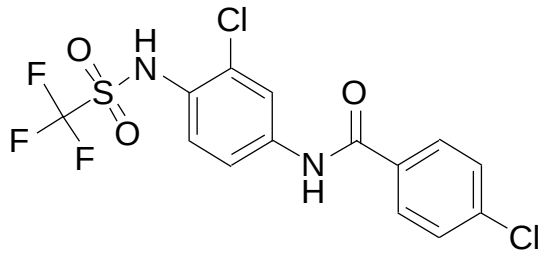

Figure 4.47 The Chemical construction of 4-chloro-N-(3-chloro-4-(trifluoromethylsulfonamido)phenyl)benzamide

◆ **4-cyano-N-(3-chloro-4-(trifluoromethylsulfonamido)phenyl)benzamide (42)**

Yield 50.5%. ^{1}H-NMR (400MHz, DMSO-d_6) δ: 10.704 (s, 1H), 8.112(d,2H,J=8.4), 8.082(d,1H,J=2.0), 8.055 (d,2H,J=8.4), 7.729(dd,1H,J=8.8,2.0), 7.450 (d,1H,J=8.8). ^{13}C-NMR (100MHz, DMSO-d_6) δ: 164.924, 138.887, 137.632, 133.018(2C), 131.546, 130.209, 125.353, 129.071(2C), 121.488, 120.060, 118.714, 114.631. DUIS-MS calculated for $C_{15}H_9ClF_3N_3O_3S$, [M-H]-: 401.99, found 401.8, Purity: 97.2%.

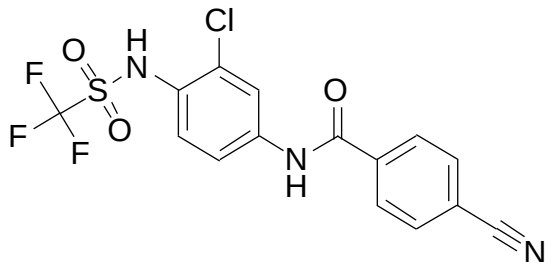

Figure 4.48 The Chemical construction of 4-cyano-N-(3-chloro-4-(trifluoromethylsulfonamido)phenyl)benzamide

◆ **N-(3-chloro-4-(trifluoromethylsulfonamido)phenyl)-3-(trifluoromethyl)benzamide (43)**

Yield 49.7%. ^{1}H-NMR (400MHz, DMSO-d_6) δ: 10.730 (s,1H), 8.307 (s,1H), 8.279(d,1H, J=7.6), 8.110(s, 1H), 8.003 (d,1H,J=7.6), 7.814 (t,1H, J=7.6), 7.775 (d,1H, J=8.8), 7.463 (d,1H, J=8.8). ^{13}C-NMR (100MHz, DMSO-d_6) δ: 164.85, 139.87, 135.73, 132.42, 131.80, 130.54, 130.31, 130.20,129.89,129.58,129.27(q,1C), 128.96(m,1C), 124.83(m,1C), 128.47,125.76,123.05,120.34(q,CF_3), 121.58, 120.13, 118.66. DUIS-MS calculated for $C_{15}H_9ClF_6N_2O_3S$, [M-H]-: 444.98, found 444.8, Purity: 98.6%.

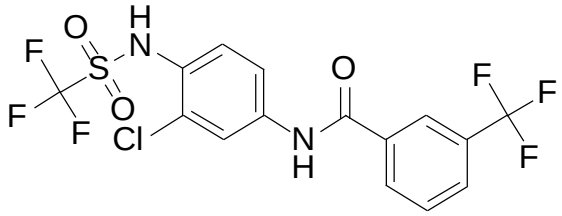

Figure 4.49 The Chemical construction of N-(3-chloro-4-(trifluoromethylsulfonamido)phenyl)-3-(trifluoromethyl)benzamide

◆ **4-chloro-N-(3-chloro-4-(trifluoromethylsulfonamido)phenyl)-3-nitrobenzamide (44)**

Yield 49.7%. ^{1}H-NMR (400MHz, DMSO-d_6) δ: 10.791(s,1H), 8.645(s,1H), 8.268 (d,1H, J=8.4), 8.081(s,1H), 8.100(d,1H,J=8.4), 7.744(d,1H,J=8.8), 7.470(d,1H,J=8.8), ^{13}C-NMR (100MHz, DMSO-d_6) δ: 163.291， 147.871， 139.510，134.831, 133.388, 132.544, 131.783, 130.537, 128.907, 125.408, 121.885, 121.579, 120.144. DUIS-MS calculated for $C_{14}H_8Cl_2F_3N_3O_5S$, [M-H]-: 455.94, found 455.8, Purity: 97.8%.

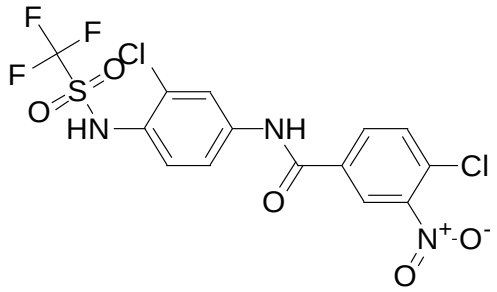

Figure 4.50 The Chemical construction of 4-chloro-N-(3-chloro-4-(trifluoromethylsulfonamido)phenyl)-3-nitrobenzamide

◆ **N-(3-chloro-4-(trifluoromethylsulfonamido)phenyl)-3,5-bis(trifluoromethyl) benzamide (45)**

Yield 48.8%. ^{1}H-NMR (400MHz, DMSO-d_6) δ: 10.851 (s,1H), 8.609 (s,2H), 8.403 (s, 1H), 8.073 (s,1H), 7.746 (d,1H, J=8.8), 7.482 (d, 1H, J=-8.8) ^{13}C-NMR (100MHz, DMSO-d_6) δ: 163.344 , 137.156, 131.625,

131.536,131.207,130.784,130.544(q,2C), 130.874, 130.312, 129.093(m,2C), 125.874(m,1C), 127.632,124.921,122.206119.491(q,2CF_3), 121.975, 121.751, 120.253. DUIS-MS calculated for $C_{16}H_8ClF_9N_2O_3S$, [M-H]-: 512.97, found 512.8, Purity: 97.3%.

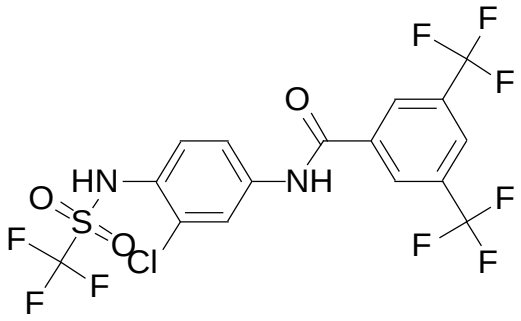

Figure 4.51 The Chemical construction of N-(3-chloro-4-(trifluoro methylsulfonamido)phenyl)-3,5-bis(trifluoromethyl) benzamide

◆ **4-chloro-N-(3-fluoro-4-(methylsulfonamido)phenyl)benzamide (46)**

Yield 52.7%. ^{1}H-NMR (400MHz, DMSO-d_6) δ: 10.573(s,1H)， 9.478(s,1H), 7.990 (d,2H, J=8.0)， 7.843(d,1H,J=12.8), 7.636 (d,2H,J=8.0)， 7.538, (d,1H,J=8.6) , 7.372(t,1H,J=8.6) ， 3.011 (s,3H). ^{13}C-NMR (100MHz, DMSO-d_6) δ: 165.093, 157.637,155.207(1C), 138.871,138.767(1C), 137.168, 133.687, 130.136(2C), 129.021(2C), 128.429, 120.470,120.339(1C), 116.747,116.718(1C), 108.451,108.200(1C), 40.067. DUIS-MS calculated for $C_{14}H_{12}ClFN_2O_3S$, [M-H]-:341.02, found 340.9; Purity: 96.8%.

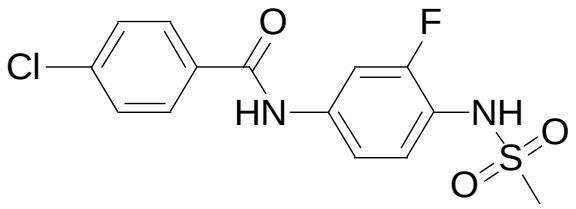

Figure 4.52 The Chemical construction of 4-chloro-N-(3-fluoro-4-(methylsulfonamido)phenyl)benzamide

◆ **4-cyano-N-(3-fluoro-4-(methylsulfonamido)phenyl)benzamide (47)**

Yield 48.9%. ^{1}H-NMR (400MHz, DMSO-d_6) δ: 10.680 (s,1H)， 9.506 (s,1H), 8.111(d,2H,J=8.4), 8.051 (d,2H,J=8.4), 7.849(d,1H, J=12.4)， 7.541(d,1H, J=8.8)，7.390(t,1H, J=8.8), 3.017(s,3H). ^{13}C-NMR (100MHz, DMSO-d_6) δ: 164.823, 157.563,155.130(1C), 138.997, 138.551, 138.448(1C), 132.999(2C), 129.039(2C), 128.377, 120.792,120.659(1C), 118.723, 116.841,116.810(1C), 114.574, 108.540,108.289(1C), 56.503. DUIS-MS calculated for $C_{15}H_{12}FN_3O_3S$, [M-H]-: 332.05, found 332.0, Purity: 98.8%.

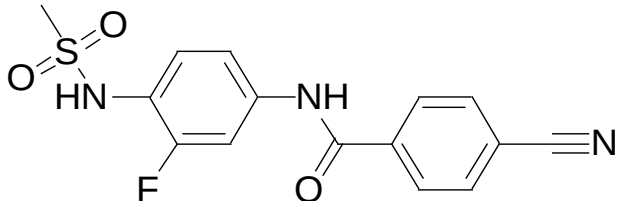

Figure 4.53 The Chemical construction of 4-cyano-N-(3-fluoro-4-(methylsulfonamido)phenyl)benzamide

◆ **N-(3-fluoro-4-(methylsulfonamido)phenyl)-3-(trifluoromethyl)benzamide (48)**

Yield 43.5%. ^{1}H-NMR (400MHz, DMSO-d_6) δ: 10.663(s,1H), 9.504(s,1H), 8.295(s,1H), 8.281(d,1H,J=8.0), 8.001(d,1H,J=8.0), 7.850(d,1H,J=12.8), 7.805(d,1H,J=8.0), 7.548(d,1H,J=8.8), 7.396 (d,1H, J=8.8). 3.021(s,3H). ^{13}C-NMR (100MHz, DMSO-d_6) δ: 164.712, 157.592,155.158(1C), 138.634,138.534(1C), 135.882, 132.364, 130.297, 130.212,129.892,129.573,129.893(q,1C), 128.444,125.782,123.070,120.360(q,CF_3), 128.378, 124.728(m,1C), 123.070, 120.710,120.579(1C), 116.898,116.867(1C), 108.626,108.377(1C), 40.062. DUIS-MS calculated for $C_{15}H_{12}F_4N_2O_3S$, [M-H]-: 375.04, found 374.9, Purity: 98.2%.

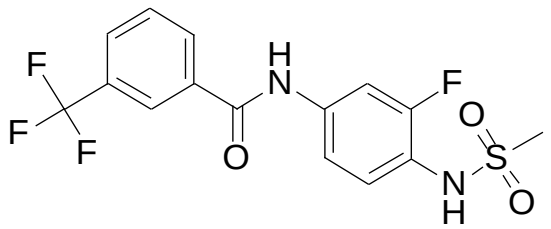

Figure 4.54 The Chemical construction of N-(3-fluoro-4-(methyl sulfonamido)phenyl)-3-(trifluoromethyl)benzamide

◆ **4-chloro-N-(3-fluoro-4-(methylsulfonamido)phenyl)-3-nitrobenzamide (49)**

Yield 42.6%. ^{1}H-NMR (400MHz, DMSO-d_6) δ: 10.733(s,1H), 9.521(s,1H), 8.639(s,1H), 8.266 (d,1H, J=8.4), 7.999(d,1H,J=8.4), 7.830(d,1H,J=12.8), 7,528(d,1H,J=8.8), 7.404(t,1H,J=8.8, 3.023(s,3H). ^{13}C-NMR (100MHz, DMSO-d_6) δ: 163.136, 157.520,155.099(1C), 149.891, 138.312,138.209(1C), 134.965, 133.335,

132.516, 128.799, 128.372, 125.352, 120.951,120.922(1C), 116.917,116.556(1C), 108.640,108.399(1C), 40.063. DUIS-MS calculated for $C_{14}H_{11}ClFN_3O_5S$, [M-H]-: 386.00, found 385.9; Purity: 96.3%.

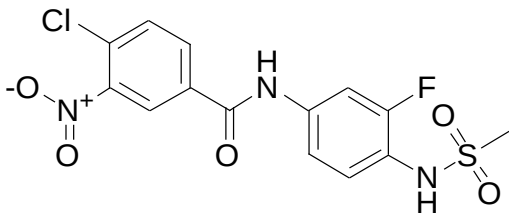

Figure 4.55 The Chemical construction of 4-chloro-N-(3-fluoro-4-(methylsulfonamido)phenyl)-3-nitrobenzamide

◆ **N-(3-fluoro-4-(methylsulfonamido)phenyl)-3,5-bis(trifluoromethyl) benzamide (50)**

Yield 41.7%. ^{1}H-NMR (400MHz, DMSO-d_6) δ: 10.845(s,1H)， 9.537(s,1H)，8.613(s,2H)，8.400(s,1H)，7.844(d,1H,J=12.8)，7.541(d,1H,J=8.8)，7.423(d,1H, J=8.8)，3.031（s,3H）. ^{13}C-NMR (100MHz, DMSO-d_6) δ: 163.215, 157.495,155.061(1C), 138.210,138.109(1C), 137.232, 131.508,131.188,130.856,130.526(q,2C) ，129.081(m,2C), 128.270, 127.653,124.933,122.219,119.504(q,2CF_3), 125.823(m1C)，121.081,120.950(1C)， 117.063,117.035(1C)，108.812,108.561(1C)， 40.059. DUIS-MS calculated for $C_{16}H_{11}F_7N_2O_3S$, [M-H]-: 443.03, found 442.9, Purity: 97.8%.

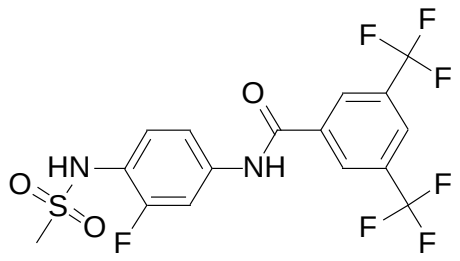

Figure 4.56 The Chemical construction of N-(3-fluoro-4-(methyl sulfonamido)phenyl)-3,5-bis(trifluoromethyl) benzamide

◆ **4-chloro-N-(3-fluoro-4-(ethylsulfonamido)phenyl)benzamide (51)**

Yield 50.2%. ^{1}H-NMR (400MHz, DMSO-d_6) δ: 10.509 (s,1H), 9.506 (s,1H), 7.986 (d,2H, J=8.4), 7.830(dd,1H, J_1= 2.0, J_2= 12.8) , 7.637 (d,2H,J=8.4), 7.518 (d,1H, J=8.8), 7.372 (t,1H,J=8.8), 3.078 (q,2H,J=7.2), 1.275 (t,3H,J=7.2). ^{13}C-NMR (100MHz, DMSO-d_6) δ: 165.076, 157.435,155.009(1C), 138.703,138.600(1C), 137.160, 133.676, 130.133, 129.020, 128.327, 120.455,120.332(1C), 116.735,116.704(1C), 108.383,108.132(1C), 46.702, 8.478. DUIS-MS calculated for $C_{15}H_{14}ClFN_2O_3S$, [M-H]-: 355.03, found 354.9, Purity: 97.5%.

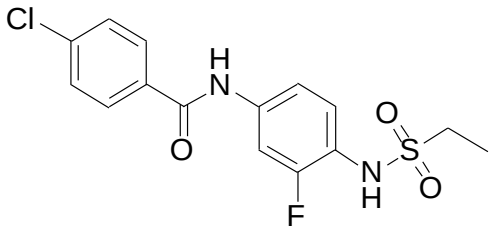

Figure 4.57 The Chemical construction of 4-chloro-N-(3-fluoro-4-(ethylsulfonamido)phenyl)benzamide

◆ **4-cyano-N-(3-fluoro-4-(ethylsulfonamido)phenyl)benzamide (52)**

Yield 53.2%. ^{1}H-NMR (400MHz, DMSO-d_6) δ: 10.682 (s, 1H), 9.533 (s,1H), 8.110 (d,2H, J=8.4), 8.049 (d,2H,J=8.4), 7.836(d, 1H, J=12.8), 7.526 (d,2H,J=8.8), 7.391 (t,1H,J=8.8), 3.084 (q,2H, J=7.2), 1.276 (t,3H,J=7.2) . ^{13}C-NMR (100MHz, DMSO-d_6) δ: 164.802, 157.365,154.936(1C), 138.989, 138.393,138.291(1C), 132.995(2C), 129.038(2C), 128.252, 120.785,120.652(1C), 128.726, 116.835,116.804(1C), 114.563, 108.482,108.232(1C), 46.724, 8.475. DUIS-MS calculated for $C_{16}H_{14}FN_3O_3S$, [M-H]-: 346.07, found 345.9 Purity: 97.7%.

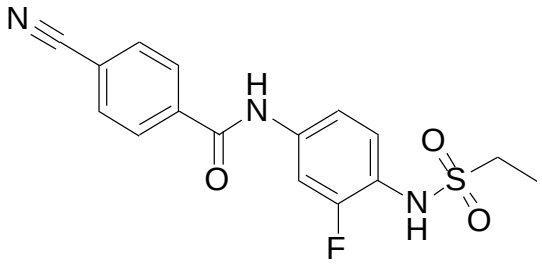

Figure 4.58 The Chemical construction of 4-cyano-N-(3-fluoro-4-(ethylsulfonamido)phenyl)benzamide

◆ **N-(3-fluoro-4-(ethylsulfonamido)phenyl)-3-(trifluoromethyl)benzamide (53)**

Yield 52.3%. ^{1}H-NMR (400MHz, DMSO-d_6) δ: 10.662(s,1H), 9.531(s,1H), 8.292(s,1H), 8.268 (d,1H,J=7.2), 7.997 (d,1H,J=7.2), 7.826(m, 2H), 7.530(d,1H,J=8.0), 7.397 (d,1H,J=8.0), 3.089(q,2H,J=7.0), 1.281(t,3H,J=7.0). ^{13}C-NMR (100MHz, DMSO-d_6) δ: 164.689, 157.393,154.968(1C), 138.479,138.375(1C), 135.872, 132.357,

130.289, 130.211,129.883,129.562,129.242(q,1C), 128.868(m,1C), 128.261, 124.726(m,1C), 120.708,120.576(1C), 116.886,116.854(1C), 108.565,108.313(1C), 46.737, 8.490. DUIS-MS calculated for $C_{16}H_{14}F_4N_2O_3S$, [M-H]-: 389.06, found 388.9, Purity: 97.5%.

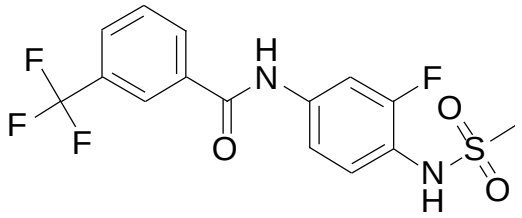

Figure 4.59 The Chemical construction of N-(3-fluoro-4-(ethyl sulfonamido)phenyl)-3-(trifluoromethyl)benzamide

◆ **4-chloro-N-(3-fluoro-4-(ethylsulfonamido)phenyl)-3-nitrobenzamide (54)**

Yield 52.5%. ^{1}H-NMR (400MHz, DMSO-d_6) δ: 10.748(s,1H), 9.546 (s,1H), 8.642(s,1H), 8.268(dd,1H, J_1= 2.0, J_2= 8.4) , 7.997 (d,1H,J=8.4), 7.826 (d,1H,J=12.8), 7.516(dd,1H,J=8.8,2.0), 7.403 (t,1H,J=8.8), 3.089 (q,2H,J=7.3), 1.277 (t, 3H,J=7.3) . ^{13}C-NMR (100MHz, DMSO-d_6) δ: 163.116, 157.328,154.999(1C), 147.872, 138.169,138.071(1C), 134.955, 133.349, 132.502, 128.784, 128.239,128.233(1C), 125.371, 120.943,120.811(1C), 116.911,116.880(1C), 109.583,109.331(1C), 46.766, 6.479. DUIS-MS calculated for $C_{15}H_{13}ClFN_3O_5S$, [M-H]-: 400.02, found 399.9, Purity: 98.8%.

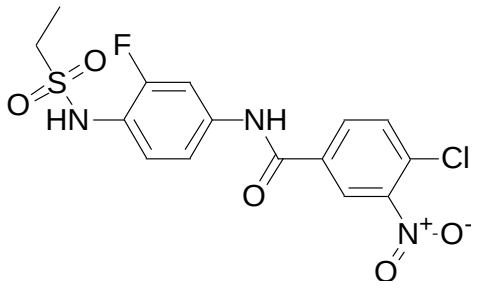

Figure 4.60 The Chemical construction of 4-chloro-N-(3-fluoro-4-(ethylsulfonamido)phenyl)-3-nitrobenzamide

◆ **N-(3-fluoro-4-(ethylsulfonamido)phenyl)-3,5-bis(trifluoromethyl)benzamide (55)**

Yield 47.9%. ^{1}H-NMR (400MHz, DMSO-d_6) δ: 10.872 (s,1H), 9.563 (s,1H), 8.618 (s,2H), 8.400 (s,1H), 7.842 (d,1H,J=12.8), 7.533 (d,1H,J=8.8), 7.423 (t, 1H, J=8.8), 3.099 (q,2H,J=7.2), 1.283 (t,3H,J=7.2). ^{13}C-NMR (100MHz, DMSO-d_6) δ: 163.197, 157.304,154.872(1C), 138.070,137.972(1C), 137.220, 131.506,131.176,130.840,130.539(q,2C), 129.081(m,2C), 128.170, 125.772(m,1C), 127.645,124.932,122.219,119.504(2CF_3), 121.066,120.940(1C), 117.065,117.028(1C), 108.757,108.504(1C), 46.795, 8.491. DUIS-MS calculated for $C_{17}H_{13}F_7N_2O_3S$, [M-H]-: 457.05, found 456.9, Purity: 98.5%.

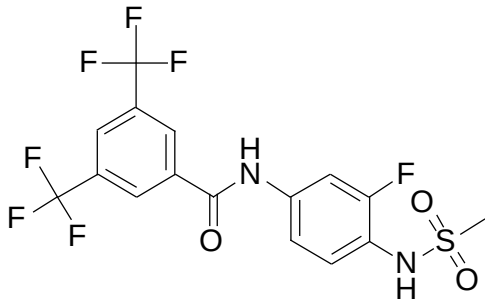

Figure 4.61 The Chemical construction of N-(3-fluoro-4-(ethyl sulfonamido)phenyl)-3,5-bis(trifluoromethyl)benzamide

◆ **4-chloro-N-(3-fluoro-4-(trifluoromethylsulfonamido)phenyl)benzamide (56)**

Yield 45.6%. ^{1}H-NMR (400MHz, DMSO-d_6) δ: 16.200(s,1H)，10.587(s,1H), 7.986 (d,2H, J=8.4), 7.872 (d,1H, J=12.8), 7.639(d,2H,J=8.4), 7.576(d,1H, J=8.4), 7.391(t,1H,J=8.4). ^{13}C-NMR (100MHz, DMSO-d_6) δ: 165.260, 159.039,158.573(1C)，140.280, 140.311,140.132(1C)， 137.260， 133.592， 130.173(2C)，129.042(2C), 119.343,119.136(1C), 116.821,116.789(1C), 108.320,108.069(1C). DUIS-MS calculated for $C_{14}H_9ClF_4N_2O_3S$, [M-H]-: 394.99, found 394.9, Purity: 97.8%.

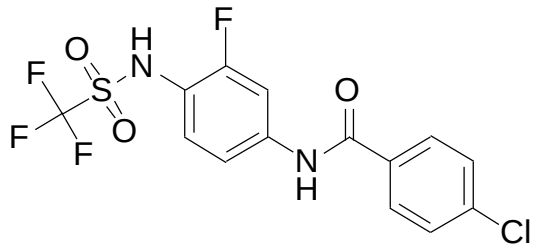

Figure 4.62 The Chemical construction of 4-chloro-N-(3-fluoro-4-(trifluoromethylsulfonamido)phenyl)benzamide

◆ 4-cyano-N-(3-fluoro-4-(trifluoromethylsulfonamido)phenyl)benzamide (57)

Yield 47.6%. ^{1}H-NMR (400MHz, DMSO-d_6) δ: 10.770(s, 1H), 8.111(d,2H,J=8.0), 8.055(d,2H,J=8.0), 7.892(d,1H,J=12.8), 7.587(d,1H,J=8.8), 7.417(t,1H,J=8.8). ^{13}C-NMR (100MHz, DMSO-d_6) δ: 165.018, 158.667,156.213(1C), 138.888, 133.163,133.138(1C), 133.012(2C), 130.305, 129.088(2C), 121.943,121.911(1C)，118.704, 116.933,116.902(1C), 114.657, 108.401,108.154(1C).

DUIS-MS calculated for $C_{15}H_9F_4N_3O_3S$, [M-H]-: 386.02, found 385.9 Purity: 97.9%.

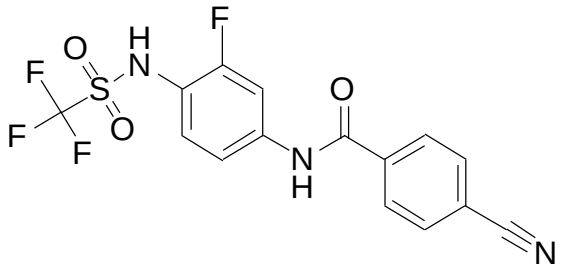

Figure 4.63 The Chemical construction of 4-cyano-N-(3-fluoro-4-(trifluoromethylsulfonamido)phenyl)benzamide

◆ **N-(3-fluoro-4-(trifluoromethylsulfonamido)phenyl)-3-(trifluoromethyl)benzamide (58)**

Yield 47.5%. ^{1}H-NMR (400MHz, DMSO-d_6) δ: 10.776 (s,1H), 8.299 (S,1H), 8.286 (d,2H, J=7.6), 8.002 (d, 1H, J=7.6), 7.906 (d, 1H, J=12.4), 7.833(t, 1H, J=7.6), 7.605 (d, 1H, J=8.2), 7.418 (t,1H, J=8.2) . ^{13}C-NMR (100MHz, DMSO-d_6) δ: 164.897, 158.680,156.226(1C), 140.421,140.341(1C), 135.781, 132.419, 132.377, 130.296, 130.265, 130.223,129.902,129.58,1129.260(q,1C), 128.917(m,1C) , 124.806(m,1C), 123.059,122.488(1C), 116.989,116.962(1C), 108.499,108.247(1C). DUIS-MS calculated for $C_{15}H_9F_7N_2O_3S$, [M-H]-: 429.01, found 428.9, Purity: 98.3%.

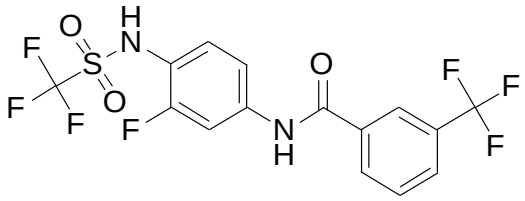

Figure 4.64 The Chemical construction of N-(3-fluoro-4-(trifluoro methylsulfonamido)phenyl)-3-(trifluoromethyl)benzamide

◆ **4-chloro-N-(3-fluoro-4-(trifluoromethylsulfonamido)phenyl)-3-nitrobenzamide (59)**

Yield 43.5%. ^{1}H-NMR (400MHz, DMSO-d_6) δ: 10.760(s,1H), 10.483(s,1H),8.654(s,1H) , 8.279 (dd,1H, J=8.4,1.2), 7.999 (t,1H,J=8.0), 7.855(d,1H,J=12.8,), 7.612(m,2H). ^{13}C-NMR (100MHz, DMSO-d_6) δ: 163.342, 158.672,156.220(1C), 147.883, 140.242,140.139(1C), 134.865, 133.378, 132.536, 130.371, 128.903, 125.405, 121.886,121.343(1C), 117.010,116.980(1C), 108.500,108.251(1C). DUIS-MS calculated for $C_{14}H_8ClF_4N_3O_5S$, [M-H]-: 439.97, found 439.8, Purity:98.1%.

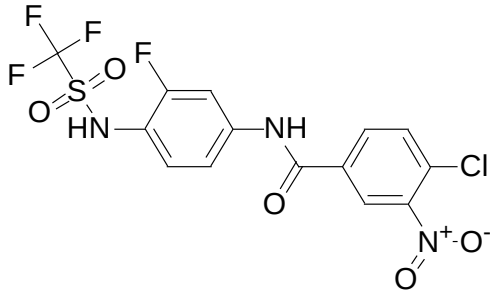

Figure 4.65 The Chemical construction of 4-chloro-N-(3-fluoro-4-(trifluoromethylsulfonamido)phenyl)-3-nitrobenzamide

◆ **N-(3-fluoro-4-(trifluoromethylsulfonamido)phenyl)-3,5-bis(trifluoromethyl)benzamide (60)**

Yield 40.2%. ^{1}H-NMR (400MHz, DMSO-d_6) δ: 10.944(s,1H), 8.612(s,2H), 8.397(s,1H)，7.900(d, 1H, J=12.4),7.594(d, 1H, J=8.6)， 7.448(t, 1H, J=8.6). ^{13}C-NMR (100MHz, DMSO-d_6) δ: 163.430, 158.665,156.211(1C), 140.171,140.067(1C), 137.148, 131.525,131.193,130.861,130.531(q,2C), 130.349, 129.150,129.125(3C), 125.843（m,1C）, 127.629,124.914,122.200,119.486(q,2CF_3)， 117.129,117.100(1C), 108.645,108.396(1C). DUIS-MS calculated for $C_{16}H_8F_{10}N_2O_3S$, [M-H]-: 497.00, found 497.0, Purity: 98.2%.

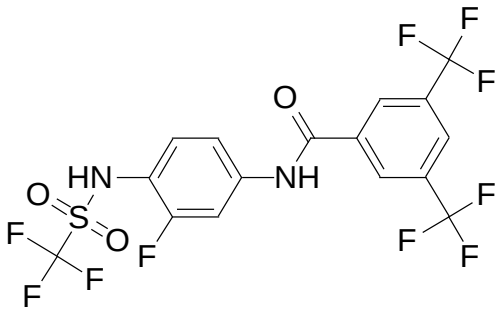

Figure 4.66 The Chemical construction of N-(3-fluoro-4-(trifluoromethyl sulfonamido)phenyl)-3,5-bis(trifluoromethyl)benzamide

4.4.2. Biological studies

4.4.2.1. Cell culture.

Three breast cancer cell lines including SKBR-3, MCF-7, and MDA-MB-231; human embryonic kidney cell line HEK293; mice macrophages cell C-38 were obtained from ATCC (Rockville, MD). The cells were maintained in RPMI1640 medium supplemented with 10% fetal bovine serum (FBS), 2 mmol/L L-Glutamine, 1 mmol/L sodium pyruvate, 100 U/mL penicillin-streptomycin. FBS was heat inactivated for 30 min in a 56 ℃ water bath before use. Cell cultures were grown at 37 ℃, in a humidified atmosphere of 5% CO_2 in a VWR CO_2 incubator (Bridgeport NJ).

4.4.2.2. Cell viability analysis

The effects of the new derivatives on the viability of three breast cancer cell lines were assessed using the 3-(4,5-dimethylthiazol-2-yl)-2,5-diphenyl-2H- tetrazolium bromide assay in four replicates. Cells were grown in RPMI1640 medium in 96-well, flat-bottomed plates for 24 h, and were exposed to various concentrations of the compounds dissolved in DMSO (DMSO final concentration ≤0.1%) in media for 48 h. Controls received DMSO vehicle at a concentration equal to that in drug-treated cells. The medium was removed, replaced by 200 µL of 0.5 mg/ml of 3-(4,5-dimethylthiazol-2-yl) -2,5-diphenyl-2H-tetrazolium bromide in fresh media, and cells were incubated in the CO_2 incubator at 37 ℃

for 2 h. Supernatants were removed from the wells, and the reduced 3-(4,5-dimethylthiazol-2-yl) -2,5-diphenyl- 2H-tetrazolium bromide dye was solubilized in 200 µL/well DMSO. Absorbance at 570 nm was determined on a plate reader. Statistical and graphical information was determined using GraphPad Prism software (GraphPad Software Incorporated) and Microsoft Excel (Microsoft Corporation). IC_{50} values were determined using nonlinear regression analysis.

4.4.2.3. Western blot

SKBR-3 cells were treated with JCC76 (1 µM), compound 16 (0.1, 0.3, 1 µM) and compound 17 (0.1, 0.3, 1 µM) for 48 h. The cells were lysed, briefly sonicated, and centrifuged at 12000*g* for 10 min. 30 g of protein for each sample was boiled with 4x loading buffer for 5 minutes, electrophoresed on a 10% SDS-polyacrylamide gel, and transferred onto polyvinylidene difluoride (PVDF) membrane. The membrane was blocked for 1 hour with 5% nonfat milk in PBST and then incubated with specific primary antibody (Cell Signaling). After washing, the membrane was incubated with horseradish-conjugated secondary antibody (Cell Signaling). The bands were visualized by chemiluminescence with ECL reagent (Thermo Scientific).

4.4.2.4. Small chaperone activity assay.

Alpha-crystalline chaperone activity assay: 24 µlmg/ml insulin stock solution was added to the single well of 384 well plate, 3 µl 5mg/ml alpha-crystalline, 71 µl PBS buffer with appropriate concentration of compound dissolved inside were added as well. The mixture was thoroughly mixed and incubated at 37 ℃ for 5 min, whereupon 2 µL of 1M DTT in water was added to initiate the insulin aggregation. The absorbance (A) at 400 nm was monitored over 45min using a plate reader. A mixture of insulin in the absence or presence of alpha-crystalline with 0.1% DMSO was used as control.

4.5. ACKNOWLEDGEMENTS

This research was supported by Center for Gene Regulation in Health and Disease (GRHD) of Cleveland State University and the Summer Undergraduate Research program. Aicha Quamine was supported by a McNair scholarship. The instruments used in the study were supported by National Science Foundation Major Research Instrumentation Grants (CHE-0923398 and CHE-1126384).

4.6 REFERENCES

1. Figueroa-Magalh ães, M. C.; Jelovac, D.; Connolly, R. M.; Wolff, A. C. Treatment of HER2-positive breast cancer The Breast2014, 23(2), 128–136
2. Normanno, N.; Luca, A. D.; Bianco, C.; Strizzi, L.; Mancino, M.; Maiello, M. R.; Carotenuto, A.; Feo, G. D.; Caponigro, F.; Salomon, D. S. Epidermal growth factor receptor (EGFR) signaling in cancer. Gene 2006, 366 (1), 2–16
3. Onitilo, A. A.; Engel, J. M.; Greenlee, R. T.; Mukesh, B. N. Breast cancer subtypes based on ER/PR and Her2 expression: comparison of clinicopathologic features and survival. Clinical Medicine & Research 2009, 7 (1-2), 4–13.
4. Ryan, Q.; Ibrahim, A.; Cohen, M. H.; Johnson, J.; Ko, C.-W.; Sridhara, R.; Justice, R.; Pazdur, R. FDA drug approval summary: lapatinib in combination with capecitabine for previously treated metastatic breast cancer that overexpresses HER-2.. The Oncologist 2008, 13 (10), 1114–1119.

5. Valabrega, G.; Montemurro, F.; Aglietta, M. Trastuzumab: mechanism of action, resistance and future perspectives in HER2-overexpressing breast cancer. Annals of Oncology 2007, 18 (6), 977–984
6. Barok, M.; Joensuu, H.; Isola, J. Trastuzumab emtansine: mechanisms of action and drug resistance. Breast Cancer Research 2014, 16 (2).
7. 15. Hudis, C. A. N. Engl. Trastuzumab — Mechanism of Action and Use in Clinical PracticeJ. Med 2007, 357 (1), 39–51
8. Kang, S. H.; Kang, K. W.; Kim, K.-H.; Kwon, B.; Kim, S.-K.; Lee, H.-Y.; Kong, S.-Y.; Lee, E. S.; Jang, S.-G.; Yoo, B. C. Upregulated HSP27 in human breast cancer cells reduces Herceptin susceptibility by increasing Her2 protein stability. BMC Cancer 2008, 8 (1).
9. Li, K. C.; Heo, K.; Ambade, N.; Kim, M. K.; Kim, K.-H.; Yoo, B. C.; Yoo, H.-S. Reduced expression of HSP27 following HAD-B treatment is associated with Her2 downregulation in NIH: OVCAR-3 human ovarian cancer cells. Molecular Medicine Reports 2015, 12 (3), 3787–3794.
10. Kim, M. K.; Kim, S. C.; Kim, W. K.; Kim, K.; Kim, K.-H.; Yoo, B. C. HSP27 phosphorylation inhibitor regulates Her2 expression in human breast cancer cell
11. Robert L. Lichter, and Roderick E. Wasylishen。Fluoropyridines. Carbon-13 chemical shifts and carbon-fluorine coupling constants. J. Am. Chem. Soc., 1975, 97 (7), 1808–1813
12. Del Bene JE, Alkorta I, Elguero J. Probing (1)J(C-F) and (n)J(F-F) spin-spin

coupling constants for fluoroazines: an ab initio theoretical investigationJ Phys Chem A.2010,114(7),2637-43.

13. Yang, J. Tian ran you ji hua he wu he ci gong zhen tan pu ji; Hua xue gong ye chu ban she: Beijing, 2011.

CHAPTER V

CONCLUSION AND FUTURE DIRECTIONS

5.1 Conclusion

Through HSP27 inhibition several client proteins will be downregulated, HER2 is one of those client proteins. Inhibiting HSP27 became an indirectly HER2 overexpressed breast cancer therapeutic strategy. In previously study we have identified a lead compound JCC76 which was generated from COX-2 inhibitor, Nimesulide. The lead compound JCC76 exhibit selective inhibition against HER2 overexpressed breast cancer cell and inhibit the function of HSP27.

In the first study totally 23 compounds were synthesized through a five steps reaction scheme adapted from JCC76 synthesized scheme. The structure of new analogs was confirm by proton and carbon NMR and LC-MS. The purity of products was exam by LC-UV set up wavelength at 260nm. Cell viability assay was used to test the analogs ability to inhibit cell proliferation. Western-blot and chaperone assay were used to

investigate the anti-proliferate cellular mechanism.

The major structural difference between new analogs and lead compound JCC76 is the flipped sulfonamide moiety. The SAR study indicate that in the B moiety 2,5-dimethoxybenzy group contributes more in cell proliferation inhibition compared to 2,5-dimethybenzy group. For the B moiety, SAR study suggests that it is critical for the compounds' anti-proliferate activity against SKBR-3 cells, the difference of potency between the least potent compound and the most potent one could be 250 folds. Electron withdrawing groups on the benzyl amide group harm the biological activity and bulky electron donating substitution groups such as iodo, methoxy on benzyl amide moiety enhance the compounds' overall activity. From 23 compounds, two were selected for the further studies because of their potency and selectivity. In the chaperone inhibition experiment, the selected compounds, 16 and 17, inhibited the protective function of small chaperone, α-crystalline, against DTT induced insulin denaturation and aggregation. This result indicates that the ligand based structural optimization analogs preserved the chaperone inhibition of the lead compound. In the HER2 downregulation experiment, the results indicate a dose-dependent downregulation of HER2 for both compounds, especially compound 16 at 1 and 0.3μM concentration where at 1μM it showed a 3 fold decrease in HER2 compared to JCC76 at same concentration.

In the second study we try to improve inhibitors' water solubility and cell uptake by decrease molecular size and weight. Totally 60 compounds were synthesized. The structure of new analogs were confirm by proton and carbon NMR and LC-MS. The

purity of products was detected by LC-UV set up wavelength at 260nm. Cell viability assay was used to test the analogs ability to inhibit cell proliferation.

To improve solubility 2,5-dimethybenzy group was replace by 4 difference small function groups, three sulfonamide with small alky chain were choose and 5 benzyl amide group which are highly polar and show potent SKBR-3 cell growth inhibition were used. Through the combination of these substitution groups 60 compounds were designed. The SAR study indicates several compounds with 3-trifluoromethylbenzamide groups showed potent and selective inhibition of SKBR-3 cells. However, unexpectedly, some analogs showed potent proliferation inhibition against macrophage cells, C38, suggesting that these compounds may interfere some unknown critical pathways in macrophage cell.

5.2 Future direction

Through cell viability assay compounds that specifically targeting HER2 overexpressed breast cancer cell SKBR-3 have been choose. However whether this compounds activate by inhibiting HSP27 which destabilize HER2 result in SKBR-3 proliferate hindrance or not haven’t been confirm. To investigate the mechanism of new analogs western-blot and chaperone assay will be used to approve new compounds are HSP27 inhibitors

To further improve HSP27 inhibition, small molecule inhibitor may not be enough. A new technology Proteolysis targeting chimera (PROTAC) which can downregulate

selected protein through increase degradation by ubiquitin-proteasome system. Synthesis new compounds using PROTAC may increase HSP27 degradation which result in HER2 downregulation and more potent inhibition against HER2 overexpressed breast cancer.